The Role of the Silica Frustule in Diatom Carbon Acquisition and Photosynthesis

by

Tamsyne Jade Smith-Harding

BSc., BSc. (Honours)

Thesis submitted to Flinders University for the degree of Doctor of Philosophy

College of Science and Engineering

November 2018

TABLE OF CONTENTS

THESIS ABSTRACT

Diatoms are arguably the most ecologically successful group of eukaryotic microalgae in aquatic systems. Fixing 25-50% of the 50 billion tonnes of organic carbon generated in the oceans annually, they dominate marine primary productivity. Although inorganic carbon is plentiful in the oceans, 90% is present as HCO_3^- and <1% present as CO_2, the substrate for carbon fixation by ribulose-1,5-bisphosphate carboxylase/oxygenase (RUBISCO). RUBISCO has a low affinity for CO_2 and all known RUBISCOs are sub-saturated at present day levels. Carbon concentrating mechanisms (CCMs) act to increase the concentration of CO_2 at the active site of RUBISCO. In microalgae, including some diatoms, one such mechanism involves the dehydration of HCO_3^- at the cell surface by external carbonic anhydrase (CA_{ext}), maintain a high equilibrium of CO_2 available for uptake at the plasmamembrane. Since H^+ exchange with water is slow, a pH buffer is necessary to maintain high catalytic rates. It has been suggested that the silica frustule may act as a buffer for CA_{ext} in diatoms and that CA_{ext} activity is modulated by the silica content of the frustule. The overall objective of this thesis was to determine the role of the frustule in CA_{ext} activity, overall CCM function and photosynthesis in the cosmopolitan marine diatom *Chaetoceros muelleri*. Chapter 1 investigated the role of CA_{ext} in inorganic carbon (C_i) acquisition and photosynthesis over the course of growth in *C. muelleri*. Whilst CA_{ext} activity increased over time in response to CO_2 depletion, the role that it played in C_i acquisition for photosynthesis was variable. Specifically, CA_{ext}-mediated C_i supply increased between the first two sampling points, but was negligible later in the growth phase, where C_i acquisition was likely by direct uptake of HCO_3^- by anion exchange transporters at the cell surface. Chapter 2 explored the impacts of silica limitation, which produces poorly silicified frustules, on CA_{ext} activity, overall CCM function and photosynthesis. Silica-limited *C. muelleri* cells had less heavily silicified frustules and were twice the size of their silica-replete counterparts. Although CA_{ext} activity did not differ between

silica treatments when the difference in cell size was accounted for, overall CCM function was greater in silica cells. Since larger cells are more prone to CO_2 limitation the increase in cell size, rather than frustule silica content, likely regulates CA_{ext} activity in *C. muelleri*. Since the operation of a CCM may act as a sink for excess light energy, Chapter 3 explored the effects of silica limitation on photoprotective mechanisms and the production of harmful reactive oxygen species. Silica-limited *C. muelleri* cells were found to be more prone to photoinhibition than silica-replete cells, likely as a consequence of a downregulation of the CCM. Photoprotective mechanisms were upregulated in silica-limited cells. The upregulation of these mechanisms likely protected silica-limited cells from the production of harmful reactive oxygen species. In general, the physiological flexibility displayed by *C. muelleri* in response to C_i and silica availability likely contributes to the observed dominance of bloom-forming diatoms in coastal environments and may give them a competitive advantage under future climate scenarios.

DECLARATION

I certify that this thesis does not incorporate without acknowledgment any material previously submitted for a degree or diploma in any university; and that to the best of my knowledge and belief it does not contain any material previously published or written by another person except where due reference is made in the text.

Tamsyne J Smith-Harding

November, 2018

ACKNOWLEDGEMENTS

Like many of life's endeavours, this thesis has only come to fruition because I've had the support of many along the way. To my supervisors, Professor Jim Mitchell and Professor John Beardall, thank you for giving me the opportunity to learn. To Jim, thank you for encouraging me to explore ideas, to seek 'the story' and dessert-fuelled discussions on science and life. To John, thank you for sharing your wealth of knowledge on photosynthetic 'beasts', for being generous with your time whenever I was 'sorry to bother you', for the delicious homegrown produce and for the lemon tarts at Christmas time.

I have been fortunate enough to be a part of two 'lab families' and as such, have twice as many 'family members' to thank. To (soon to be) Dr Melissa Wartman, thank you for letting me rant when it was needed, for providing every pen and USB I used throughout my PhD (you were gifting them to me, right?) and for sharing my love of food and terrible sense of humour. To Dr Tom Lines, thank you for the discussions over coffee and for helping me to troubleshoot the oxygen electrode countless times. To (soon to be) Dr Prachi Varshney, thank you for keeping me sane during late night experiments and for the constant encouragement. To Dr Manoj Kamalanathan, thank you for your enthusiasm for science (it is so infectious!), the laughs and your friendship. To Dr Yussi Marlene Palacios Delgado, thank you for the fun and the laughs. To Shirley Davey-Prefumo, thank you for your help growing cultures and all of your encouragement. To Dr Eloise Prime, thank you for the diatom chats and for listening when I needed it (also, Nitwit, Blubber, Oddment and Tweak). To all members, past and present, of the Beardall Algal Ecophysiology Lab at Monash University and the Mitchell Microbial Systems Laboratory at Flinders University - thank you for sharing the ups and downs with me,

for the conversations, the coffees, for teaching me techniques and for the fun! Thank you also to all the friends I made in the Monash Biology department – all of the chats, work and not-work related, we had in the hallways and the tearoom made my time at Monash fun.

Thank you to Fiona Hibbert in the School of Biological Sciences for helping with all of my paperwork at Monash and for your always friendly chats when we came across each other in the hallway. Thank you also to Associate Professor Cathy Abbott in the College of Science and Engineering for signing my forms and checking in on me.

Thank you also to the Australian Research Council and Monash University for project funding and Flinders University for my postgraduare scholarship, without which I would not have been able to complete this thesis.

To Steve and Robyn Brett, thank you for employing me part-time while I finished writing up and for your patience when it took longer than we expected. To Dave Hill, thank you for your interest in my work and for your encouragement.

To my friends - Eloise, Clare, Alana, Nathan, Jayne and Gerard, thank you for your encouragement, for not talking about my thesis when I needed a break and for getting me away from the computer!

To Gayle and Ferg Burdon, thank you for inviting me into your home and letting me live with you when I first moved to Victoria. To Mom and Dad, thank you for supporting me, for sacrificing everything to move us across the world – I don't think there are enough words to express my appreciation for all you have done. To my little, big brother Wayde, thank you for

always being my best friend. To Justin, thank you for making the move with me, for going through the journey with me, for celebrating the successes and making me laugh when I thought I couldn't do it. To Blade, Patch, Filch and friends, thank you for all the fun and cuddles.

"An understanding of the natural world and what's in it is a source of not only a great curiosity but great fulfillment."

David Attenborough

"Let us step into the night and pursue that flighty temptress, adventure."

Albus Dumbledore

LIST OF TABLES

Chapter 4

LIST OF FIGURES

Chapter 3

Chapter 4

ABBREVIATIONS

α	Relative light harvesting efficiency
μ	Specific growth rate
AZ	Acetazolamide
C	Carbon
CA_{ext}	External carbonic anhydrase
CCM	Carbon dioxide concentrating mechanism
C_i	Inorganic carbon
CO_2	Carbon dioxide
CO_3^{2-}	Carbonate
DBL	Diffusive boundary layer
DD	Diadinoxanthin
DT	Diatoxanthin
ESAW	Enriched seawater artificial water
F_v/F_m	Maximum quantum yield of PSII
F_m	Maximal fluorescence
F_o	Minimal fluorescence
HCO_3^-	Bicarbonate

I_k	Light saturation parameter
$K_{0.5}CO_2$	Half-saturation constant of photosynthesis for CO_2
$K_{0.5}C_i$	Half-saturation constant of photosynthesis for C_i
$K_{0.5}HCO_3^-$	Half-saturation constant of photosynthesis for HCO_3^-
N	Nitrogen
N_2	Nitrogen gas
NPQ	Non-photochemical quenching
O_2	Oxygen
PAM	Pulse-amplitude-modulation fluorometry
PFD	Photon flux density
PSII	Photosystem II
rETR	Relative electron transport rate
$rETR_{max}$	Maximum relative electron transport rate
ROS	Reactive oxygen species
RUBISCO	Ribulose-1,5-bisphosphate carboxylase/oxygenase
V_{max}	Maximum rate of CO_2-saturated photosynthesis

Chapter 1: General Introduction

1.1 GLOBAL IMPORTANCE OF PHYTOPLANKTON PHOTOSYTHESIS

Phytoplankton are unicellular photoautotrophs that may exist as single cells, or in chains or colonies. They are found in all aquatic environments where the prevailing physico-chemical properties, such as light, nutrient availability, temperature, pH and alkalinity, support their growth (Armbrust 2009) and are fundamental contributors to global carbon cycling. Despite accounting for a mere 0.2% of Earth's total photoautotrophic biomass (Field et al. 1998) they are responsible for an estimated 40% of total global primary productivity (Falkowski 1994). Over geological timescales oxygen production by early unicellular marine photoautotrophs oxygenated the Earth's atmosphere, giving rise to the evolution of aerobes (Falkowski et al. 1998, Sánchez-Baracaldo 2015). Phytoplankton-derived organic carbon is either consumed by other organisms or, in marine systems, exported to the deep ocean (Azam 1998).

Phytoplankton cells, grazed upon by herbivorous zooplankton, form the basis of coastal and open ocean food webs (Armbrust 2009). Furthermore, it is estimated that 10-50% of carbon fixed by phytoplankton in the marine environment is consumed by bacteria (Azam et al. 1983). Dissolved and/or particulate organic matter exuded by phytoplankton cells is an important component of microbial food webs in the ocean (Fuhrman 1999). In particular, the dissolved organic matter released by dying phytoplankton cells provides an important energy source for marine bacteria and heterotrophic flagellates (Alldredge et al. 1993, Giordano et al. 1994, Fuhrman 1999). A significant cause of phytoplankton mortality, viral lysis results in the bursting of cells and release of dissolved organic matter (Fuhrman 1999). In addition, living phytoplankton cells are known to release dissolved and particulate organic matter that supports the growth of bacterial population (Alldredge et al. 1993, Giordano et al. 1994). A large proportion of the organic matter released by phytoplankton cells is consumed by bacteria

(Fuhrman 1999). These bacteria are predated upon by heterotrophic flagellates, thereby returning some of the phytoplankton-derived organic carbon to the food web via the 'microbial loop' (Azam et al. 1983). For this reason, the carbon fixed by phytoplankton plays an important role in driving marine food webs (Falkowski et al. 2000, Armbrust et al. 2004).

The organic carbon that is not consumed in the photic zone is exported to the ocean interior by the sinking of aggregated dead cells and organic matter in the form of marine snow, where it is either consumed by deep-sea organisms or sequestered for centuries to millennia (Bowler et al. 2010). Approximately 1-3% of organic carbon produced annually by phytoplankton is exported to the deep sea, with greater export in the polar regions (De La Rocha and Passow 2007). This flux of organic carbon to the deep ocean, known as the 'biological carbon pump', is estimated to have reduced atmospheric CO_2 concentrations by 150-220 ppm (Falkowski et al. 2000),and thus playing an important role in regulating global climate over geological timescales(Falkowski et al. 1998, Falkowski et al. 2000, Fung et al. 2005). As a consequence, phytoplankton haveevolved physiological strategies to respond to fluctuations in CO_2 concentrations.

1.2 THE ENZYMATICS OF CARBON LIMITATION IN PHYTOPLANKTON

Inorganic carbon (C_i) is plentiful in the marine environment and is generally not thought to be limiting to phytoplankton photosynthesis (Reinfelder 2011). Rather, it is typically an insufficient supply of light, nitrogen and/or phosphorus that constrains primary production in phytoplankton communities (Raven 1994). Additionally, in some areas of the oceans low concentrations of trace metals may limit phytoplankton photosynthesis. In particular, severe

limitation of photosynthesis is associated with iron limitation in large areas of the equatorial Pacific, north-east subarctic Pacific and Southern Oceans (Martin and Fitzwater 1988, Kolber et al. 1994, Behrenfeld et al. 1996, Watson et al. 2000). However, whilst the concentration of C_i itself is not usually limiting, a range of abiotic and biotic factors have the potential to cause photosynthetic carbon limitation in marine phytoplankton.

In the oceans C_i is found as bicarbonate (HCO_3^-), carbonate (CO_3^{2-}) and carbon dioxide (CO_2) (Zeebe and Wolf-Gladrow 2001). At the alkaline pH (8-8.3) found in the oceans, the C_i pool is predominantly comprised of the ionic forms, with 90% present as HCO_3^-, over 9% as CO_3^{2-} and less than 1% as CO_2 (Figure 1.1) (Raven 1994, Riebesell 2000). This relatively low concentration of CO_2, the sole substrate for the carbon fixing enzyme ribulose-1,5-bisphosphate carboxylase/oxygenase (RUBISCO), has the potential to result in carbon limitation for phytoplankton photosynthesis. RUBISCO is the central enzyme involved in photosynthetic carbon fixation. During photosynthesis CO_2 is transported, actively or by diffusion, to the active site of RUBISCO where it is converted to organic carbon. In marine environments CO_2 is present at 12-15 μM (Beardall and Giordano 2002). In contrast to the low concentration of CO_2 in marine environments, microalgal RUBISCOs show a poor affinity for CO_2 with half-saturation constants ($K_{0.5}$) of 14.5-186 μM (Beardall and Giordano 2002, Heureux et al. 2017). As a consequence, in the absence of a means for concentrating CO_2 at the active site, all microalgal RUBISCOs are sub-saturated at present day CO_2 levels.
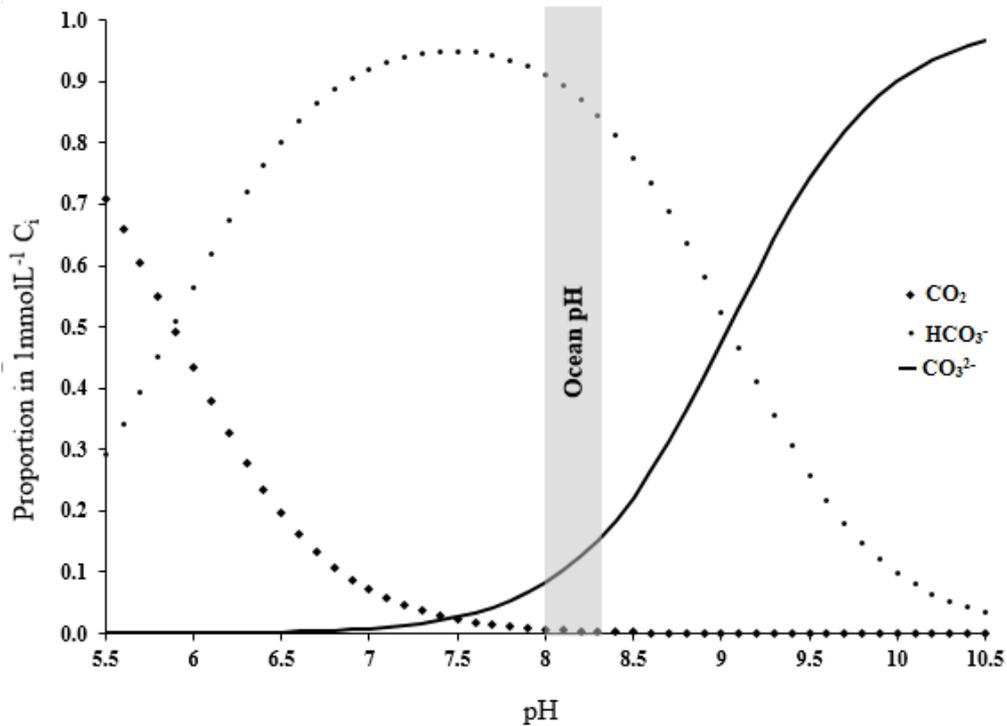
Figure 1.1. The proportion of the forms of C_i found in marine systems as a function of pH (at 20°C and a salinity of 35‰). At the alkaline pH of the oceans (8-8.3) the C_i pool is comprised of ~90% HCO_3^-, ~9% CO_3^{2-} and less than 1% CO_2. Redrawn from Beer et al. (2014).

Despite its abundance HCO_3^- does not readily diffuse across cellular membranes (Young et al. 2001). In addition, the uncatalysed conversion of HCO_3^- to CO_2 at the pH range of the ocean is relatively slow (Zeebe and Wolf-Gladrow 2001). Conversely, while CO_2 can diffuse across cellular membranes more readily than HCO_3^- (Wolf-Gladrow and Riebesell 1997, Young et al. 2001), its supply at the cell surface is restricted by its diffusion kinetics in water (Wolf-Gladrow and Riebesell 1997, Reinfelder 2011). The diffusion of CO_2 in water is approximately 10^4 times slower than in air (Granum et al. 2005). In addition, the movement of CO_2 is slow in the area directly surrounding the cell, known as the diffusive boundary layer (Granum et al. 2005). Uptake of CO_2 at the cell surface may result in depletion of CO_2 in the diffusive boundary layer, creating a concentration gradient relative to the surrounding medium (Riebesell et al. 1993,

Shen and Hopkinson 2015). Since the diffusive boundary layer is unstirred, the molecular diffusion of CO_2 to the surface of the cell is slow. Consequently, the diffusion kinetics of CO_2 in seawater mean that carbon acquisition by passive CO_2 diffusion alone is usually insufficient to meet the needs of RUBISCO (Raven 1994, Granum et al. 2005). The diffusion problem is exacerbated by the fact that RUBISCO is a bifunctional enzyme that is able to fix CO_2, in carbon fixation and O_2 in photorespiration. CO_2 and O_2 compete for binding at the active site of RUBISCO. The chemical species bound by RUBISCO is regulated by the $CO_2:O_2$ present at the active site, with a higher ratio favouring carbon fixation. Conversely, a low $CO_2:O_2$ favours photorespiration and can inhibit carbon fixation (Lorimer 1981). The process of photorespiration involves the uptake of O_2 and eventual loss of fixed carbon, making the process wasteful in terms of net carbon gain (Reinfelder 2011).

The inefficient nature of RUBISCO is attributed to its evolution in a non-photorespiratory atmosphere, where CO_2 concentrations were much higher and O_2 concentrations lower than present day (Moroney and Somanchi 1999, Hetherington and Raven 2005). Under such conditions, RUBISCO was likely to have been CO_2 saturated (Hetherington and Raven 2005). As a consequence oxygenase activity was likely to have been repressed, with high CO_2 concentrations at the active site of RUBISCO favouring carboxylase activity (Hetherington and Raven 2005). However, under present day conditions, where CO_2 in the marine environment is sub-saturating for RUBISCO, there is the potential for oxygenase activity to outcompete carboxylation. To compensate for the low concentration of CO_2 in the marine environment and the inefficient nature of RUBISCO under present day atmospheric conditions many microalgae have evolved carbon dioxide concentrating mechanisms (CCMs) (Giordano et al. 2005, Reinfelder 2011, Raven et al. 2017) to elevate the concentration of CO_2 at the active site of RUBISCO, promoting photosynthetic carboxylation over photorespiration (Raven et al. 2008).

1.3 CARBON DIOXIDE CONCENTRATING MECHANISMS (CCMs) IN MARINE MICROALGAE

In marine environments, most CCMs enable organisms to utilise HCO_3^- for photosynthesis. In phytoplankton, HCO_3^- in the environment is made accessible for photosynthesis by one of two processes; the active uptake of HCO_3^- by transporters across the plasmalemma and/or the catalysis of HCO_3^- dehydration to CO_2 by an external carbonic anhydrase (CA_{ext}) enzyme, followed by active transport at some other membrane (Young et al. 2001, Giordano et al. 2005). This thesis investigates the use of CA_{ext} in the indirect utilization of HCO_3^-.

1.3.1 Indirect Uptake of HCO_3^-: External Carbonic Anhydrase (CA_{ext})

Ubiquitous in living organisms, carbonic anhydrase (CA) is a zinc metalloenzyme that catalyses the reversible conversion of HCO_3^- and CO_2:

$$CO_2 + H_2O \leftrightarrow HCO_3^- + H^+ \quad (1.1)$$
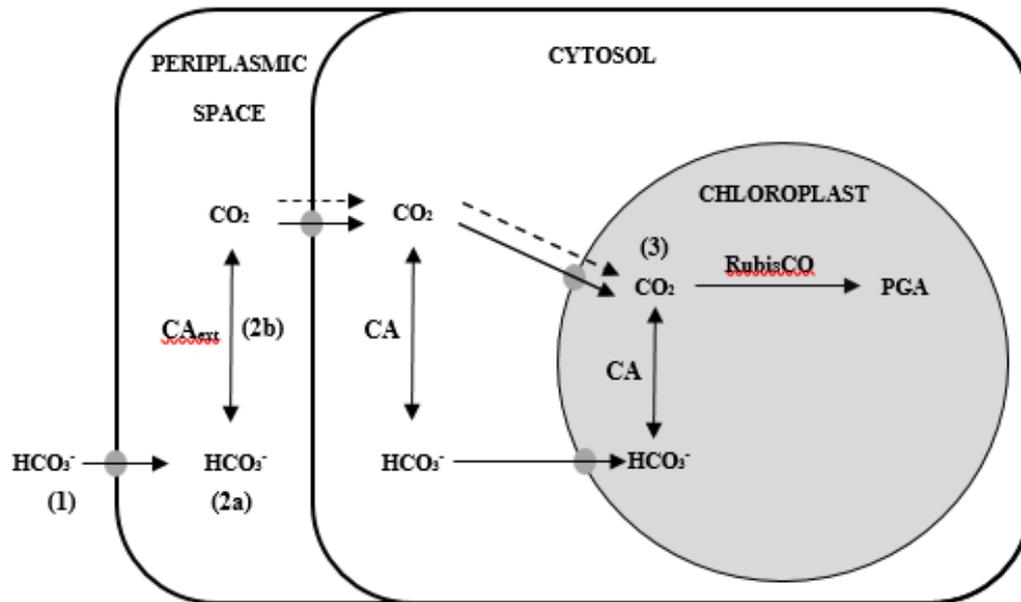
Figure 1.2. The processes by which HCO_3^- in the marine environment may be made accessible for photosynthesis in phytoplankton. (1) HCO_3^- is taken up by active transport (⬤→) across the plasmalemma. (2) (a) HCO_3^- may be actively transported across internal membranes and converted to CO_2 by an intracellular (cytosolic or chloroplastic) carbonic anhydrase (CA); and/or (b) HCO_3^- may be converted to CO_2 via dehydration by external carbonic anhydrase (CA_{ext}) in the periplasmic space. (3) The CO_2 derived by these processes is then transported, actively or passively (⋯▶), to the active site of RUBISCO. Redrawn from Badger and Price (1994) and Giordano et al. (2005).

In some aquatic photoautotrophs, including phytoplankton, external carbonic anhydrase (CA_{ext}), located in the periplasmic space or embedded in the plasma membrane (Nimer et al. 1997), catalyses the dehydration of HCO_3^- to CO_2. This reaction acts to improve the supply of CO_2 available for uptake at the cell surface (Nimer et al. 1997, Elzenga et al. 2000, Reinfelder 2011). CA_{ext} use as a means for increasing the supply rate of CO_2 by dehydration of HCO_3^- at the cell surface has been identified in a wide variety of freshwater and marine algal taxa

including the chlorophytes (Elzenga et al. 2000, Young et al. 2001), prymnesiophytes (Elzenga et al. 2000), dinoflagellates (Berman-Frank et al. 1994, Berman-Frank et al. 1995) and diatoms (Morel et al. 2002, Martin and Tortell 2008), in laboratory cultures and natural populations (Berman-Frank et al. 1994, Berman-Frank et al. 1995, Martin and Tortell 2006).

The expression of CA_{ext} is typically modulated by the concentration of CO_2 in the external growth medium, although in some cases expression may be constitutive (Rost et al. 2003, Moroney et al. 2011). In addition to the direct impact of CO_2 concentration on CA_{ext} expression and activity, a range of environmental parameters, such as light, temperature and pH have the potential to regulate CCM activity (Beardall et al. 1998, Beardall and Giordano 2002). When cells are grown under high CO_2 conditions CA_{ext} activity is often partially, or in some cases fully, repressed (Williams and Colman 1993, Lane and Morel 2000). In the marine diatom *Thalassiosira weissflogii*, the expression of CA_{ext} was immediately reduced upon the transfer of cells from 100 µatm CO_2 to 750 µatm CO_2 growth medium, with a 10-fold decline in the amount of protein expressed observed after 24 hours (Lane and Morel 2000). In some species, CA_{ext} activity may be suppressed upon exposure to high CO_2 conditions. For example, CA_{ext} activity was decreased by 98% in the freshwater green alga *Chlorella saccharophila* cells grow in 2% CO_2 medium compared to those grown at air-equilibrium levels of CO_2 (Williams and Colman 1993). Conversely, when *T. weissflogii* cells are transferred from 750 µatm to 100 µatm CO_2 the expression of the CA_{ext} protein increases after 5 hours, with a corresponding increase in CA_{ext} activity (Lane and Morel 2000). Similarly, in the freshwater green alga *Chlamydomonas reinhardtii* CA_{ext} activity was induced by transfer to low CO_2 (0.035%; 350 µatm) conditions, with a 10-fold increase approximately 6 hours after exposure (Bozzo and Colman 2000). Whilst CA_{ext} activity is typically induced by growth under low CO_2 conditions, variation in the occurrence and extent of this induction has been shown to vary between species.

In a study by Rost et al. (2003) the CA_{ext} activity observed in cultures of the marine diatom *Skeletonema costatum* was 60-fold higher in cells grown at 36 ppm CO_2 (0.0036%) compared to cultures grown at 1800 ppm (0.18%), suggesting regulation of CA_{ext} activity by CO_2 concentration. However, CA_{ext} activity in the marine flagellate *Phaeocystis globosa* remained mostly constant over a range of CO_2 concentrations, decreasing only 2-fold between cells grown at 36 ppm (0.0036%) and 180 ppm (0.018%) CO_2, before remaining relatively constant up to 1800 ppm (0.18%) CO_2 (Rost et al. 2003). These results indicate that the CA_{ext} of *P. globosa* may be constitutive rather than modulated by external CO_2 concentrations. In the coccolithophorid *Emiliania huxleyi* CA_{ext} activity remained consistently low in cultures grown at 39 ppm (0.0036%), 180 ppm (0.018%), 360 ppm (0.036%) and 1800 ppm (0.18%) CO_2, indicating that CA_{ext} plays a minor role in C_i acquisition in this species (Rost et al. 2003). Inhibition of CA_{ext} resulted in a significant decrease in net photosynthesis in *S. costatum* and *P. globosa,* with decreases of 58% and 19%, respectively in cells grown at 180 ppm (0.018%), indicating CA_{ext} may play an important role in carbon acquisition for photosynthesis in the species (Rost et al. 2003). Conversely, no difference in net photosynthesis was observed in *E. huxleyi* when CA_{ext} was inhibited, suggesting CA_{ext} does not play a significant role in carbon acquisition this species (Rost et al. 2003). These results suggest that CA_{ext} is an important component of many, but not all, microalgal CCMs, acting to improve the supply of CO_2 at the cell surface when external concentrations are low.

1.3.2 Differences in the Need for CCMs Amongst Phytoplankton

Phototrophs differ in their need for a CCM, depending on the efficiency of C fixation by their RUBISCOs. The catalytic efficiency of C fixation is determined by RUBISCO's relative selectivity factor (S_{rel}), defined as:

$$S_{rel} = K_{0.5}O_2 \, V_mCO_2/K_{0.5}CO_2V_mO_2 \; \textit{(1.2)}$$

where $K_{0.5}$ and V_m represent the half-saturation constants and substrate-saturated rates of catalysis for carboxylase and oxygenase activity, respectively (Tortell 2000, Beardall and Giordano 2002). S_{rel} gives an indication of the ability of an organism's RUBISCO to discriminate between CO_2 and O_2 and, thus, its ability to favour carboxylase over oxygenase activity (Tortell 2000, Beardall and Giordano 2002). Higher S_{rel} values indicate a greater selectivity for CO_2 and thus an enhanced ability to perform carboxylation over oxygenase activity (Tortell 2000). As a consequence, organisms with high S_{rel} values are expected to have less of a necessity for carbon acquisition using CCMs. There is good support for this assumption as species with low S_{rel} values, such as cyanobacteria, are found to have higher measures of apparent CCM activity (Tortell 2000). In fact, cyanobacterial CCMs are particularly active, increasing the CO_2 concentration at the active site of RUBISCO up to 1000-fold (Badger and Price 2003). Conversely, phytoplankton with higher S_{rel} values, show lower apparent CCM activity (Tortell 2000). Whilst diatoms generally have higher S_{rel} values, and lower apparent CCM activity, than cyanobacteria (Tortell 2000), a two-fold variation in S_{rel} was measured in 11 diatom species (Young et al. 2016). This variation in S_{rel}, as well as similar differences in a number of kinetic properties of RUBISCO observed between the 11 diatom species, likely results in variation in CCM activity (Young et al. 2016). However, despite variation in the abilities of different taxa to concentrate C_i all phytoplankton have the potential to benefit from the use of a CCM, if light and nutrient levels are sufficient to support photosynthesis, given that no known RUBISCO is saturated at current day CO_2 levels (Raven et al. 2008). To date, all cyanobacteria and most of the eukaryotic phytoplankton studied have been found to use some form of CCM (Giordano et al. 2005).

1.4 THE DIATOMS

Diatoms, belonging to the Phylum Bacillariophyta, are the most abundant and diverse groups of eukaryotic phytoplankton in marine systems (Bowler et al. 2010). As the dominant primary producers in the marine environment, diatoms generate an estimated 25-50 % of the organic C produced in the oceans (Nelson et al. 1995, Bowler et al. 2010, Granum et al. 2005). This organic matter is rapidly consumed and fuels short-chain food webs that support commercially important coastal fisheries (Armbrust et al. 2004). In the ocean, diatoms sink rapidly to the ocean floor due to their heavy siliceous cell walls (Kooistra et al. 2003, Raven and Waite 2004). Once there, diatom organic matter may either be consumed by deep-sea organisms or sequestered into the ocean floor for hundreds to thousands of years (Armbrust 2009, Bowler et al. 2010).. Diatoms are amongst the most successful groups of phytoplankton in the modern oceans (Vardi et al. 2009). Their considerable success has been attributed by some as, at least in part, due to their silicified cell wall (Hamm et al. 2003).

1.5 THE DIATOM FRUSTULE

The characteristic feature of the diatoms is their silicified cell wall, known as the frustule (Armbrust et al. 2004). Diatoms have an absolute requirement for silicon in the formation of the frustule (Brzezinski et al. 1990). Silicification of the frustule is tightly linked to the diatom cell cycle, meaning that the growth of diatoms is highly dependent on the availability of silicon in the growth medium (Brzezinski et al. 1990, Martin-Jézéquel et al. 2000). Under silica-limited conditions the growth rate of diatoms is markedly reduced (Lewin 1955, Paasche 1973a). The frustules under these conditions are weakly silicified and poorly formed, sometimes lacking structural components (Booth and Harrison 1979).

The frustule surface is decorated with a series of nano-features, such as pores, channels, ridges, spikes and spines, which are under genetic control (Hildebrand 2008, Armbrust 2009). These features are species-specific, although some intraspecific heterogeneity has been observed (Hale and Mitchell 2001, Hildebrand 2008). The frustule and its nano-features may play roles in anti-predator defence (Hamm et al. 2003), nutrient uptake (Hale and Mitchell 2001, Mitchell et al. 2013), buoyancy control (Raven and Waite 2004) and protection against UV radiation (Ingalls et al. 2010). Additionally, frustules show morphological flexibility under fluctuating environmental conditions, including salinity, affording diatoms the ability to acclimate to changing environments (Leterme et al. 2010, Leterme et al. 2013). Besides investigations into the potential roles of the frustule in nutrient uptake and buoyancy, there has been a paucity of research into the physiological role of the diatom frustule (Milligan and Morel 2002).

1.6 A PHYSIOLOGICAL ROLE FOR THE FRUSTULE: A BUFFER FOR CAext?

The rate of the CA_{ext} reaction is limited by the proton-transfer step (step 2; Figure 1.2), which is particularly slow in water (Silverman and Lindskog 1988, Milligan and Morel 2002). As a consequence, a pH buffer is required to enhance catalytic rates. In the marine environment, bicarbonate, borate and silicate have the potential to act as buffers for biological reactions (Silverman and Lindskog 1988, Pocker 2000). However, the concentration of HCO_3^- in the marine environment is insufficient for expression of full CA_{ext} activity (Milligan and Morel 2002). Additionally, the chemical properties of boric and silicic acid, namely that both are only weak acids, make both likely to be ineffective buffers for the CA_{ext} reaction (Milligan and Morel 2002).

With these considerations in mind Milligan and Morel (2002) proposed that the polymerised silica in the frustule, being more acidic than silicic acid and available in close proximity to the diatom CA_{ext}, could act as a potential buffer for HCO_3^- dehydration by CA_{ext} (Figure 1.3). To test this hypothesis the CA_{ext} buffering capacity of the silica in the frustule in both cleaned frustules and live *Thalassiosira weissflogii* was tested. It was found that the addition of HEPES buffer to a suspension of live cells did not enhance CA activity relative to a suspension lacking HEPES buffer *T. weissflogii*. Conversely, CA activity decreased in the absence of HEPES buffer in experiments using bovine CA or *Chlamydomonas* spp. cells, which have a glycoprotein cell wall. In addition, whilst bovine CA activity was reduced in the absence of a HEPES buffer, the addition of cleaned *T. weissflogii* frustules resulted in full bovine CA activity relative to a suspension containing HEPES buffer. This suggests that *T. weissflogii* frustules as buffer the CA reaction as effectively as a phosphate buffer. However, it should be noted that differences in the buffering capacity of frustules depending on the cleaning method used were observed. Milligan and Morel (2002) attributed these differences to the presence of protonated organic matter in samples where the organic coating had been oxidised using perchlorate and heat treatment. However, it is possible that the cleaning methods used altered the pKa of the silica in the frustule (Raven, 2018, pers. comm.), and thus, the buffering capacity of the frustule. However, on the whole, Milligan and Morel's results suggest that the silica in the diatom frustule is an effective pH buffer for the CA_{ext} reaction.
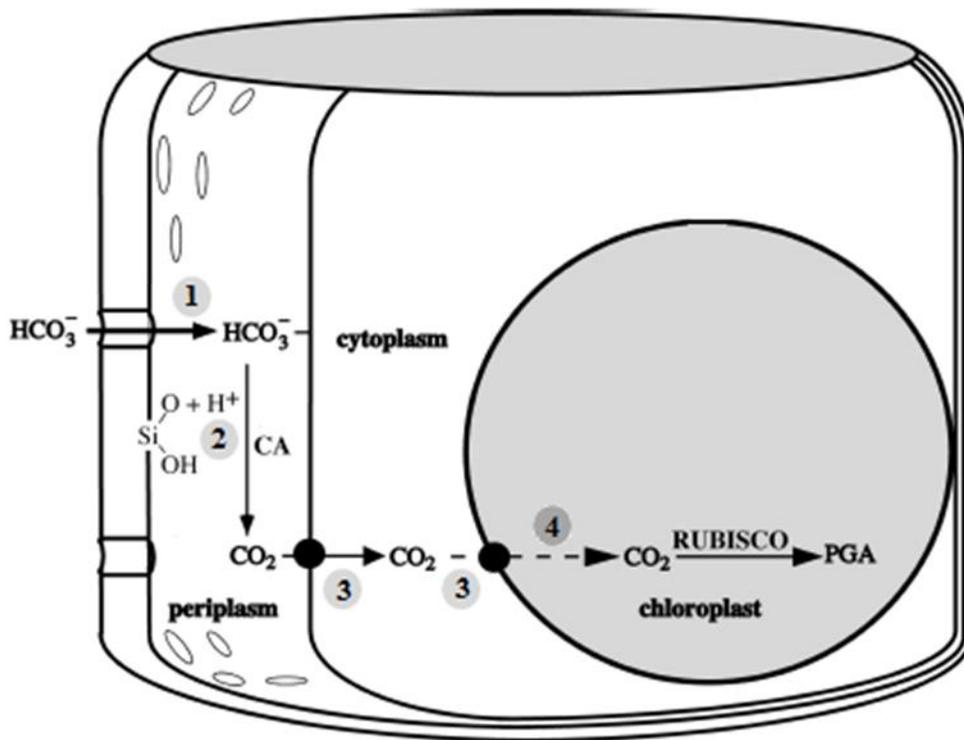
Figure 1.3. The proposed mechanism by which the silica in the diatom frustule acts as a buffer for external carbonic anhydrase (CA_{ext}). HCO_3^- in the external media is taken up by active transport across the plasmalemma (**1**). CA_{ext} in the periplasm catalyses the dehydration of HCO_3^- to CO_2, the silica in the diatom frustule acts as a buffer, increasing the rate of the proton-transfer step (**2**). CO_2 is moved within the cell by passive or active transport across membranes (**3**), potentially improving the supply of CO_2 for carbon fixation by RUBISCO (**4**). Figure modified from (Morel et al. 2002).

Further work suggested that CA_{ext} activity is influenced by frustule silica content. In particular, more heavily silicified frustules were observed in *T. weissflogii* cells grown in CO_2-limited (100 ppm) conditions (Milligan et al. 2004) and in *T. weissflogii* and *Thalassiosira pseudonana* cells grown at high pH, where the availability of CO_2 is low (Mejía et al. 2013). In both studies, the authors proposed that the observed increase in frustule silicification enhances CA_{ext} activity,

and thus, C_i acquisition under CO_2 limitation. In addition, a positive relationship between silicon availability in the growth medium, which influences the extent of frustule silicification, and CA_{ext} activity was observed in *Skeletonema costatum* (Gong and Hu 2014). Whilst these results give indirect support to the idea that CA_{ext} activity is mediated by silicon availability in diatoms, the actual impacts of the changes in silicification and CA_{ext} activity under CO_2 and silica limitation, respectively, on diatom photosynthesis, C_i acquisition and CCM function have not been explored.

1.7 THESIS OBJECTIVES AND STRUCTURE

The overall objective of this thesis is to determine the roles, if any, that the silica frustule plays in CCM function and photosynthesis in diatoms. Specifically, this thesis aims to:

(1) Establish whether CA_{ext} is a component of the CCM of the common marine diatom, *Chaetoceros muelleri* (Chapter 2) and, if so;

(2) Determine the role that CA_{ext} plays in C_i acquisition and photosynthesis in response to decreases in C_i availability with progression of population growth (Chapter 2).

(3) Investigate the impacts of silica limitation on CA_{ext} activity, photosynthesis and overall CCM function (Chapter 3).

(4) Investigate the impacts of silica limitation on photoprotective mechanisms and the production of harmful reactive oxygen species (Chapter 4).

The data chapters in this thesis have been prepared as manuscripts for publication. As such, there are redundancies in the 'Introduction' and 'Materials and Methods' sections. Chapter 2 was published in the December 2017 issue of *Journal of Phycology*. Chapter 3 will be submitted to *New Phytologist*, whilst Chapter 4 will be submitted to *Journal of Phycology*. A single reference list with all cited literature is included at the end of the thesis.

Chapter 2: The Role of External Carbonic Anhydrase in Photosynthesis During Growth of the Marine Diatom *Chaetoceros muelleri*

2.1 ABSTRACT

Carbon dioxide concentrating mechanisms (CCMs) act to improve the supply of CO_2 at the active site of ribulose-1,5-bisphosphate carboxylase/oxygenase (RUBISCO). There is substantial evidence that in some microalgal species CCMs involve an external carbonic anhydrase (CA_{ext}) and that CA_{ext} activity is induced by low CO_2 concentrations in the growth medium. However, much of this work has been conducted on cells acclimated to air-equilibrium concentrations of CO_2, rather than to changing CO_2 conditions that may occur during microalgal blooms. We investigated the role of CA_{ext} in inorganic carbon (C_i) acquisition and photosynthesis at three sampling points, one in late exponential phase and two in the subsequent linear growth phase, in the cosmopolitan marine diatom *Chaetoceros muelleri*. We observed that CA_{ext} activity increased with decreasing C_i, particularly CO_2, concentration, supporting the idea that CA_{ext} is modulated by external CO_2 concentration. Additionally, we found that the contribution of CA_{ext} activity to carbon acquisition for photosynthesis varies over time, increasing between the first and second sampling points before decreasing at the last sampling point, where external pH was high. Lastly, decreases in maximum quantum yield of photosystem II (F_v/F_m), chlorophyll, maximum relative electron transport rate ($rETR_{max}$), relative light harvesting efficiency (α) and maximum rates of CO_2-saturated photosynthesis (V_{max}) were observed over time. Despite this decrease in photosynthetic capacity an upregulation of CCM activity, indicated by a decreasing half-saturation constant of photosynthesis for CO_2 ($K_{0.5}CO_2$), occurred over time. The flexibility of the CCM during the course of growth in *C. muelleri* may contribute to the reported dominance and persistence of this species in phytoplankton blooms.

2.2 INTRODUCTION

With an estimated 200,000 species, diatoms are amongst the most abundant and diverse groups of eukaryotic phytoplankton (Mann and Droop 1996). They are widely distributed in the oceans, occurring wherever there are sufficient light and nutrients to support their growth (Armbrust 2009, Bowler et al. 2010). More specifically, diatoms dominate well-mixed coastal and upwelling regions and are the most abundant photoautotrophs along the sea-ice edge of polar ecosystems (Bowler et al. 2010). Diatoms produce between 25-50% of the estimated 50 billion tonnes of organic carbon (C) generated in the oceans annually (Falkowski 1994, Granum et al. 2005, Bowler et al. 2010), thus playing an important role in global carbon cycling.

Inorganic carbon (C_i), plentiful in the photic zone, is not traditionally thought to be limiting to phytoplankton growth in the marine environment (Reinfelder 2011), although there is some evidence to the contrary (Riebesell et al. 1993, Riebesell et al. 2007). Despite this plentiful supply, surface depletion of C_i is often observed during intense phytoplankton blooms (Codispoti et al. 1982, Riebesell et al. 1993). Additionally, other abiotic and biotic factors can contribute to C_i limitation in phytoplankton. In aquatic systems the C_i pool is present as bicarbonate (HCO_3^-), carbonate (CO_3^{2-}) and carbon dioxide (CO_2) (Reinfelder 2011). At the alkaline pH of seawater (8-8.3), C_i occurs predominantly in the ionic forms, with 90% present as HCO_3^-, > 9% as CO_3^{2-} and <1% present as CO_2, the substrate for the carbon-fixing enzyme ribulose-1,5-bisphosphate carboxylase/oxygenase (RUBISCO) (Raven 1994, Riebesell 2000). RUBISCO has a low affinity for CO_2 and, at the relatively low CO_2 concentrations found in the marine environment, the enzyme is sub-saturated (Giordano et al. 2005). In addition, the process of photorespiration involves O_2 competing with CO_2 for binding at the active site of RUBISCO (Giordano et al. 2005). Consequently, at low CO_2 concentrations, photorespiration,

the outcome of which is a net carbon loss, may outcompete photosynthetic carbon fixation (Reinfelder 2011). The supply of CO_2 for photosynthesis is further impeded by its slow diffusion in water, which is 10^4 times slower than in air (Raven 1994, Granum et al. 2005). Diffusion is particularly slow in the area directly surrounding the cell (i.e. the diffusive boundary layer; DBL) (Granum et al. 2005) where CO_2 is depleted as consequence of cellular uptake. Since the DBL is unstirred, molecular diffusion through this area to the cell surface is slow.

To overcome the constraints associated with CO_2 accumulation, most aquatic photoautotrophs have evolved mechanisms to concentrate CO_2 at the active site of RUBISCO, collectively known as carbon dioxide concentrating mechanisms (CCMs) (Giordano et al. 2005, Reinfelder 2011). In phytoplankton, most CCMs facilitate the use of HCO_3^- in photosynthesis via two processes; namely, active uptake of HCO_3^- by anion exchange and/or HCO_3^- dehydration at the cell surface by external carbonic anhydrase (CA_{ext}) followed by active transport at some other membrane (Giordano et al. 2005). CA_{ext} speeds up the dehydration of HCO_3^- to CO_2, which is slow in seawater, improving the available supply for diffusive transport across the plasmalemma (Young et al. 2001, Giordano et al. 2005).

There is considerable evidence for direct uptake of HCO_3^- in some diatoms. Specifically, observations of HCO_3^- use (Burkhardt et al. 2001), photosynthetic rates exceeding those possible by CO_2 supply from the medium in the absence of CA_{ext} (Matsuda et al. 2001) and decreased photosynthesis when HCO_3^- uptake is inhibited (Dixon and Merrett 1988) in diatoms provide support for direct HCO_3^- uptake. Furthermore, genomic analyses have identified up to ten putative HCO_3^- transporter genes in *Phaeodactylum tricorntum* (Kroth et al. 2008,

Nakajima et al. 2013) and one such gene in *Thalassiosira pseudonana* (Kroth et al. 2008). In particular, ten genes that are homologous to the mammalian SL4 HCO_3^- transporter family were identified in *P. tricornutum* (Nakajima et al. 2013). Three of these genes, PtSLC4-2, PtSLC4-1, and PtSLC4-4, were transcribed only under low CO_2 (0.039%) conditions (Nakajima et al. 2013, Matsuda et al. 2017, Tsuji et al. 2017b). Additional work on PtSLC4-2 found that expression enhanced C_i uptake and photosynthesis, suggesting an important role in the CCM of *P. tricornutum* (Nakajima et al. 2013). In addition, orthologs of the SL4 genes found in *P. tricornutum* were also identified in *T. pseudonana*, suggesting a role for HCO_3^- transporters in the CCM of this species (Nakajima et al. 2013, Tsuji et al. 2017b).

Similarly, physiological and molecular lines of evidence support a role for CA_{ext} in diatom CCMs. CA_{ext} activity has been detected in numerous diatom species, although inter- (Colman and Rotatore 1995, Burkhardt et al. 2001) and intra-specific (John-McKay and Colman 1997, Szabo and Colman 2007) variation exists. When present, CA_{ext} is induced by exogenous C_i, and more specifically CO_2, concentrations, suggesting a role in C_i acquisition. Specifically, CA_{ext} activity increases with decreasing CO_2 (Burkhardt et al. 2001, Hopkinson et al. 2013) and, like in the green alga *Chlamydomonas reinhardtii* (Bozzo and Colman 2000), can be induced less than 20 hours after cells are transferred to low CO_2 (generally 0.01-0.05%) medium (Clement et al. 2016). Conversely, CA_{ext} activity is partially, or sometimes fully, repressed when cells are grown in high CO_2 (2-5%) medium (John-McKay and Colman 1997, Szabo and Colman 2007, Clement et al. 2016). Analyses of the *T. pseudonana* genome identified 13 putative CA genes (Tachibana et al. 2011, Samukawa et al. 2014). Two of these CAs, Tpd-CA1 and Tpz-CA1, were localised to the cell periphery, indicating that they are external CAs (Tachibana et al. 2011, Samukawa et al. 2014). Expression of these genes was

greatly enhanced in cells grown at low CO_2, suggesting a role for these genes in C_i acquisition. In contrast, none of the 10 putative CA genes identified in *P. tricornutum* were found to be external CAs (Tachibana et al. 2011). Together with evidence for plasma-membrane bound HCO_3^- transporters in this species (Nakajima et al. 2013), these results suggest direct uptake of HCO_3^- in this species.

However, in most instances observations on the relationship between CA_{ext} activity or expression and CO_2 concentration are made in relatively dense cultures grown under air-equilibrium CO_2 conditions. Research into the response of CA_{ext} activity to C_i depletion over the course of population growth, as observed during phytoplankton blooms, is scarce. Whilst Mukerji et al. (1978) observed a switch from CO_2 to HCO_3^- use over time in batch cultures of the chlorophyte *Dunaliella tertiolecta,* CA_{ext} activity was not measured, making it difficult to ascertain whether this change was due to induction of CA_{ext}-mediated HCO_3^- use. However, Berman-Frank et al. (1994) measured CA_{ext} activity in response to C_i concentration over the duration of a bloom of the dinoflagellate *Peridinium gatunense* in Lake Kinneret, Israel. As with the described laboratory experiments, Berman-Frank et al. (1994) found that CA_{ext} activity was modulated by C_i, and more specifically CO_2, concentrations. The highest CA_{ext} activity was recorded at the later stages of the bloom, when C_i and CO_2 decreased to 1.8 mM and <10µM, respectively. Laboratory experiments confirmed these findings (Berman-Frank et al. 1994, Berman-Frank et al. 1995), highlighting the usefulness of laboratory experiments in exploring CCMs in bloom-forming microalgae as *in situ* studies may be difficult due to uncertainty in the occurrence and timing of blooms.

Given the dominant role of bloom-formers in global primary productivity in the oceans (Rost et al. 2003), elucidating the mechanisms used by these species to acquire C_i will improve our understanding of how a relatively small number of species drive global carbon cycling. Here, we investigate the role that CA_{ext} plays in C_i acquisition and photosynthesis at different stages of growth in the cosmopolitan marine diatom *Chaetoceros muelleri* (Lemmerman). The genus *Chaetoceros* (Ehrenberg) is one of the largest and more diverse genera of planktonic diatoms in the marine environment (Rines and Theriot 2003). With cosmopolitan distribution, *Chaetoceros* species are often the most numerous in phytoplankton communities, and blooms may persist for weeks (Rines and Theriot 2003). In addition, *Chaetoceros muelleri* is an important aquaculture feed species due to its high nutritional value and ease of growth (Pacheco-Vega and Sánchez-Saavedra 2009).

2.3 MATERIALS AND METHODS

2.3.1 Growth Conditions

Chaetoceros muelleri Lemmermann (CS-176) was obtained from the Australian National Culture Collection, CSIRO, Hobart, Australia. Cultures were grown in 0.2 µm filtered (Type GTTP Polycarbonate filters, Millipore Australia) enriched seawater artificial water (ESAW) medium at pH 8.2 (Berges et al. 2001). Growth medium had no added buffers, to allow changes in the carbonate system to replicate those found during phytoplankton blooms. Cultures were maintained at $18 \pm 1°C$ under continuous light supplied at 80 µmol photons $\cdot$ m^{-2} $\cdot$ s^{-1} (Aleph 3 LP41 LED Panel; cool white light, Knoxville VIC, Australia) and stirred continuously on an orbital shaker at 110 rpm (Thermoline Scientific, NSW Australia). Cells were acclimated to experimental conditions for at least six generations before the start of experiments. For

experiments, triplicate 1L cultures at an initial density of 10^4 cells $\cdot$ mL^{-1} were prepared in 2L Nalgene Polycarbonate narrow mouthed bottles (Thermo Scientific Nalgene, USA).

2.3.2 Growth Rate

Cells were enumerated daily using an Olympus CH-2 light microscope (Japan). Ten µL aliquots of culture were fixed with Lugol's iodine and counted on an Improved Neubauer Brightline haemocytometer (Boeco, Germany). Specific growth rates (μ,day^{-1}) were calculated using the formula:

$$\mu \text{ day}^{-1} = \ln (N_2/N_1)/(T_2-T_1) \quad (2.1)$$

where N_1 and N_2 are the cell numbers at time 1 (T_1) and time 2 (T_2), respectively.

Growth curves were used to determine appropriate timing for all further measurements (Figure 2.1a). Measurements of photosynthetic and C_i acquisition parameters were made at three sampling points: the first in late exponential phase and the 2 others in the subsequent linear growth phase. In addition, we compared our CA$_{ext}$ activity data to previously unpublished data from our laboratory (Reinecke 1997) for air-bubbled cultures of the same strain of *C. muelleri* used here. In those experiments, *C. muelleri* was grown in fe/2 medium (Guillard and Ryther 1962) at 18ºC with light supplied continuously at 140 µmol photons $\cdot$ m^{-2} by fluorescent lamps (cool white light, Sylvania Grolux). Reinecke's cultures were bubbled continuously with air (measured CO_2 in cultures = 12.36 µM; 0.04%). Prior to measurements of CA$_{ext}$ activity, cells were acclimated to experimental conditions for at least 8 generations and then maintained in exponential phase by semi-continuous culture (Reinecke 1997).

2.3.3 CO_2 and HCO_3^- Concentration

Measurements of C_i concentration, pH, temperature and salinity were taken and used to calculate $[CO_2]$ and $[HCO_3^-]$ according to Weiss (1974), Dickson and Riley (1979) and Millero (2010). Analyses were made on cell-free samples prepared by filtering 28 mL of culture through a 0.4 µm syringe filter (PALL Life Sciences Acrodisc ® Supor ® Membrane). C_i was determined by measuring the amount of $CO_2(g)$ liberated from the reaction of C_i in the sample with hydrochloric acid (HCl) in an enclosed chamber. Air, which had been stripped of CO_2 by passage through soda lime granules (4-8 mesh, Ajax Finechem, NSW Australia), was bubbled into a sealed glass chamber containing 20 mL 0.1M HCl (Merck, Darmstadt Germany). Two mL of sample were injected into the chamber through a rubber septum. The air in the head space of the vessel was passed through the desiccant magnesium perchlorate $(Mg(ClO_4)_2$; Alfa Aesar, MA, USA) and analysed continuously by an Infra-Red Gas Analysis (IRGA) system (LI-840A CO_2/H_2O Gas Analyser, Licor, Nebraska USA) until the sample had been stripped of CO_2. Data were plotted by the inbuilt software (LI-840A v2.0.0) as the concentration of $CO_2(g)$ versus time. The area under the curve was used to calculate C_i concentration by comparison with a standard curve of known sodium bicarbonate $(NaHCO_3)$ concentrations. The pH and temperature (°C) of samples were measured using a sensION+ PH31 pH meter (Hach, Colorado USA). Salinity (%) was measured using a portable refractometer. The theoretical CO_2 supply rate from spontaneous HCO_3^- dehydration in the medium was calculated according to Miller and Colman (1980).

2.3.4 Photosynthetic Parameters

Photosynthetic parameters of cells at each of the three growth phases were determined using a PhytoPAM Analyser (Heinz Walz GmbH, Effeltrich, Germany). For analyses, 4 mL samples

of culture were dark adapted for 15 minutes before first being exposed to a weak light beam to determine minimal fluorescence (F_o) and then a saturating flash to determine maximal fluorescence (F_m) of cells. The difference between F_m and F_o was used to determine variable fluorescence (F_v). From these measurements the maximum quantum yield of photosystem II (F_v/F_m) was determined as:

$$F_v/F_m = (F_m-F_o)/F_m \ (2.2)$$

The effective quantum yield of PSII (ΦPSII) and relative electron transport rate (rETR) as a function of light was determined by exposing cells to photon flux densities (PFD) from 16 – 610 µmol photons $\cdot$ m^{-2} $\cdot$ s^{-1} for 30 seconds at each PFD. ΦPSII at each PFD was determined as:

$$\Phi PSII = (F_m'-F_o')/F_m' \ (2.3)$$

where F_o' and F_m' are the minimal and maximal fluorescence at each PFD.

rETR was then calculated, and plotted against PFD by the in-built PhytoWIN software (PhytoWIN v2.13), as:

$$rETR = \Phi PSII \ x \ PFD \ x \ 0.5 \ (2.4)$$

where 0.5 accounts for 50% of light energy absorbed by the cell being used by PSII. From these plots of rETR vs PFD the relative light harvesting efficiency (α), calculated as the initial slope, and maximum relative electron transport rate (rETR$_{max}$), calculated as the asymptote of the curve, were determined by the in-built software.

2.3.5 Pigment Analyses

Culture samples were harvested by centrifugation at 2,500 g for 10 minutes (Heraeus Multifuge 3ST+, Thermo Scientific, Brookfield, WI, USA). The supernatant was discarded and the pellet retained. Pellets were suspended in 5 mL of 90% ice-cold acetone and stored overnight at 4ºC for chlorophyll extraction. After extraction, samples were centrifuged at 2,500g for 10 minutes and the supernatant retained for chlorophyll measurement. The chlorophyll concentration was determined from the extinction coefficients of the supernatant at 630 and 664 nm in a Cary-50 UV-visible spectrophotometer (Varian, Inc., California USA). Chlorophyll a and c concentrations ($\mu g \cdot 10^{-6}$ cells) were calculated as using the following diatom-specific formulae (Jeffrey and Humphrey 1975):

$$\text{Chlorophyll } a \text{ (chl } a) = 11.47*E_{664} - 0.40*E_{630} \quad (2.5)$$

$$\text{Chlorophyll } c_1 + c_2 \text{ (chl } c_1 + c_2) = 24.36*E_{630} - 3.73*E_{664} \quad (2.6)$$

where E_x denotes the extinction coefficient at wavelength x.

$\text{chl} \cdot 10^{-6} \text{ cells} = [\text{chl}]*\text{volume extracted (VE)}/C_n*\text{volume filtered (VF)} \quad (2.7)$

where [chl] is the concentration of chlorophyll (a or $c_1 + c_2$), VE = 5 mL, C_n is the relevant daily cell number and VF= 20 mL.

2.3.6 CA$_{ext}$ Activity

CA$_{ext}$ activity was measured using an electrometric assay (Wilbur and Anderson 1948, Miyachi et al. 1983) adapted as described by (Young et al. 2001). Cells were harvested by centrifuging suspensions at 2,500 g for 10 minutes (Heraeus Multifuge 3ST+, Thermo Scientific, Brookfield, WI, USA), washed twice in ice-cold 50 mM Na_2HPO_4 buffer (BDH Chemicals,

Victoria Australia; pH adjusted to 8.2) and resuspended in 15 mL of ice-cold 50 mM Na_2HPO_4 buffer at a final concentration of 4 x 10^6 cells/L. CA_{ext} activity was determined as the time taken for the pH of cell-free 50mM Na_2HPO_4 (control) or 50 mM Na_2HPO_4 with cells in a sealed chamber at 4°C to drop by 1 pH unit after injection of CO_2-saturated 2.3 mL 22 g L^{-1} NaCl to an equal volume of sample. Samples were constantly stirred and cooled using a circulating water bath. The procedure was repeated at least 6 times for each sample and the average time per sample used in calculations. CA_{ext} activity, expressed as relative enzyme activity (REA) was calculated as follows:

Relative Enzyme Activity (REA) $=10$ $[(T_{control}/T_{cells}]-1)$ (*2.8*)

where $T_{control}$ and T_{cells} are the times (s) taken for a 1 pH unit drop in control and cell samples, respectively.

2.3.7 C_i Affinity– Photosynthesis vs C_i Curves

The affinity of cells for C_i was determined by measuring O_2 evolution at a range of C_i concentrations (P vs C_i) in a Clark-type O_2 electrode (Hansatech Oxygraph). Samples were harvested by centrifugation at 1,500 g for 10 minutes, washed twice in C_i-free ESAW medium and resuspended in C_i-free ESAW medium at a final density of ~ 2 x 10^7 cells $\cdot$ mL^{-1}. To prepare C_i-free ESAW medium a sample of medium was acidified to pH ~2 with 32% HCl, bubbled with nitrogen (N_2) gas for at least 90 minutes, buffered with 200 µM Tris-base (Sigma, St. Louis, Missouri, USA) and adjusted to pH 8.2 with freshly prepared saturated sodium hydroxide (NaOH). Two mL of sample were placed in the O_2-electrode chamber and measurements of O_2 evolution made at saturating light for photosynthesis (determined from Rapid Light Curves; 200 µmol photons $\cdot$ $m^{-2} \cdot$ s^{-1} at sampling point 1, 140 µmol photons $\cdot$ m^{-2}

$\cdot$ s^{-1} at sampling point 2 and 90 µmol photons $\cdot$ m^{-2} $\cdot$ s^{-1} at sampling point 3) and 18°C. Samples were left in the chamber until all residual C_i in the medium was consumed and the CO_2 compensation point was reached. Photosynthetic oxygen evolution was then measured after addition of 10 sequential C_i concentrations (4.98 µM – 2000 µM C_i). The data obtained were fitted to the Michaelis-Menten model in GraphPad Prism 6.07, from which measures of the half-saturation constant of photosynthesis for C_i ($K_{0.5}C_i$ and the maximum rate of CO_2-saturated photosynthesis (V_{max}) were determined. Assuming complete equilibrium of C_i in the O_2-electrode chamber, the half-saturation constants of photosynthesis for CO_2 ($K_{0.5}CO_2$) and HCO_3^- ($K_{0.5}$ HCO_3^-) were calculated using pH, salinity and temperature as described earlier under the sub-heading 'CO_2 and HCO_3^- concentration'.

The CO_2 drawdown capacity of cultures (µmol $\cdot$ L^{-1} $\cdot$ h^{-1}) was calculated as:

$$C_n \text{ x } V_{max} \quad (2.9)$$

where C_n is the relevant daily cell number (cells/L) and V_{max} is the CO_2-saturated photosynthetic rate (µmol O_2 $\cdot$ h^{-1} $\cdot$ 10^{-6} cells).

2.3.8 The Role of CA_{ext} in Photosynthetic O_2 Evolution - Inhibition of CA_{ext}

Samples were prepared as described for P vs C_i measurements. Once the CO_2 compensation point was reached, O_2 evolution was followed for 2 minutes after the addition of 33µM C_i (sub-saturating as determined by P vs C_i analyses). The change in O_2 evolution was then followed after the addition of 100 µM of the membrane-impermeable CA inhibitor acetazolamide (AZ; Sigma-Aldrich, St. Louis, Missouri, USA) for 2 minutes (Miyachi et al. 1983). The effect of CA_{ext} on photosynthetic O_2 evolution was expressed as the percent reduction in O_2 evolution, calculated as:

$$(\Delta O_2 \text{ evolution after AZ addition/}O_2 \text{ evolution before AZ addition}) \text{ x } 100\% \quad (2.10)$$

2.3.9 Statistical Analyses

The statistical significance of any differences observed between sampling points was determined by a one-way ANOVA followed by a *post hoc* Tukey's HSD multiple comparison test in GraphPad Prism 6.07 (GraphPad Software, La Jolla California USA). The theoretical CO_2 supply rate was compared with the CO_2 drawdown capacity of cultures at each sampling point using an unpaired two-tailed t-test. Differences were considered statistically significant if $p < 0.05$.

2.4 RESULTS

2.4.1 Daily Measurements: Growth and Carbonate Chemistry

Cell numbers increased at a specific growth rate (μ) of 0.69 day^{-1} from 1 x 10^4 cells $\cdot$ mL^{-1} at inoculation to 4 x 10^4 cells $\cdot$ mL^{-1} at day 2 (Figure 2.1a). Cultures reached a maximum growth rate of 1.73 day^{-1} by day 3 at which point cell density was 2.3 x 10^5 cells $\cdot$ mL^{-1}. Cell numbers increased further, reaching 5.4 x10^5 cells $\cdot$ mL^{-1} at day 4 ('sampling point 1'), although growth dropped to 0.85 day^{-1}. Growth slowed further to 0.24 day^{-1} at day 5 ('sampling point 2') with a 25% increase in cells numbers to 6.7 x 10^5 cells $\cdot$ mL^{-1}. The increase in culture population slowed further after sampling point 2 to 0.14 day^{-1}, with cell numbers increasing 16% to 7.7 x 10^5 cells $\cdot$ mL^{-1} by day 6 ('sampling point 3'). The pH of the growth medium increased with increasing cell number (Figure 2.1b). In general, the trend observed in the pH was similar to that observed in daily cell number (Figure 2.1b). The pH increased slowly from 8.00 at

inoculation before reaching 9.13 at sampling point 1. The pH increased further to 10.01 by sampling point 2 (Tukey's HSD, $p < 0.05$) but remained stable between sampling points 2 and 3 (Tukey's HSD, $p = 0.50$). Conversely, the concentration of CO_2 (Figure 2.1c) and HCO_3^- (Figure 2.1d) decreased with increasing cell number. HCO_3^- decreased rapidly in the first 4 days, dropping 69% from 1920 µM at inoculation to 596 µM at sampling point 1. There was a further 89% reduction in HCO_3^- concentration between sampling point 1 and 2, with the concentration reaching 68 µM before levelling off, reaching 35 µM by sampling point 3. The trend in CO_2 concentration was similar, although more pronounced, to that observed in HCO_3^- concentration. CO_2 concentration decreased rapidly with cell number, dropping 97% from 15 µM at inoculation to 0.4 µM by sampling point 1. The concentration of CO_2 continued to decrease rapidly, decreasing a further 99% to 0.005 µM before levelling off to 0.002 µM by sampling point 3.
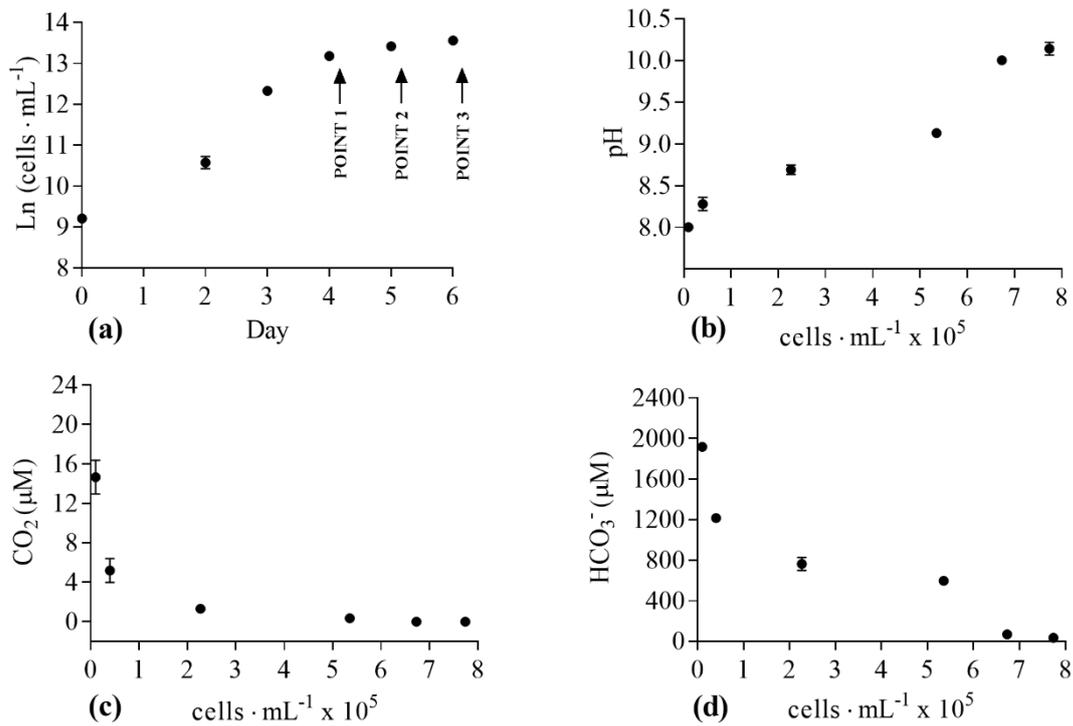
Figure 2.1. (a) Daily cell number ('points 1, 2 and 3' indicate the timing of samples for photosynthetic and C_i acquisition parameters) and changes in (b) external HCO_3^- concentration, (c) external CO_2 concentration and (d) pH with cell number. Values are means ($\pm$ standard error of the mean) of measurements from triplicate independent cultures.

2.4.2 Photosynthetic Parameters

All of the photosynthetic parameters measured followed the same general trend, with an overall decrease over time (Table 2.1). The maximum quantum yield (F_v/F_m) decreased 25% from 0.59 at sampling point 1 to 0.44 at sampling point 3 (one-way ANOVA, $F_{2,\,4} = 381.3$, $p < 0.005$). However, the decrease in F_v/F_m was markedly greater between sampling points 2 and 3 where a 23% decrease was observed (Tukey's HSD, $p < 0.05$), compared to an 11% decrease between sampling points 1 and 2 (Tukey's HSD, $p < 0.005$). There was a 16% decrease in the relative

light harvesting efficiency (α) from 0.250 at sampling point 1 to 0.211 at sampling point 3 (one-way ANOVA, $F_{2, 4} = 164.5$, $p < 0.05$). However, unlike the case of F_v/F_m, the decreases in α observed between sampling points 1 and 2 and sampling points 2 and 3 were similar with 7% (Tukey's HSD, $p < 0.05$) and 9% reductions (Tukey's HSD, $p < 0.0001$), respectively. There was a 53% decrease in total chlorophyll concentration (one-way ANOVA, $F_{2, 4} = 123.5$, $p < 0.05$) and, as with α, the decreases for each of the two time periods were similar with a decrease of approximately 31% between sampling points 1 and 2 (Tukey's HSD, $p < 0.05$) and sampling points 2 and 3 (Tukey's HSD, $p < 0.05$). Lastly, there was a 63% reduction in maximum electron transport rate ($rETR_{max}$) overall (one-way ANOVA, $F_{2,6} = 70.78$, $p < 0.0001$). $rETR_{max}$ decreased 35% from 37 at sampling point 1 to 24 at sampling point 2 (Tukey's HSD, $p < 0.005$) before decreasing a further 43% to 14 at sampling point 3 (Tukey's HSD, $p < 0.005$).

Table 2.1. The maximum quantum yield (F_v/F_m), relative light harvesting efficiency (α), total chlorophyll concentration (chlorophyll $a + c1,c2$; µg · 10^{-6} cells) and relative maximum electron transport rate ($rETR_{max}$) at three stages of growth in *Chaetoceros muelleri*. Values are means (± standard error of the mean) of triplicate measurements.

	Sampling Point		
	1	**2**	**3**
F_v/F_m	0.59 ± 0.01	0.52 ± 0.01	0.44 ± 0.01
α	0.250 ± 0.002	0.232 ± 0.003	0.211 ± 0.003
Total Chl	0.64 ± 0.02	0.44 ± 0.01	0.30 ± 0.01
$rETR_{max}$	37 ± 0.97	24 ± 2.16	14 ± 0.49

2.4.3 Affinity for C_i

The affinity of photosynthetic O_2 evolution for HCO_3^- and CO_2 increased over time, as evidenced by decreases in the half-saturation constants of photosynthesis ($K_{0.5}$) for both C_i species (Table 2.2). Overall, $K_{0.5}CO_2$ (one-way ANOVA, $F_{2,6} = 16.12$, $p < 0.005$) and $K_{0.5}HCO_3^-$ (one-way ANOVA, $F_{2,6} = 16.12$, $p < 0.005$) decreased 76% between sampling point 1 and 3. The largest decreases for $K_{0.5}CO_2$ (Tukey's HSD, $p < 0.05$) and $K_{0.5}HCO_3^-$ (Tukey's HSD, $p < 0.05$) were observed between sampling points 2 and 3, with a 69% reduction in both. Similarly, the maximum rate of CO_2 saturated photosynthesis (V_{max}) decreased over time (Table 2.2). V_{max} was at its highest of 0.081 µmol O_2 · h^{-1} · 10^{-6} cells at sampling point 1 before

decreasing 48% by sampling point 2 (Tukey's HSD, $p < 0.001$). V_{max} continued to decrease, with a further 44% reduction between sampling points 2 and 3 (Tukey's HSD, $p < 0.05$). The affinity of cells for CO_2 uptake ($V_{max}/K_{0.5}CO_2$) remained stable at all sampling points (one-way ANOVA, $F_{2,6} = 3.12$, $p = 0.11$).

Table 2.2. Half-saturation constants of photosynthesis for CO_2 and HCO_3^- ($K_{0.5}CO_2$ µM and $K_{0.5}HCO_3^-$ µM), CO_2-saturated photosynthetic rate (V_{max}; µmol $O_2 \cdot h^{-1} \cdot 10^{-6}$ cells) and affinity for CO_2 uptake ($V_{max}/K_{0.5}CO_2$) of *Chaetoceros muelleri* at each of the measured stages of growth. Values are means (± standard error of the mean) of triplicate measurements. All measurements were made at pH 8.2.

	Sampling Point		
	1	**2**	**3**
$K_{0.5}CO_2$	0.258 ± 0.013	0.203 ± 0.040	0.063 ± 0.012
$K_{0.5}HCO_3^-$	105.60 ± 5.14	83.23 ± 16.27	25.64 ± 5.05
V_{max}	0.081 ± 0.004	0.042 ± 0.004	0.024 ± 0.001
$V_{max}/K_{0.5}CO_2$	0.32 ± 0.02	0.22 ± 0.02	0.41 ± 0.09

2.4.4 CO_2 Drawdown Capacity and Theoretical CO_2 Supply

The CO_2 drawdown capacity of cultures decreased 34% from 21. 6 µmol $\cdot L^{-1} \cdot h^{-1}$ at sampling point 1 to 14.3 µmol $\cdot L^{-1} \cdot h^{-1}$ at sampling point 2 (Figure 2.2; Tukey's HSD, $p < 0.05$), before levelling off to 9.1 µmol $\cdot L^{-1} \cdot h^{-1}$ at sampling point 3 (Tukey's HSD, $p = 0.08$). There was an

initial sharp decline in the theoretical uncatalysed CO_2 supply rate from bicarbonate from 57.4 $\mu mol \cdot L^{-1} \cdot h^{-1}$ at sampling point 1, to 1 $\mu mol \cdot L^{-1} \cdot h^{-1}$ at sampling point 2 (Figure 2.2; Tukey's HSD, $p < 0.001$), before the rate levelled off to 0.41 $\mu mol \cdot L^{-1} \cdot h^{-1}$ at sampling point 3 (Tukey's HSD, $p = 0.9957$). At sampling point 1 the theoretical CO_2 supply rate was 2.7 times greater than the CO_2 drawdown capacity of cultures (Figure 2.2; unpaired t-test, $t_4 = 4.24$, $p < 0.05$). Conversely, at sampling points 2 and 3 the CO_2 drawdown capacity of cells was 14.2 times (unpaired t-test, $t_4 = 10.28$, $p < 0.001$) and 22.3 times (Figure 2.2; unpaired t-test, $t_4 = 15.26$, $p < 0.001$) greater, respectively, than the theoretical CO_2 supply rate.
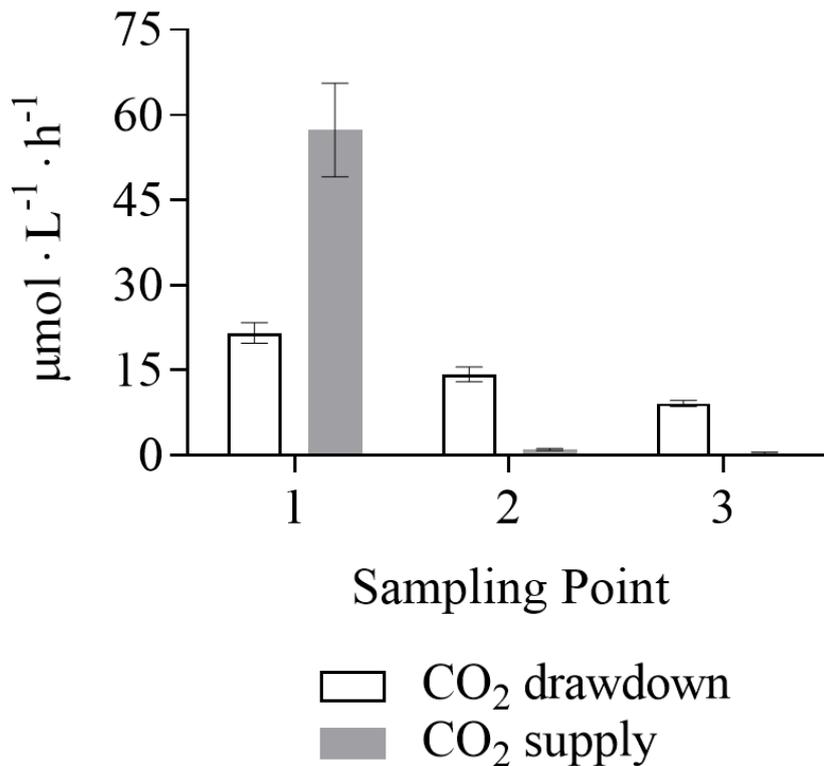
Figure 2.2. Comparisons between the CO_2 drawdown capacity of *Chaetoceros muelleri* cultures ($\mu mol \cdot L^{-1} \cdot h^{-1}$) and the theoretical CO_2 supply from spontaneous HCO_3^- dehydration in the medium at each of three measured stages of growth. Values are means ($\pm$ standard error of the mean) of measurements from triplicate independent cultures.

2.4.5 CA_{ext} Activity

CA_{ext} activity increased by a factor of 7.6 from 0.94 REA units $\cdot$ 10^{-6} cells at sampling point 1 to 7.16 REA units 10^{-6} cells at sampling point 2 (Figure 2.3; Tukey's HSD, $p < 0.001$). Activity remained stable between sampling points 2 and 3, with only a 0.14 % increase observed (Tukey's HSD, $p > 0.9999$). The trend observed in CA_{ext} activity was similar to those observed in the measured carbonate chemistry parameters. CA_{ext} activity increased with increases in pH and decreases in HCO_3^- and CO_2 concentration (Figure 2.4).

Acetazolamide (AZ), an inhibitor of CA_{ext}, reduced photosynthetic O_2 evolution to some degree at all three of the growth phases tested (Figure 2.5). Photosynthetic O_2 evolution decreased 5% at sampling point 1. AZ had a greater impact at sampling point 2 (Tukey's HSD, $p < 0.05$), inhibiting photosynthetic O_2 evolution by 21%. However, the effect seen at sampling point 3 was negligible (Tukey's HSD, $p < 0.005$), with only 0.5% reduction in photosynthetic O_2 evolution after the addition of AZ.
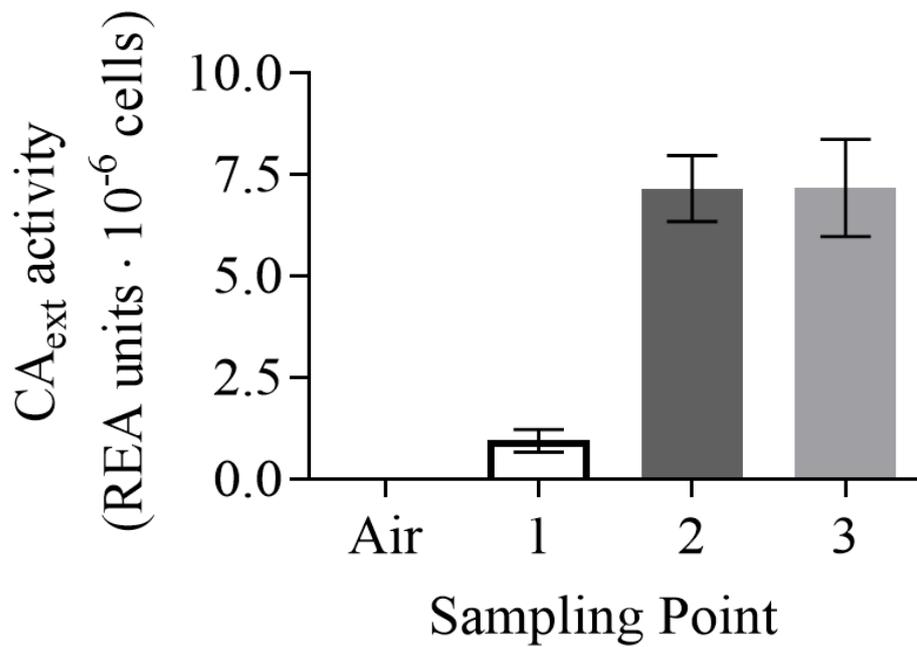
Figure 2.3. The mean CA_{ext} activity (REA units $\cdot$ 10^{-6} cells) in *Chaetoceros muelleri* at each of three measured stages of growth. Values are means ($\pm$ standard error of the mean) of measurements from triplicate independent cultures. The measurement for 'air' cultures is previously unpublished data from our laboratory for air-bubbled semi-continuous cultures of the same strain of *C. muelleri* (Reinecke 1997).
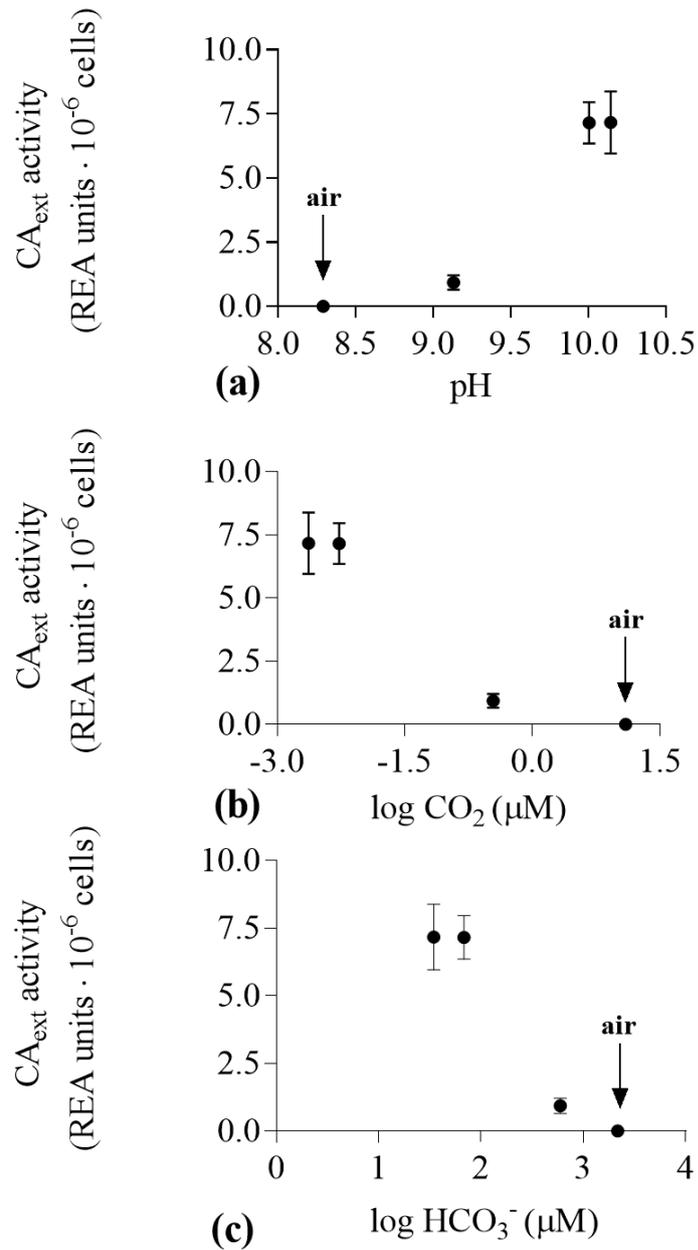
Figure 2.4. The relationship between the growth medium carbonate chemistry and CA_{ext} activity. (a) external pH (b) external CO_2 concentration (μM) and (c) external HCO_3^- concentration (μM). Values are means ($\pm$ standard error of the mean) of measurements from triplicate independent cultures. The measurements for 'air' are previously unpublished data from our laboratory for air-bubbled semi-continuous cultures of the same strain of *C. muelleri* Reinecke (1997).
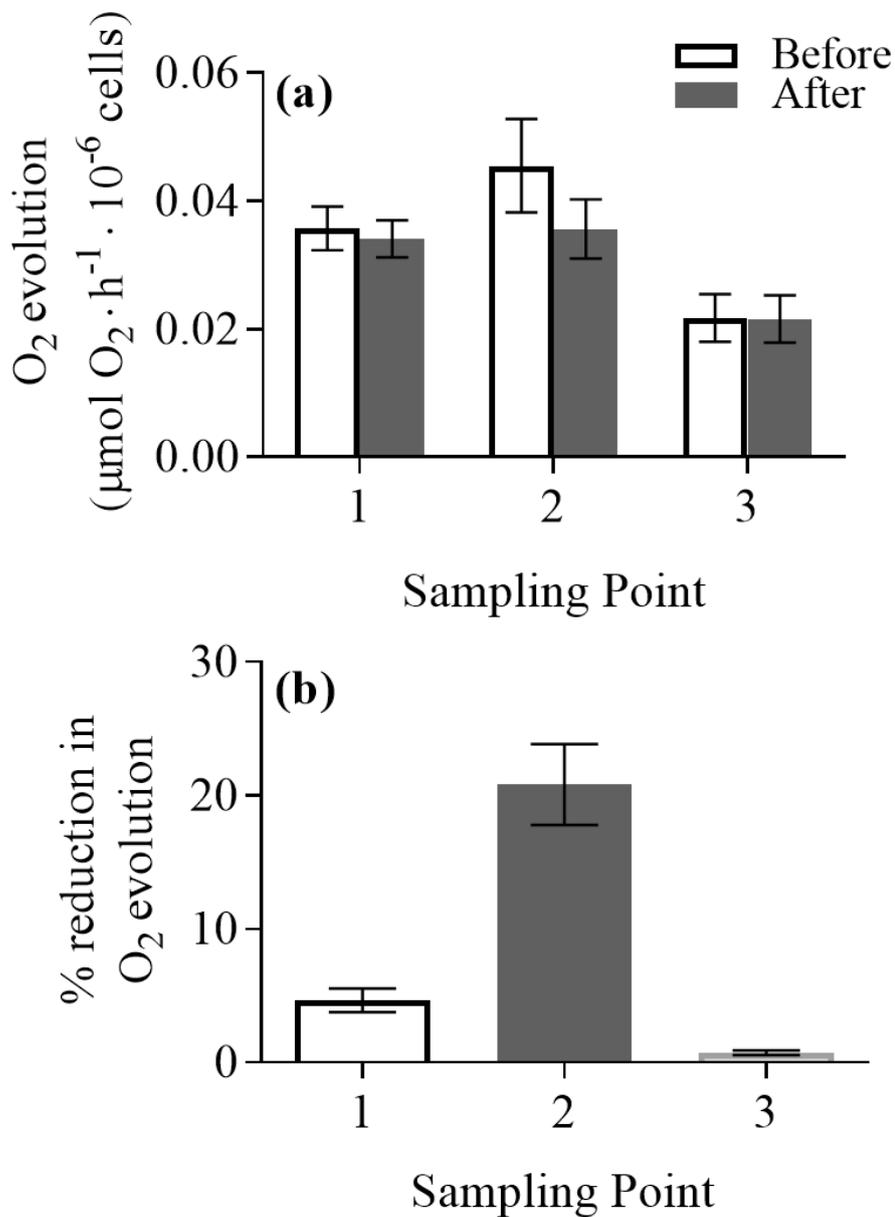
Figure 2.5. (a) The rate of photosynthetic O_2 evolution at 33 µM Ci before and after the addition of acetazolamide, an inhibitor of CA_{ext}, and (b) the mean reduction (%) in photosynthetic O_2 evolution after the addition of acetazolamide in *Chaetoceros muelleri* at each of the three measured growth phases. Values are means (±standard error of the mean) of measurements from triplicate independent cultures.

2.5 DISCUSSION

Time-series measurements of CA_{ext} activity over the course of population growth progression in phytoplankton species, for laboratory cultures or natural populations, are scarce. However, our finding that CA_{ext} activity increases with progression of the population growth as C_i decreases agrees with the available literature. In the laboratory, CA_{ext} activity was highest in the later stages of growth in a high-calcifying strain of the coccolithophorid *Emiliania huxleyi*, in the pennate diatom *P. tricornutum* and in the prymnesiophyte *Phaeocystis globosa* (Nimer et al. 1994, Iglesias-Rodriguez and Merrett 1997, Elzenga et al. 2000). In *E. huxleyi*, CA_{ext} activity increased with decreases in C_i concentration and calcification, for which HCO_3^- is a substrate, later in the growth cycle. Consequently, the authors surmised that CA_{ext} activity was influenced by HCO_3^- concentration in this strain (Nimer et al. 1994). As in *E. huxleyi*, CA_{ext} activity was only detected in the later stages of growth in *P. tricornutum*. Subsequent measurements suggested that CA_{ext} activity was induced by C_i limitation (Iglesias-Rodriguez and Merrett 1997). Elzenga et al. (2000) reported similar findings in *P. globosa*, whereby CA_{ext} activity increased with increasing pH and decreasing C_i over time. Further experiments concluded that CA_{ext} activity in *P. globosa* was specifically induced by CO_2 availability. Additionally, similar increases in CA_{ext} activity with increasing pH (constant C_i concentrations) or decreasing C_i concentrations (constant pH) were observed in *T. pseudonana* (Hopkinson et al. 2013). The resulting trends were identical, strongly suggesting the CA_{ext} activity was specifically modulated by CO_2 concentration (Hopkinson et al. 2013). Similar observations have been made in natural populations of the dinoflagellate *Peridinium gatunense* in Lake Kinneret, Israel (Berman-Frank et al. 1994). The relationship between CA_{ext} activity and C_i concentration was monitored over the course of an annually-occurring bloom of *P. gatunense*. Whilst CA_{ext} activity fluctuated in the early stages of the bloom, the highest activity was measured when C_i concentrations were depleted to <1.8 mM by the rapidly growing

population. More specifically, there was an exponential increase in CA_{ext} activity when CO_2 concentrations were <10μM (Berman-Frank et al. 1994). Our CA_{ext} activity of 0. 94 REA units · 10^{-6} cells is similar to those reported in studies using the electrometric assay used here. In particular, CA_{ext} activities between 0.1 - 1.5 REA units · 10^{-6} cells have been reported in exponentially growing cultures in a number of microalgal species (Mitchell and Beardall 1996, Iglesias-Rodriguez and Merrett 1997, Young et al. 2001, Spijkerman et al. 2014). In contrast, the values of 7.157 and 7.167 REA units · 10^{-6} cells measured at sampling points 2 and 3, respectively, are considerably higher than those typically reported in the literature, even for cultures grown under high pH   or low CO_2 conditions (Spijkerman et al. 2014) that would be expected to induce upregulation of CA_{ext} activity. These measurements are, however, usually made earlier in the growth phase where CA_{ext} is likely to be lower. Our observation of an ~8-fold increase in CA_{ext} activity between sampling point 1 and 2 is consistent with observations made in the previously discussed studies on *P. tricornutum*, *P. globasa* and *P. gatunense*. In particular, CA_{ext} activity increased 4-, 26- and up to 50-fold between the early and later stages of growth in *P. tricornutum*, *P. globasa* and *P. gatunense*, respectively (Berman-Frank et al. 1994, Iglesias-Rodriguez and Merrett 1997, Elzenga et al. 2000). Our findings are in agreement with the literature in that CA_{ext} activity increased with increasing pH and C_i depletion caused by exponentially growing cultures of *C. muelleri*. In addition, we observed that at sampling point 1, where CA_{ext} activity was lowest, the theoretical supply of CO_2 from spontaneous HCO_3^- dehydration exceeded the CO_2 drawdown capacity of cultures. This suggests that uncatalysed CO_2 supply from the bicarbonate in the medium at this stage of growth is sufficient to meet the needs of photosynthesis. Conversely, at sampling points 2 and 3 the CO_2 drawdown capacity of cultures exceeded CO_2 supply from the bicarbonate in the medium, suggesting the operation of a CCM (Burns and Beardall 1987), consistent with the high CA_{ext} activity observed at sampling points 2 and 3 in our cultures. This apparent induction of CA_{ext} in

response to an insufficient spontaneous CO_2 supply from bicarbonate suggests that CA_{ext} activity in *C. muelleri* is specifically modulated by CO_2 concentration, as in other microalgal species (Berman-Frank et al. 1994, Elzenga et al. 2000). The operation of a CCM, including the use of CA_{ext}, imposes additional energy costs on phytoplankton cells, increasing the energetic budget for growth (Raven et al. 2008, Raven et al. 2014). Therefore, the induction of CA_{ext} only when uncatalysed CO_2 availability is insufficient to promote photosynthesis over photorespiration, which is energetically expensive (Raven et al. 2014) and results in a net loss of fixed C (Raven 1994, Giordano et al. 2005, Reinfelder 2011), may be a resource-conserving strategy in phytoplankton cells.

Along with a depletion of C_i, including HCO_3^- and CO_2, over the course of population growth increases in the pH of the growth medium, as observed here, influence the concentration of CO_2 available for uptake at the cell surface. At lower pH the relative concentration of CO_2 is high and the diffusive flux to the cell membrane is sufficient to support photosynthesis (Axelsson et al. 1995, Elzenga et al. 2000). As pH increases, the relative concentration of CO_2 decreases. Consequently, the catalysed conversion of HCO_3^- by an upregulation of CA_{ext} expression becomes necessary to provide an adequate supply of CO_2 to support photosynthesis at the cell membrane (Elzenga et al. 2000). However, at the upper end of the pH spectrum, where the relative CO_2 concentration continues to decrease, very high external CA activity would be required to sustain the C_i supply required to maintain photosynthesis. Therefore, at higher pH direct uptake of HCO_3^- at the cell membrane by anion exchange (AE) proteins is likely to be more efficient than CA_{ext}-mediated CO_2 supply (Axelsson et al. 1995). Whilst total CA, internal plus external, activity appeared to correlate with the maximum photosynthetic rate in the *P. gatunense* bloom monitored by Berman-Frank et al. (1994), to our knowledge the actual contribution of CA_{ext} to the supply of CO_2 for photosynthesis at different growth stages

has not been directly measured in any phytoplankton species. Here, we inferred the role of CA_{ext} activity in photosynthesis by measuring the reduction in photosynthetic O_2 evolution in the presence of acetazolamide, an inhibitor of CA_{ext}. Although the contribution of CA_{ext} to photosynthesis over the course of population growth has not previously been investigated there is evidence that, due to its relationship with C_i speciation, the pH of the growth medium influences the contribution of CA_{ext} to photosynthesis (Moroney et al. 1985, Axelsson et al. 1995, Elzenga et al. 2000).

Axelsson et al. (1995) found that at pH 8.4 photosynthesis in the macroalga *Ulva lactuca* was suppressed by acetazolamide but unaffected by 4,4'-diisothiocyanostilbene-2,2-disulphonate (DIDS), an inhibitor of some AE proteins. Conversely, treatment with DIDS decreased photosynthesis in *U. lactuca* grown at pH 9.8, whilst acetazolamide had no effect (Axelsson et al. 1995). It was concluded that *U. lactuca* is able to make use of HCO_3^- by two mechanisms, with direct uptake via AE being induced by the low CO_2 concentrations prevailing at high pH. Similarly, Elzenga et al. (2000) measured the inhibition of C fixation by acetazolamide in *P. globosa* cells at three pH levels – 8.4, 8.6 and 9.2. They observed that inhibition of C fixation doubled from 11% at pH 8.4 to 22% at pH 8.6 before decreasing to almost 0% at pH 9.2. The observations made by Elzenga et al. (2000) are remarkably similar to our observations on the role of CA_{ext} in photosynthesis over the course of population growth of *C. muelleri*. Specifically, photosynthetic O_2 evolution decreased by 5% when CA_{ext} was inhibited at sampling point 1. In agreement with our observations of low CA_{ext} activity at sampling point 1, this suggests that CA_{ext} plays a minor role in the CCM of *C. muelleri* at this stage of growth. As with CA_{ext} activity, the contribution of CA_{ext} to photosynthesis increased with increasing pH and, particularly, decreasing CO_2 between the first two sampling points. More specifically, photosynthetic O_2 evolution was inhibited by 21%, the highest we observed, at sampling point

2. This finding is similar to observations made in *T. pseudonana*, where photosynthetic O_2 evolution in the presence of acetazolamide was inhibited by ~25% only at very low (1 µM) CO_2 concentrations (Hopkinson et al. 2013). Hopkinson et al. (2013) found that CA_{ext} expression in *T. pseudonana* and in *Thalassiosira weissflogii* is conservative and does not exceed that required to maintain CO_2 concentrations at the surface of the cell at, or near, bulk concentrations. Thus, it is likely that at sampling point 2 CO_2 supply by CA_{ext} was optimised to supplement C_i supply by other uptake mechanisms, namely HCO_3^- uptake by AE transporters. This is supported by observations of simultaneous CO_2 and HCO_3^- uptake at low CO_2 in a number of diatom species (Burkhardt et al. 2001, Clement et al. 2016). By sampling point 3, where pH had increased further and the relative concentration of CO_2 was consequently very low, the contribution of CA_{ext} to photosynthesis was negligible. Despite this, high CA_{ext} activity persisted at sampling point 3. Similarly, CA_{ext} activity at high pH was greatest in diatom species that were 'HCO_3^- users' (Trimborn et al. 2008, 2009). Consequently, Trimborn et al. (2008) suggested that in HCO_3^- users, CA_{ext} hydrates CO_2 leaking from the cell, thus enhancing HCO_3^- available for uptake by AE transporters. Therefore, it is possible that at sampling point 3 C_i acquisition in *C. muelleri* was almost solely by direct uptake of HCO_3^-, with CA_{ext} playing an indirect role via C_i recycling. However, it has been suggested that external CAs may be less susceptible to regulated degradation than internal forms of the enzyme (Lane and Morel 2000). As such, the possibility that high CA_{ext} activity persists at sampling point 3 despite the negligible role observed in photosynthesis may simply be because the enzyme has not yet been targeted for degradation. Observations that transcription of some putative HCO_3^- transporter genes in *P. tricornutum* is specifically induced when cells are CO_2-limited suggests that direct HCO_3^- uptake via AE transporters is involved in the CCM of some diatoms (Nakajima et al. 2013). In contrast, despite some evidence that O_2 evolution was inhibited by DIDS in cells of the green alga *Dunaliella tertiolecta* grown at pH 9.5, and not in

those grown at pH 8, no impact of DIDS on intracellular C_i accumulation or C fixation rates was observed, suggesting a DIDS-insensitive mechanism for direct HCO_3^- uptake or a minor role of HCO_3^- transportersin the CCM at high pH in this species (Young et al. 2001). These contrasting results suggest that direct uptake of HCO_3^- mediated by DIDS-sensitive AE transporters at high pH may be species dependent and whether AE plays a role in C_i use in *C. muelleri* at the very low CO_2 concentrations present at high pH still needs to be resolved.

Although the trend in our acetazolamide inhibition data is similar to that observed for *P. globosa*, the pH of our cultures at the measured stages of growth was higher than the pH used by Axelsson et al. (1995) and Elzenga et al. (2000). In Elzenga et al. (2000) the highest contribution of CA_{ext} to C fixation in *P. globosa* was observed at pH 8.8, with a sharp decline observed at pH 9.2. Here, the inhibition of photosynthetic O_2 evolution by acetazolamide increased between sampling point 1, where the pH was 9.1, and sampling point 2, where the pH was 10, before decreasing. The high pH reached in the later stages of growth here is not unusual for batch cultures of *C. muelleri*. Ihnken et al. (2011) observed a maximal pH of 10.3 during long-term (< 5 days) pH drift experiments using the same strain of *C. muelleri*. The high activity and enhanced role of CA_{ext} in photosynthesis observed here at relatively high pH may indicate that the use of CA_{ext} in the CCM of *C. muelleri* is only required at very low CO_2 concentrations. Since all microalgal RUBISCOs are sub-saturated at air-equilibrium concentrations of CO_2 (Beardall and Giordano 2002), the bubbling of cultures with ambient air is typically used as a 'low CO_2' condition when investigating microalgal CCMs. Previous work in our laboratory reported an absence of CA_{ext} activity in air-bubbled cultures of *C. muelleri* (Reinecke 1997). Similarly, a recent study by Tsuji et al. (2017a) found no impact of acetazolamide on the $K_{0.5}C_i$ or V_{max} for photosynthetic O_2 evolution in air-bubbled cultures of *C. muelleri*. Together, these findings suggest that CA_{ext}-mediated uptake of C_i is only induced

at very low CO_2 concentrations in this species. Whilst it is well known that in species with a CCM, cells growing at high (2-5%) and low CO_2 (0.03-0.05%) are physiologically different, Vance and Spalding (2005) reported further distinct differences between *Chlamydomonas reinhardtii* cells grown at 'low CO_2' (0.03-0.3%) and those grown at 'very low CO_2' (0.005-0.01%). Of note here, they found that in cells grown under very low CO_2 expression of *Cah1*, a gene encoding CA_{ext}, and the apparent affinity of cells for CO_2 were greater compared to 'low CO_2' cells (Vance and Spalding 2005).The concentration of CO_2 at our first sampling point (0.35 µM; 0.001%) was significantly lower than the range described by Vance and Spalding (2005) as 'very low CO_2'and yet, the role of CA_{ext} in the CCM of *C. muelleri* at sampling point 1 was relatively minor. However, CA_{ext} was maximally induced by sampling point 2, where the concentration of CO_2 was extremely low (0.005 µM; 0.00001%). These results, along with those of Reinecke (1997) and Tsuji et al. (2017a), support the idea CA_{ext} C. *muelleri* is induced at very low CO_2 concentrations.

Diatoms, haptophytes and red algae have Form ID, or red-type lineage, RUBISCOs (Young et al. 2016, Heureux et al. 2017).Despite some variation within the group, diatom RUBISCOs generally display a high specificity for CO_2 compared with other microalgal groups, with the exception of red algae (Tortell 2000, Young et al. 2016). Tortell (2000) found a significant negative relationship between the CO_2 specificity factor of RUBISCO and the ability of microalgal cells to concentrate C_i via CCMs. In general, RUBISCOs with faster CO_2-saturated specific reaction rates (k_{cat}^c) require lower CO_2 concentrations to saturate C fixation, likely reducing the necessity for CCM-mediated C_i uptake. However, in diatoms RUBISCO content was found to correlate positively with carboxylation efficiency (k_{cat}^c/ K_mCO^2; where K_mCO^2 is the half-saturation constant for CO^2), rather than the CO^2-saturated specific reaction rate like in C_4 plants (Young et al. 2016). Of the 11 diatom species surveyed by Young et al. (2016) *C.*

muelleri appeared to have one of the most efficient RUBISCOs, as indicated by the comparatively low half-saturation constant for CO_2 (K_mCO_2) of 23 µM, high CO_2 specificity factor and carboxylation efficiency measured in extracts of RUBISCO. Consequently, *C. muelleri* may allocate more of its resources to maintaining higher RUBISCO content rather than a CCM involving CA_{ext} to maintain photosynthesis (Young et al. 2016) until the concentration of CO_2 in the surrounding medium is too low to meet RUBISCO's needs, necessitating the induction of CA_{ext}-mediated C_i acquisition. However, since the concentration of CO_2 in our growth medium at inoculation (~15 µM) was already below the measured K_mCO_2 of 23 µM for *C. muelleri* RUBISCO, it is likely that some form of CCM is active even before the induction of CA_{ext}.

In C_4 plants, a CCM typically allows a plant to reduce its RUBISCO content and, consequently, optimise its nitrogen use efficiency (Ghannoum et al. 2005). Similarly, a relationship between the affinity of RUBISCO for CO_2 and RUBISCO content has been observed in a number of diatom(Young et al. 2016) and haptophyte species (Heureux et al. 2017). In particular, those species with high CO_2-affinity RUBISCOs typically have a greater RUBISCO content, expressed as the proportion of soluble protein, than those with low CO_2-affinity RUBISCOs (Young et al. 2016, Heureux et al. 2017). Conversely, species with low CO_2-affinity RUBISCOs were found to have lower RUBISCO content and more active CCMs (Young et al. 2016, Heureux et al. 2017). Therefore, photosynthetic organisms are concluded to use a CCM if their RUBISCO content relative to total soluble protein is low and their $K_{0.5}CO_2$ for photosynthetic O_2 evolution is below the K_mCO_2 of RUBISCO, which varies with species. Given that we observed $K_{0.5}CO_2$ values that were lower than the K_mCO_2 of 23 µM reported for *C. muelleri* (Young et al. 2016) we can conclude that, in agreement with CA_{ext} activity data, *C. muelleri* has an active CCM at all three measured stages of growth. However, although the

observed decrease in $K_{0.5}CO_2$ is indicative of enhanced CCM function over time, a decrease in V_{max}, when expressed on a per cell or chlorophyll basis (unpublished data), was also observed. This observation is inconsistent with those of Rost et al. (2003), who reported that V_{max} on a chlorophyll basis remained stable with increases in CCM function (as indicated by decreasing $K_{0.5}CO_2$) caused by decreases in CO_2 availability in a range of species, including diatoms. However, these observations were made in cells acclimated to air-equilibrium concentrations of CO_2 where nutrient concentrations were stable between treatments (Rost et al. 2003). It is possible that the observed decrease in V_{max} over time in our experiments is an artefact of the protocol used. Cells were resuspended in fresh medium at pH 8.2 for all P vs C_i measurements, resulting in sudden decreases of 0.93, 1.81 and 1.94 pH units at sampling points 1, 2 and 3, respectively. Whilst adjusting the pH prior to measurements kept the C_i environment constant between sampling points sudden decreases in pH have can impair photosynthesis in microalgae (Nalewajko and O'Mahony 1989). However, we observed a similar decline in $rETR_{max}$ over time. Since the pH of samples were not altered prior to PAM measurements it is unlikely that the observed decrease in V_{max} was due to pH shock. In our experiments, as well as in natural populations, nitrogen (N) limitation later in the growth cycle can influence CCM function and photosynthesis.

A similar decline in maximum photosynthetic rates despite increased affinity for CO_2 as reported here was observed in N limited cells of *D. tertiolecta* (Young and Beardall 2005). The authors suggested that the increased affinity for CO_2 of O_2 evolution despite decreases in photosynthetic capacity observed in *D. tertiolecta* acts to maintain efficient C fixation by RUBISCO under N limited conditions. Under N replete conditions a significant proportion of cellular N is allocated to RUBISCO. In contrast, significant decreases in the proportion of cellular N allocated to RUBISCO have been observed in N limited cells (Falkowski et al. 1989). Additionally, decreases in cellular RUBISCO concentration have been observed during the N-

limiting conditions associated with the stationary growth phase of a range of diatoms, including *C. muelleri* (Losh et al. 2013). Enhancing the CO_2 affinity of O_2 evolution by means of a CCM would act to maintain efficient photosynthetic C fixation despite a lower investment of N in RUBISCO. The N diverted from RUBISCO synthesis has been hypothesised to be preferentially allocated to daughter cells (Cleveland and Perry 1987), thus allowing growth of the population to continue for some time after the onset of N stress (Falkowski et al. 1989). Whilst N availability was not measured in our cultures decreases in F_v/F_m and total chlorophyll content, as observed here, are good indicators of N limitation (Young and Beardall 2005). Furthermore, whilst our V_{max} values are low compared to those previously reported for a number of microalgal species (Rost et al. 2003), including *C. muelleri* (Hu and Gao 2008), they are similar to the values measured for N-limited *D. tertiolecta* cells (Young and Beardall 2003). In particular, V_{max} values of ~2 nmol $O_2 \cdot min^{-1} \cdot 10^{-6}$ cells (0.12 µmol $O_2 \cdot h^{-1} \cdot 10^{-6}$ cells) were recorded in *D. tertiolecta* 40 hours after exposure to N-limitation, and continued to decrease thereafter (Young and Beardall 2003). In addition, it is plausible to assume that by sampling point 3 our cells were experiencing N limitation given that increases in lipid content, consistent with N limitation, have been observed in stationary phase for the same strain of *C. muelleri* used here (Giordano et al. 2001, Liang et al. 2006). Consequently, the enhanced CCM function observed here may act to ameliorate the effects of N limitation on the C fixation capacity of RUBISCO by increasing the efficiency of the remaining RUBISCO in the later stages of growth in *C. muelleri*, particularly given that the affinity for CO_2 uptake ($V_{max}/K_{0.5}CO_2$) remained constant over time.

Here, we have shown that at high cell densities *C. muelleri* makes use of a CCM, specifically involving CA_{ext}, to mediate C_i acquisition. CA_{ext} activity is induced by depletion of CO_2 as a result of consumption by growing cultures. Also, we have shown that CA_{ext} plays a role in

photosynthesis at higher pH, and consequently lower CO_2 concentrations, than has been reported for some other microalgal species. However, it is likely that at the very high pH, and consequently very low CO_2 concentrations, observed at the last sampling point C_i acquisition is primarily by direct HCO_3^- via AE transporters. Lastly, we provided evidence with support from the literature, that *C. muelleri* may enhance CCM activity over time to maintain efficient C fixation despite reductions in RUBISCO synthesis. As a consequence, the N usually allocated to RUBISCO can be reallocated to daughter cells, thus prolonging cell division despite N stress. Overall, the physiological strategies used to maintain relatively efficient photosynthesis beyond exponential phase may contribute to the observed dominance and persistence of diatoms, including *Chaetoceros* species, in phytoplankton blooms.

Chapter 3: Silica Limitation Effects on Diatom CO_2 Concentrating Mechanism Function, Photosynthesis and CO_2 Drawdown Capacity

3.1 ABSTRACT

The silica frustule of diatoms may act as a buffer for external carbonic anhydrase (CA_{ext}), an enzyme that catalyses the otherwise slow conversion of bicarbonate to CO_2 at the cell surface. In addition, there is evidence that CA_{ext} activity is modulated by the silica content of the frustule. Here, the impact of silica limitation, which results in poorly silicified frustules, on CA_{ext} activity and CO_2 concentrating mechanism function was investigated in *Chaetoceros muelleri*. Semi-continuous *C. muelleri* cultures were grown under silica-limited or silica-replete conditions and growth rate, cell size, biogenic silica content, theoretical CO_2 flux to the cell surface, CA_{ext} activity, affinity for CO_2 and CO_2 drawdown capacity was compared. The frustules of silica-replete cells were approximately twice as silicified as silica-limited cells. However, silica-limited cells were approximately twice the size of silica-replete cells. The observed difference in cell size resulted in a lower theoretical CO_2 flux to the cell surface in silica-limited cells. When the difference in cell size was accounted for no difference in CA_{ext} activity was observed between silica treatments. In contrast, a greater affinity for CO_2 was observed in silica replete cells, suggesting that the CO_2 concentrating mechanism of silica replete cells was more efficient than that of silica limited cells. Consequently, we hypothesised that enhanced C_i limitation resulting from the increased size of cells, rather than frustule silica content, regulates CO_2 concentrating mechanism function in silica limited *C. muelleri* cells. These findings may explain why the Equatorial Upwelling Zone of the Pacific Ocean, where diatoms dominate net production and silica availability is often low, is a net source of CO_2 to the atmosphere. In addition, our findings may have implications for future global carbon cycling, since it is predicted that enhanced thermal stratification of the surface layer in the tropics and mid-latitudes will inhibit the supply of nutrients, including silica, to the photic zone.

3.2 INTRODUCTION

Diatoms are arguably the most ecologically successful group of eukaryotic microalgae in aquatic environments. With an estimated 200,000 species (Mann and Droop 1996), they occur wherever light and nutrient levels are sufficient to meet their growth requirements (Armbrust 2009). In the oceans, diatoms dominate well-mixed coastal and upwelling regions, fuelling commercially important fisheries (Armbrust 2009). They are also typically the most abundant photoautotrophs along the sea-ice edge (Bowler et al. 2010) and are a vital food source for polar communities (Armbrust 2009). Diatoms fix 25-50% of the 50 gigatonnes of organic carbon (C) produced in the oceans each year(Nelson et al. 1995, Granum et al. 2005, Bowler et al. 2010). A considerable proportion of this organic C is exported to the deep sea, creating a net downward flux of C (Falkowski et al. 1998, Bowler et al. 2010) in what is called the 'biological carbon pump'. The sequestration of this organic C in the deep sea for centuries to millennia (Falkowski et al. 1998) is thought to have lowered atmospheric CO_2 concentrations over geological timescales, thus shaping global climate (Falkowski et al. 1998, Tréguer and Pondaven 2000).

Diatoms play a major role in the biological carbon pump due to the sinking of their heavy silica cell wall, known as a frustule. With the exception of the weakly silicified *Phaeodactylum tricornutum* (Borowitzka and Volcani 1978, Martino et al. 2007), diatoms have an absolute requirement for silica to form the frustule (Lewin 1962). Under silica-limitation slower growth rates (Guillard et al. 1973, Paasche 1973a, Paasche 1973b, Paasche 1975, Laing 1985), lower maximal cell numbers (Guillard et al. 1973, Laing 1985), changes in the chemical and macromolecular composition (Harrison et al. 1976, Harrison et al. 1977, Bucciarelli and Sunda 2003) and the biovolume (Bucciarelli and Sunda 2003) of cells are frequently observed. In

addition, the frustules of silica-limited cells are weakly silicified (Guillard et al. 1973, Paasche 1973a, Paasche 1973b, Harrison et al. 1977) and often lack structural components (Paasche 1973a, Harrison et al. 1977, Booth and Harrison 1979). The frustule confers many advantages to the diatoms, perhaps explaining their ecological success. In particular, silica cell walls may be cheaper to produce than their organic counterparts (Raven 1983). In addition, the frustule and its nano-features may play roles in anti-predator defence (Hamm et al. 2003), enhancing nutrient uptake (Hale and Mitchell 2001, Mitchell et al. 2013), UV protection (Ingalls et al. 2010) and buoyancy control (Raven and Waite, 2004). Although, the high nitrogen requirement associated with silica cell wall biomineralization may make it a less desirable ballast strategy compared to carbohydrate storage and mobilisation (Lavoie et al. 2016). The frustule also displays morphological flexibility under fluctuating environmental conditions, affording diatoms the ability to survive in harsh environments (Leterme et al. 2010, Ligowski et al. 2012, Leterme et al. 2013). However, research on the physiological functions of the frustule is scarce, although a role in inorganic carbon acquisition (C_i) has been proposed (Milligan and Morel 2002).

Due to its plentiful supply in the photic zone, C_i is not traditionally thought to be limiting to microalgal growth and photosynthesis (Reinfelder 2011), although there is some evidence that suggests otherwise (Riebesell et al. 1993, Hein and Sand-Jensen 1997, Riebesell et al. 2007).. In aquatic environments, the pool of C_i is made up of bicarbonate (HCO_3^-), carbonate (CO_3^{2-}) and carbon dioxide (CO_2) (Reinfelder 2011). At the alkaline conditions (pH 8 – 8.3) prevailing in the oceans over 90% of C_i is present as HCO_3^-, with less than 1% as CO_2, the sole substrate for the carbon fixing enzyme ribulose-1,5-bisphosphate carboxylase/oxygenase (RUBISCO) (Riebesell 2000). The supply of CO_2 to the cell is impeded further by its slow diffusion in water, which is 10^4 times slower than in air (Raven 1994, Granum et al. 2005). Along with

RUBISCO's relatively low affinity for CO_2, the short supply of CO_2 to the cell means that, in the absence of a mechanism for concentrating CO_2, all microalgal RUBISCOs are sub-saturated at present day levels (Riebesell 2000, Beardall and Giordano 2002, Raven et al. 2008). Additionally, oxygen (O_2) competes with CO_2 for the active site of RUBISCO in the process of photorespiration (Raven et al. 2008, Reinfelder 2011). Photorespiration involves a net loss of C and thus amplifies the energy cost of C fixation by RUBISCO (Raven 1994, Giordano et al. 2005, Raven et al. 2014). To overcome the problems surrounding CO_2 accumulation many microalgal species have evolved CO_2 concentrating mechanisms (CCMs) (Giordano et al. 2005, Reinfelder 2011).

CCMs act to enhance the concentration of CO_2 at the active site of RUBISCO, promoting C fixation over photorespiration (Beardall 1989). In microalgae, most CCMs make the large pool of HCO_3^- accessible for photosynthesis. One such mechanism involves the dehydration of HCO_3^- at the cell surface by external carbonic anhydrase (CA_{ext}) (Reinfelder 2011), maintaining a high equilibrium of CO_2 for passive or active uptake at the plasmamembrane. This alone, does not result in internal accumulation of CO_2, which still requires active transport at some other membrane (Giordano et al. 2005). However, the rate of HCO_3^- dehydration is limited by the proton (H^+) transfer step, as H^+ exchange with water is particularly slow (Lindskog and Coleman 1973, Silverman and Lindskog 1988). Consequently, a pH buffer is required to maintain high catalytic rates (Lindskog and Coleman 1973, Silverman and Lindskog 1988, Milligan and Morel 2002).

In seawater, bicarbonate, borate and silicate are potential buffers for the CA_{ext} reaction (Milligan and Morel 2002). However, since bicarbonate concentrations of up to 200 mM are

required for full CA activity, the 2 mM bicarbonate available in seawater is 100 times lower than is necessary for it to be an effective buffer for CA_{ext} (Milligan and Morel 2002). Additionally, the low concentration, and alkaline nature, of both boric and silicic acids diminishes their potential to be effective buffers for CA_{ext} (Milligan and Morel 2002). Conversely, the polymerised silica in diatom frustules is more acidic and present at relatively high concentrations in close proximity to the periplasm, where diatom CA_{ext} is located (Milligan and Morel 2002). For these reasons Milligan and Morel (2002) proposed that the silica frustule acts as a potential buffer for CA_{ext} in diatoms. They found support for this hypothesis by showing, through a series of experiments, that live cells and the cleaned frustules of *Thalassiosira weissflogii* buffered the CA reaction effectively. It should, however, be noted that the methods used to remove organic matter from the frustules may have altered the pK_a of the frustule Si-OH groups (Raven, 2018, pers. comm) and consequently, the buffering capacity of cleaned frustules. Later work found that under CO_2-limited conditions (100 ppm) the frustules of *T. weissfloggi* cells are more heavily silicified than cells growing in CO_2-replete medium (370 ppm and 750 ppm), suggesting a link between the external CO_2 environment and diatom silicification (Milligan et al. 2004). Similar findings were reported by Mejía et al. (2013), who found a positive correlation between the silica:fixed C quota of cells and increasing pH in *T. weissflogii* and *Thalassiosira pseudonana*. They suggested that the increased silica requirement at high pH was a response to the concomitant decrease in CO_2 availability. Both studies suggested that under CO_2 limited conditions diatoms are more heavily silicified to enhance CA_{ext} activity and thus improve C_i acquisition (Milligan et al. 2004, Mejía et al. 2013), although it should be noted the availability of resources other than silica and inorganic carbon, including N (Flynn and Martin-Jézéquel 2000), Fe (Hutchins and Bruland 1998, Takeda 1998) and light (Martin-Jézéquel et al. 2000, Zhang et al. 2017) also have the potential to influence frustule silicification. In support of this hypothesis Gong and

Hu (2014) found a positive correlation between CA_{ext} activity and silica concentration in the growth medium in *Skeletonema costatum*.

Whilst these studies lend support to Milligan and Morel's (2002) findings, the impacts of the observed changes in silicification and CA_{ext} activity, when diatoms are exposed to CO_2 and silica limitation respectively, on diatom C_i acquisition and CCM function remain unclear. Therefore, we investigated the effects of silica limitation on CA_{ext} activity, photosynthesis and CCM function in the common, bloom-forming (Rines and Theriot, 2003), marine diatom *Chaetoceros muelleri*. This aimed to improve our understanding of the influence of silica availability on the biological carbon pump, since any impacts of silica limitation on diatom C_i acquisition are likely to affect C fixation and, coupled with the reduced ballast provided by less heavily silicified frustules, CO_2 drawdown via the biological carbon pump. This is of particular importance given the predicted effects of global warming on stratification in the oceans and consequent enhanced limitation of nutrient supply to the upper mixed layer (Behrenfeld et al. 2006, Doney 2006).

3.3 MATERIALS AND METHODS

3.3.1 Growth Conditions

Chaetoceros muelleri Lemmerman (CS-176; Australian National Culture Collection, Hobart Australia) was grown at $18 \pm 1°C$ under continuous light supplied at 90 µmol photons m^{-2} s^{-1} (cool white light, BL75-S LED panel, Enttec, Rowville VIC, Australia) and stirred at 300 rpm on a magnetic stirrer (RT 15 magnetic stirrer, IKA Werke Staufen, Germany). Cultures were grown in 0.2 µm filtered (Type GTTP Polycarbonate filters, Millipore, Bayswater VIC,

Australia) enriched seawater artificial water (ESAW) medium (Berges et al. 2001) with 10.6 µM Na_2SiO_3 (silica-limited) or 106 µM Na_2SiO_3 (silica-replete). Medium was buffered to pH 8.2 with 10 mM Tris-base (Sigma, St. Louis, Missouri, USA). Cells were acclimated to experimental conditions for at least 3 generations before the start of experiments. For experiments, triplicate 300 mL cultures for each treatment were inoculated at a density of 10^4 cells mL^{-1} in 500 mL square Nalgene Polycarbonate narrow-mouthed bottles (Thermo Scientific Nalgene, Rochester NY, USA). Cultures were maintained in mid-exponential (at 3.32 x 10^5 cells/L for silica-limited cells and 11.80 x 106 cells/L for silica-replete cells) phase by performing daily dilutions with fresh ESAW medium.

3.3.2 Growth Rate

Cell numbers were determined daily using a Zeiss Axioscope A1 light microscope (Carl Zeiss, Göttingen, Germany). Cell counts were carried out on ten µL aliquots of culture, fixed with Lugol's iodine, using an Improved Neubauer Brightline haemocytometer (Boeco, Hamburg, Germany). Four replicate counts were carried out per culture and the average cell number recorded. Specific growth rates (µ day^{-1}) were calculated as:

$$\ln (N_2/N_1)/(T_2-T_1) \quad (3.1)$$

where N_1 and N_2 are the cell numbers at time 1 (T_1) and time 2 (T_2), respectively.

3.3.3 Morphometric Measurements

Morphometric data for each treatment was collected using a Zeiss Axioscope A1 fitted with an AxioCam ICc1 camera (Carl Zeiss, Göttingen, Germany). Photographs of at least 45 Lugol's

iodine preserved cells (15 cells per replicate) from each treatment were taken using a 40x objective lens in the built-in AxioVision Release 4.7.1 software (Carl Zeiss, Göttingen, Germany). To calculate the surface area and biovolume of cells measurements of length, width and thickness were then made on saved photographs using the publicly available Image J 1.50i software (Rasband, W.S., ImageJ, U. S. National Institutes of Health, Bethesda, Maryland, USA, http://imagej.nih.gov/ij/, 1997-2016) calibrated with a 100 µm objective micrometre. The average surface area (μm^2) and biovolume (μm^3) of cells was calculated according to Vadrucci et al. (2013) using the formulae for elliptic prisms. Given the limitations in obtaining three-dimensional measurements of individual cells using microscopy (Vadrucci et al. 2013) measurements of cell width and thickness were carried out on photographs of at least 15 cells in girdle view and then measurements of cell length were carried out on 15 cells which had valve view for each replicate. From these measurements, the average length, width and thickness of cells in each sample was determined and used to calculate surface area and biovolume.

3.3.4 Inorganic Carbon in the Growth Medium

The concentration of total C_i in the growth medium was determined from cell-free medium samples, prepared by filtering 28 mL of culture through a 0.4 µm syringe filter (PALL Life Sciences Acrodisc ® Supor ® Membrane, Port Washington NY, USA) into a pre-sterilised McCartney bottle. Samples were stored at 4°C until analysis. For analyses, 20 mL of 0.1M hydrochloric acid (HCl; Merck, Darmstadt, Germany) was continuously bubbled with air, which had been passed through soda lime granules to ensure complete stripping of CO_2 (4-8 mesh, Ajax Finechem, NSW, Australia), in a sealed glass chamber. Total C_i concentration was determined by measuring the amount of $CO_2(g)$ liberated from the reaction of C_i in 2 mL of

sample, injected into the chamber through a rubber septum, with the HCl. The gas liberated from this reaction passed through the desiccant magnesium perchlorate ($Mg(ClO_4)_2$; Alfa Aesar, Haverhill MA, USA) and was analysed continuously by an Infra-Red Gas Analysis (IRGA) system (LI-840A CO_2/H_2O Gas Analyser, Licor, Lincoln Nebraska, USA) until all CO_2 had been removed. Data were plotted by the inbuilt software as the concentration of CO_2(g) versus time and the area under this curve was used to calculate total C_i concentration by comparison with a standard curve of known sodium bicarbonate ($NaHCO_3$) concentrations (ranging from 0 – 3 mM). The pH, temperature (ºC) and salinity (%) of samples were determined using a sensION+ PH31 pH meter with in-built temperature probe (Hach, Loveland Colorado, USA) and a portable refractometer. The total C_i concentration, pH, temperature and salinity were used to calculate $[CO_2]$ and $[HCO_3^-]$ according to Weiss (1974), Dickson and Riley (1979) and Millero (2010). The pH and $[CO_2]$ and $[HCO_3^-]$ were then used to calculate the theoretical CO_2 supply rate from spontaneous HCO_3^- dehydration according to Miller and Colman (1980).

3.3.5 Theoretical Maximum Diffusive Flux of CO_2 to the Cell

The equation for the diffusive flux of nutrients to the cell is most accurately solved for spherical cells (Pasciak and Gavis 1975). However, for cells that are approximately cylindrical, such as *C. muelleri*, it is possible to solve the equations by approximating the cells as prolate spheroids (Pasciak and Gavis 1975). First, the shape radius (r_{shape}) of silica-limited and silica-replete cells was determined according to Pasciak and Gavis (1975). Once r_{shape} was determined, the theoretical maximum diffusive flux of CO_2 to the cell, Q_a (µmol m^2 s^{-1}), was calculated as (Riebesell et al. 1993):

$$4\pi r_{shape}D(c_\infty - c_a) \quad (3.2)$$

where r_{shape} = the shape radius (µm), D = the diffusivity of CO_2 in seawater (1.487 x 10^{-3} µm^2 s^{-1} at 18ºC and 35% salinity, calculated according to Wolf-Gladrow and Riebesell (1997)), c_∞ = the concentration of CO_2 of $r_{shape} \to \infty$, i.e. the bulk concentration of CO_2 in the medium (assuming air equilibrium = 14.7 µM at pH 8, 18ºC and 35% salinity, calculated as described under the subheading 'Inorganic Carbon in the Growth Medium') and c_a = the concentration of CO_2 at the surface of the cell, which was assumed to be 0, since CO_2 is often depleted in the diffusion boundary layer due to uptake by cells.

3.3.6 Frustule Silica Content

Forty mL culture suspensions were filtered onto pre-rinsed 0.6 µM polycarbonate filters (Type DTTP, Isopore Membrane Filter, Millipore, Bayswater VIC, Australia). Filters were placed into 50 mL polypropylene centrifuge tubes (Falcon^{TM}, BD Biosciences, Bedford MA, USA) and stored at -20°C until analysis. Frustule silica was digested by incubating filters in 18 ml of 0.5% sodium carbonate (Na_2CO_3) at 85°C for 2 hours. Samples were then cooled to room temperature, neutralised with 3.25 mL of 0.5 N hydrochloric acid (HCl) and made up to 25 mL with distilled water (Paasche 1980). The silica content of samples was then measured according to Strickland and Parsons (1972), with minor modifications. Briefly, 5 mL of each sample was added to 2 mL of molybdate reagent in a 15 mL polypropylene centrifuge tubes (Falcon^{TM}, BD Biosciences, Bedford MA, USA), mixed and left for 10 minutes for the yellow silicomolybdate complex to form (Strickland and Parsons 1972). This complex was reduced, producing a blue compound, by adding 3 mL of freshly prepared reducing solution (comprised of metol-sulphite, oxalic acid and sulphuric acid; see Strickland and Parsons, 1972) and mixing thoroughly. Samples were then left to incubate at room temperature for 3 hours for full colour development (Strickland and Parsons 1972). After incubation, the extinction coefficient of samples at 810

nm in a 1 cm cell was measured using a Cary-50 UV-visible spectrophotometer (Varian, Inc., Palo Alto California, USA). A filter/reagent blank was created by taking a clean filter through the full procedure. A standard curve of the extinction coefficients of solutions of known silica concentration, prepared using Na_2SiO_3, was used to calculate the silica content of samples.

3.3.7 External Carbonic Anhydrase Activity

Cells were harvested for CA_{ext} activity assays by centrifuging cell suspensions at 2,500 x g for 10 minutes (Heraeus Multifuge 3ST+, Thermo Scientific, Brookfield WI, USA), washing cells twice in ice-cold 50 mM phosphate buffer at pH 8.2 (Na_2HPO_4; BDH Chemicals, Victoria Australia) before resuspending in 15 mL ice-cold 50 mM phosphate buffer at a final density of at least 10^6 cells mL^{-1}. Samples were stored on ice until analysis. CA_{ext} activity was measured as the time taken for the pH of 2.3 mL of sample to drop 1 unit after the injection of 2.3 mL of a solution of CO_2-saturated 22 gL^{-1} NaCl in a sealed chamber (Wilbur and Anderson 1948, Miyachi et al. 1983, Young et al. 2001). CO_2-saturated NaCl solution was prepared by discharging 8 g of pure food grade CO_2 (Seltz Soda Charger, iSi GmbH, Vienna Austria) into 300 mL of 22 g L^{-1} NaCl using a soda siphon. Samples were stirred and maintained at 4°C with a circulating water bath during measurements. Control measurements were made using ice-cold 50 mM phosphate buffer without cells. CA_{ext} activity, expressed as relative enzyme activity (REA) was calculated as:

$$10 \left[(T_{control}/T_{cells})-1 \right] \quad (3.3)$$

where $T_{control}$ and T_{cells} are the times (s) taken for a 1 pH unit drop in control and cell samples, respectively.

3.3.8 Affinity for Inorganic Carbon – Photosynthesis vs Inorganic Carbon Experiments

The affinity of cells for C_i was determined by measuring photosynthetic oxygen (O_2) evolution at a range of C_i concentrations (P vs C_i) using a Clark-type O_2 electrode (Hansatech, Norfolk, United Kingdom). Cells were harvested by centrifugation at 2,500 g for 10 minutes, washed twice in C_i-free ESAW medium before being resuspended in C_i-free ESAW medium at a final density of ~10^7 cells mL^{-1}. C_i-free medium was prepared on the day of experiments by acidifying a sample of medium to pH ~2, bubbling with nitrogen gas (N_2) for at least 90 minutes and then adjusting the pH to 8.2 with a freshly prepared saturated sodium hydroxide (NaOH) solution. Measurements were made at 230 µmol photons m^{-2} s^{-1} (saturating light for photosynthesis; determined from Rapid Light Curve measurements using a PhytoPAM Analyser (Heinz Walz GmbH, Effeltrich, Germany)) and 18°C. Two mL samples were placed in the O_2-electrode chamber and left to photosynthesise until all residual C_i in the medium had been consumed and the CO_2 compensation point was reached. Afterwards, photosynthetic O_2 evolution was measured for 2 minutes after each of 11 sequential additions of $NaHCO_3$ ranging from 5-2,500 µM (Pierangelini et al. 2014a). The Michaelis-Menten model was then fit to the data to calculate the half-saturation constant of photosynthesis for C_i ($K_{0.5}C_i$) and the maximum rate of CO_2-saturated photosynthesis (V_{max}) in GraphPad Prism 6.07 (GraphPad Software, La Jolla California USA). Assuming complete equilibrium of the C_i system during experiments, the half-saturation constant of photosynthesis for CO_2 ($K_{0.5}CO_2$) was calculated from the $K_{0.5}C_i$ using pH, salinity and temperature as described earlier under the sub-heading 'Inorganic Carbon in the Growth Medium'.

The CO_2 drawdown capacity of cultures (µmol L^{-1} h^{-1}) was then calculated as:

$$C_n \text{ x } V_{max} \quad \textit{(3.4)}$$

where C_n is the cell number (cells/L) and V_{max} is the CO_2 saturated photosynthetic rate (μmol O_2 h^{-1} 10^6 $cells^{-1}$), assuming a ratio of CO_2 to O_2 of 1, of cells at the CO_2 concentration in the medium at the time of harvest for P vs C_i experiments.

3.3.9 Statistical Analyses

The statistical significance of any difference observed between silica-replete and silica-limited cultures was determined by performing an unpaired two-tailed t-test in GraphPad Prism 6.07 (GraphPad Software, La Jolla California USA). Differences were deemed to be statistically significant if $p < 0.05$.

3.4 RESULTS

3.4.1 Growth Rate, Cell Size and Frustule Silicification

Silica-limited *C. muelleri* cultures grew 2.3 times slower (unpaired t-test; $t(4) = 11.65$, $p = 0.0003$) than silica-replete cultures (Table 3.1). In addition, the cell number reached by time of harvest during mid-exponential phase was 3.5 times lower in silica-limited cultures (unpaired t-test; $t(4) = 58.29$, $p < 0.0001$) than in silica-replete cultures (Table 3.1).
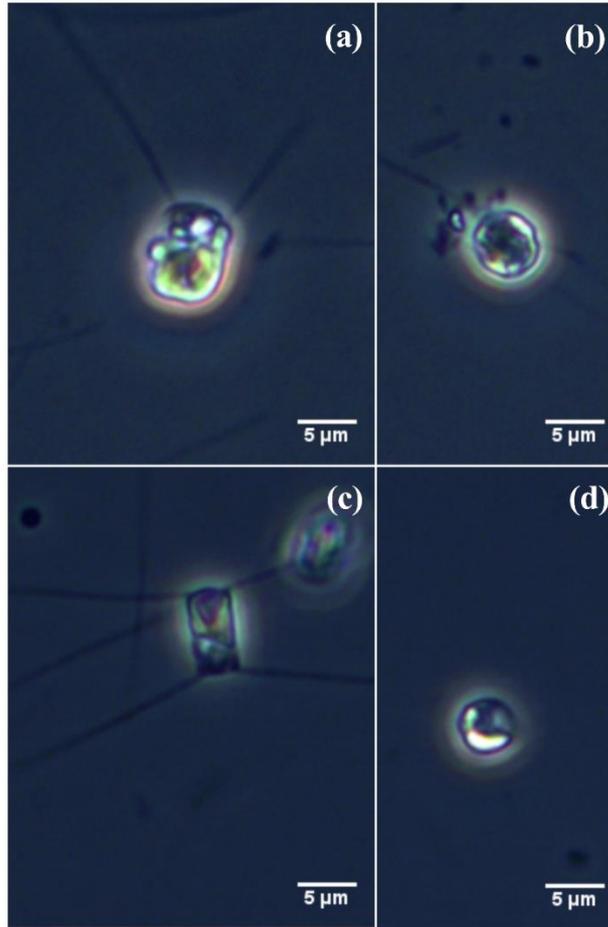
Figure 3.1. Examples of silica-limited and silica-replete *Chaetoceros muelleri* cells at the time of cell harvest. (a) silica-limited cell in girdle view, (b) silica-limited cell in valve view, (c) silica-replete cell in girdle view and (d) silica-replete cell in valve view.

Table 3.1. Growth, cells measurements and frustule silica content of *Chaetoceros muelleri* cells grown in silica-limited or silica-replete ESAW medium.

	silica-limited (Mean ± SEM; n = 3)	silica-replete (Mean ± SEM; n = 3)
Growth		
Specific growth rate (μ, day^{-1})	0.27 ± 0.02	0.63 ± 0.02
Cell number at mid-exponential phase (cells mL^{-1})	3.32 x 10^5 ± 0.05 x 10^5	11.80 x 10^5 ± 0.13 x 10^5
Cell Measurements		
Width (µm)	5.34 ± 0.14	3.68 ± 0.06
Length (µm)	6.42 ± 0.02	4.31 ± 0.06
Thickness (µm)	7.25 ± 0.20	7.80 ± 0.13
Surface Area (µm^2)	188 ± 6	123 ± 3
Biovolume (µm^3)	196 ± 9	97 ± 3
Frustule Silica Content		
Frustule silica per cell (pg cell^{-1})	3.08 ± 0.09	5.40 ± 0.04
Frustule silica content: Surface Area (pg µm^{-2})	0.017 ± 0.001	0.044 ± 0.001

Overall, silica-limited cells were twice as large as silica-replete cells, with biovolumes of 195.6 µm^3 and 97.1 µm^3 (Table 3.1), respectively (unpaired t-test; t(4) = 9.86, p = 0.0006). In particular, *C. muelleri* cells grown in silica-limited medium had 1.5 times the surface area

(unpaired t-test; t(4) = 9.88, p = 0.0006), were 49% longer (unpaired t-test; t(4) = 33.94, p < 0.0001) and 45% wider (unpaired t-test; t(4) = 10.94, p = 0.0004) than silica-replete cells (Figure 3.1, Table 3.1). There was, however, no difference in the thickness of cells (unpaired t-test; t(4) =2.23, p = 0.09) between treatments (Figure 3.1, Table 3.1).

In addition, silica-limited cells were less heavily silicified than their silica-replete counterparts (Table 3.1). More specifically, silica-replete cells had 1.7 times the frustule silica content per cell compared to silica-limited cells (unpaired t-test; t(4) = 23.05, p < 0.0001). Given that silica-replete cells were smaller than their silica-limited counterparts, the difference in frustule silica content between treatments was greater when normalised for surface area. Specifically, the frustule silica content of silica-replete cells was 2.6 times greater than that of silica-limited cells (Table 3.1, unpaired t-test; t(4) 22.74, p < 0.0001).

3.4.2 Inorganic Carbon in the Growth Medium and Theoretical Maximum Diffusive Flux of CO_2 to the Cell

The pH of the external growth medium was 0.11 units lower in silica-limited cultures (unpaired t-test; t(4) = 4.04, p = 0.02) than in silica-replete cultures (Table 3.2). However, the concentration of C_i in the external growth medium did not vary between silica treatments (Table 3.2), with no statistically significant difference in the total C_i concentration (unpaired t-test; t(4) = 0.07, p = 0.55), HCO_3^- concentration (unpaired t-test; t(4) = 1.01, p = 0.37) or CO_2 concentration (unpaired t-test; t(4) = 2.32, p = 0.08) observed between treatments. In addition, the rate of CO_2 supply from spontaneous HCO_3^- dehydration (Table 3.2) did not vary between treatments (unpaired t-test; t(4) = 2.52, p = 0.065). The diffusive flux of CO_2 to the cell was 1.2 times greater in silica-limited cells (unpaired t-test; t(4) = 19.76, p < 0.0001) than in silica-

replete cells (Table 3.2). Conversely, when normalised to cell biovolume, the diffusive flux of CO_2 μm^{-3} was 1.6 times greater (unpaired t-test; $t(4) = 10.57$, $p = 0.0005$) in silica-replete cells (Table 3.2).

Table 3.2. Carbonate chemistry parameters of cell-free silica-limited or silica-replete ESAW medium and the theoretical maximum diffusive flux of CO_2 to the surface of *Chaetoceros muelleri* cells grown in silica-limited or silica-replete ESAW medium.

	silica-limited	silica-replete
	(Mean ± SEM; n = 3)	(Mean ± SEM; n = 3)
Carbonate Chemistry		
pH	8.29 ± 0.02	8.40 ± 0.02
Total Ci (μM)	972 ± 58	919 ± 57
HCO_3^- (μM)	811 ± 49	740 ± 51
CO_2 (μM)	3.04 ± 0.30	2.20 ± 0.20
Spontaneous CO_2 supply (μmol L^{-1} h^{-1})	7.8 ± 0.7	5.6 ± 0.5
Theoretical Maximum Diffusive Flux of CO_2 (Q_a)		
To cell (μmol μm^{-2} s^{-1})	1.84 ± 0.02	1.49 ± 0.01
Q_a : BV ((μmol μm^{-2} s^{-1}) μm^{-3})	9.43 x 10^{-3} ± 0.39 x 10^{-3}	15.34 x 10^{-3} ± 0.40 x 10^{-3}

3.4.3 CA$_{ext}$ Activity and Affinity for Inorganic Carbon

When measured per 10^6 cells, CA$_{ext}$ activity was significantly higher in silica-limited cells than in silica-replete cells (unpaired t-test; t(4) = 5.29, p = 0.006), with 1.7 times more activity measured in silica-limited cells (Figure 3.2a). However, when normalised for cell surface area there was no significant difference (unpaired t-test; t(4) = 0.99, p = 0.38) in CA$_{ext}$ activity between treatments (Figure 3.2b).

Cells grown in silica-replete medium had a significantly greater affinity of photosynthetic O_2 evolution for C_i (unpaired t-test; t(4) = 2.82, p = 0.048) and CO_2 (unpaired t-test; t(4) = 2.82, p = 0.048), as shown by a half-saturation constant of photosynthesis for CO_2 (K$_{0.5}CO_2$) that was less than half of that for cells grown in silica-limited medium (Table 3.3; Figure 3.3). The maximum rate of CO_2-saturated photosynthesis (V$_{max}$) on a per cell basis of silica-limited cells was 1.8 faster (unpaired t-test; t(4) = 4.83, p = 0.008) than that of silica-replete cells (Table 3.3, Figure 3.3). However, when results were normalised to cell biovolume no significant difference (unpaired t-test; t(4) = 0.52, p =0.63) in V$_{max}$ was observed between treatments (Table 3.3). Lastly, the capacity of silica-replete cultures for CO_2 drawdown, calculated using the cell number and CO_2 concentration of the medium at the time of harvest for experiments, was more than double (unpaired t-test; t(4) = 4.65, p = 0.0097) that of silica-limited cultures (Figure 3.4).
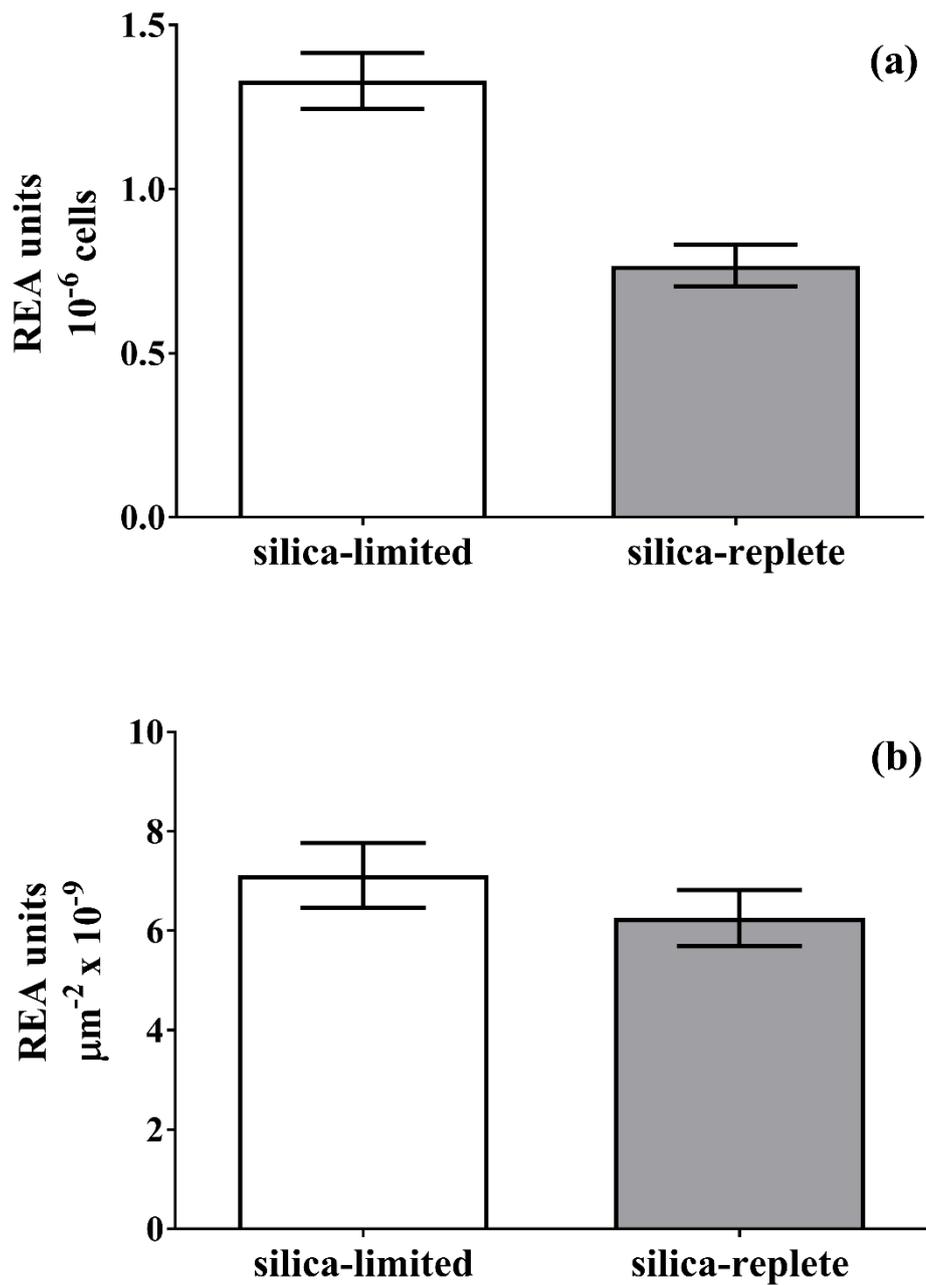
Figure 3.2. (a) External carbonic anhydrase (CA_{ext}) activity (relative enzyme activity (REA)) per 10^6 cells and (b) normalised for the average cell surface area of each treatment of *Chaetoceros muelleri* cells grown in silica-limited or silica-replete ESAW medium. Values are means (± standard error of the mean) of measurements from triplicate independent cultures.

Table 3.3. P vs C_i parameters for *Chaetoceros muelleri* cells grown in silica-replete and silica-limited ESAW medium.

	silica-limited (Mean ± SEM; n = 3)	silica-replete (Mean ± SEM; n = 3)
$K_{0.5}C_i$ (µM)	76 ± 16	31 ± 3
$K_{0.5}CO_2$ (µM)	0.345 ± 0.071	0.141 ± 0.014
V_{max} (µmol O_2 h^{-1} 10^{-6} cells)	0.073 ± 0.006	0.039 ± 0.004
V_{max}: BV (µmol O_2 h^{-1} $µm^{-3}$)	$3.7 \times 10^{-4} \pm 3.4 \times 10^{-5}$	$4.0 \times 10^{-4} \pm 5.2 \times 10^{-5}$
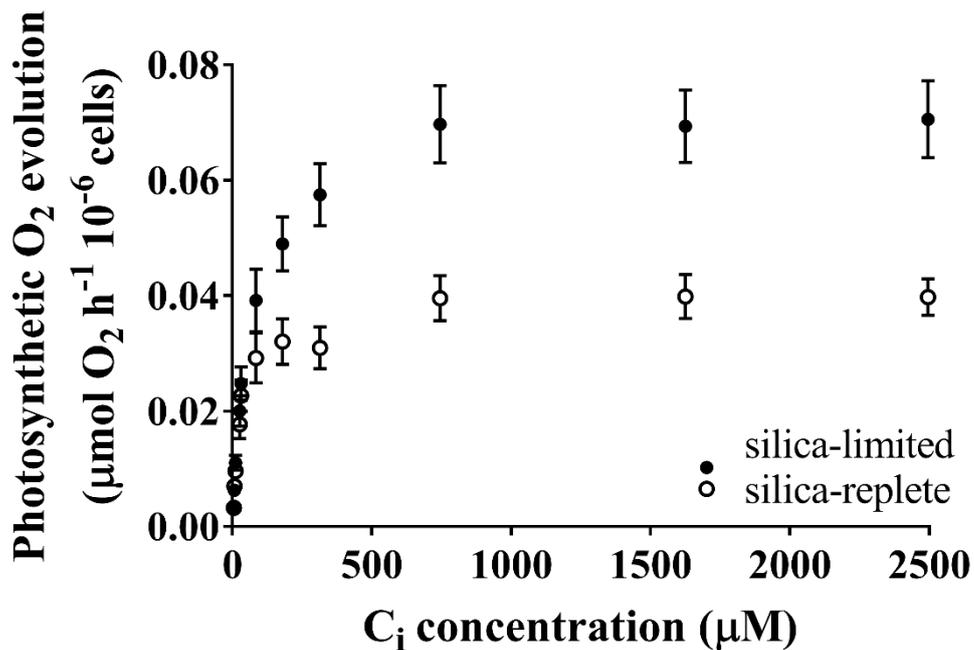
Figure 3.3. The rate of photosynthetic O_2 evolution (µmol O_2 h^{-1} 10^{-6} cells) as a function of inorganic carbon concentration (µM) of *Chaetoceros muelleri* cultures grown in silica-limited or silica-replete ESAW medium. Values are means (± standard error of the mean) of measurements from triplicate independent cultures.
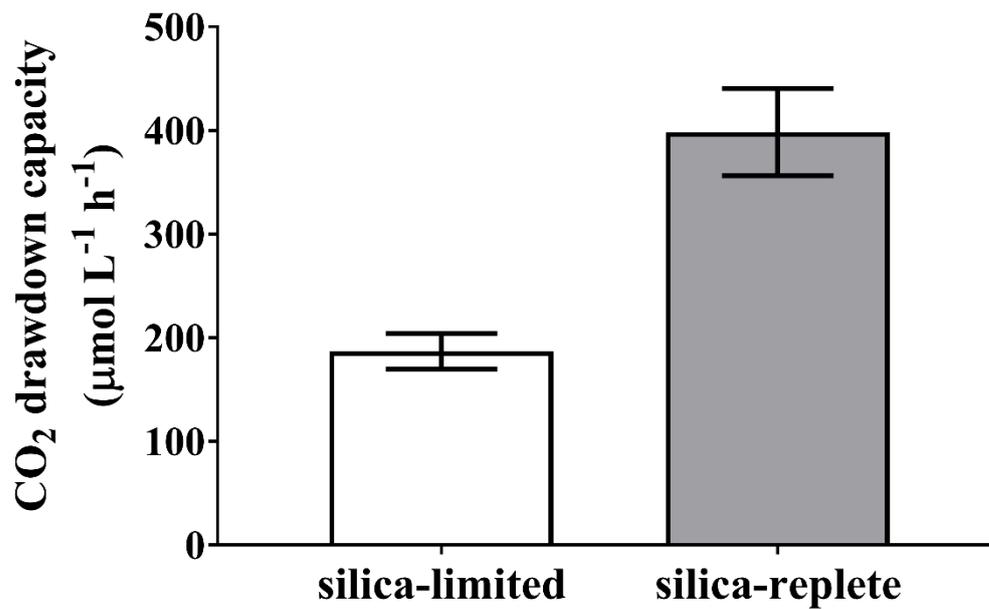
Figure 3.4. The CO_2 drawdown capacity (μmol L^{-1} h^{-1}) of *Chaetoceros muelleri* cultures grown in silica-limited or silica-replete ESAW medium. Calculations were made using the cell number and CO_2-saturated photosynthetic rate each treatment at the time of harvest for experiments. Values are means ($\pm$ standard error of the mean) of measurements from triplicate independent cultures.

3.5 DISCUSSION

It has been proposed that the frustule acts as a buffer for CA_{ext} (Milligan and Morel 2002) and that the amount of silica in the frustule mediates CA_{ext} activity in diatoms (Milligan et al. 2004, Mejía et al. 2013). Despite evidence that silica availability is positively correlated with CA_{ext} activity (Gong and Hu 2014), the resulting impacts on C_i acquisition and CCM function have not been explored. Therefore, our objective was to determine the impact of silica limitation on CA_{ext} activity and CCM function in the cosmopolitan marine diatom, *C. muelleri*.

Silicification of the frustule is tightly linked to the cell cycle (Brzezinski et al. 1990, Hildebrand 2008), meaning that growth is mediated by silica availability (Lewin 1962, Martin-Jézéquel et al. 2000). As is almost always reported for diatoms subjected to silica limitation (Guillard et al. 1973, Paasche 1973a, Paasche 1973b, Harrison et al. 1977), slower growth rates and poorly silicified frustules were observed here for silica-limited *C. muelleri* cells (Table 3.1), are almost always reported in diatoms subjected to silica limitation The availability of resources besides silica (nitrogen, phosphorus,trace metal and light availability) can also influence growth rates in phytoplankton and frustule silicification in diatoms (Hutchins and Bruland 1998, Takeda 1998, Flynn and Martin-Jézéquel 2000, Martin-Jézéquel et al. 2000, Raven and Waite 2004, Zhang et al. 2017). To eliminate potential growth limitation by nutrients other than silica, cultures were maintained in mid-exponential growth phase by performing daily dilutions with fresh, nutrient replete silica-limited or silica-replete medium. Whilst the concentrations of these other nutrients at the time of our experiments were not measured, we found no difference in CO_2 and HCO_3^- availabilities or the supply of CO_2 by spontaneous dehydration of HCO_3^- between silica treatments (Table 3.2). It is reasonable to assume that, as with C_i concentrations, daily dilutions ensured that the concentration of nutrients besides silica remained sufficient to support growth between treatments. Therefore, we can conclude that any of the observed differences between silica treatments can be attributed to the concentration of silica in the medium.

In addition to slower growth rates and less silicified frustules, we observed a significant effect of silica limitation on cell size in *C. muelleri*. In particular, we observed that the biovolume of silica-limited cells was twice that of their silica-replete counterparts (Table 3.1). Since diatom cells become smaller with each mitotic division (Willén 1991), this difference may simply be due to the slower growth rates observed in silica-limited cultures. Although, greater elasticity

of silica-limited frustules may exacerbate the lengthwise elongation of frustules observed during division of *Chaetoceros* spp. (Pickett-Heaps 1998) and thus, account for the greater biovolume observed in silica-limited cells. Bucciarelli and Sunda (2003) reported that *T. pseudonana* cells became progressively larger after the onset of silica limitation, suggesting that increased biovolume is a direct response to silica availability rather than a side effect of slower growth. Such differences in biovolume can influence the diffusive flux of CO_2 to the cell (Pasciak and Gavis 1974), even when the CO_2 concentration and supply by spontaneous HCO_3^- dehydration are the same. Whilst the diffusive flux of CO_2 to the cell increases linearly with the cell radius, the CO_2 requirement of the cell increases with the cube of the cell radius (Riebesell et al. 1993, Shen and Hopkinson 2015), assuming that photosynthetic capacity per unit volume is uniform. It should be noted, however, that if larger cells are more vacuolated as has been observed in some diatoms, the photosynthetic capacity per unit volume will not be uniform (Raven 1995). Consequently, larger cells may be more susceptible to CO_2 limitation (Finkel et al. 2010, Shen and Hopkinson 2015). Here, we found that whilst the calculated theoretical maximum diffusive flux of CO_2 to the cell was greater in silica-limited cells when calculated per cell (Table 3.2), when the difference in biovolume between treatments was accounted for the reverse was true (Table 3.2). This lower calculated theoretical maximum diffusive flux of CO_2 in larger silica-limited *C. muelleri* cells would likely exacerbate CO_2 limitation and necessitate additional up-regulation of the CCM compared to silica-replete cells.

Shen and Hopkinson (2015) measured CA_{ext} activity in six centric diatom species with spherical radii ranging from $3 - 67$ µm and found that activity increased as a function of cell size. We observed a similar relationship between cell size and CA_{ext} activity in *C. muelleri* cells exposed to different silica treatments. Specifically, we found that CA_{ext} activity per 10^6 cells in silica-limited cells was approximately twice that of silica-replete cells, which were half the

size (Figure 2a). This finding supports the idea that the CCM is up-regulated in silica-limited cells to overcome increased CO_2 deficiency that probably occurs as a consequence of increased biovolume. However, it disagrees with the hypothesis that CA_{ext} activity is mediated by frustule silica content. In contrast, higher cellular silica quotas were reported for *T. weissflogii* cells grown at 100 ppm CO_2 compared to those grown at 370 or 750 ppm CO_2 (Milligan et al. 2004). Similarly, a strong positive relationship was found between pH and silica: fixed C in *T. pseudonana* and *T. weissflogii* (Mejía et al. 2013). The authors of both studies proposed that the frustule is more heavily silicified at low CO_2 to enhance the CA_{ext} buffering capacity of the frustule and, consequently, CO_2 supply. Reports of an up-regulation of CA_{ext} activity in *T. weissflogii* cells grown at 100 ppm CO_2 (Milligan and Morel 2002) provide some support this hypothesis. However, increased frustule silicification has also been observed diatoms exposed to low light (Martin-Jézéquel et al. 2000, Zhang et al. 2017), N limitation (Flynn and Martin-Jézéquel 2000) and Fe limitation (Hutchins and Bruland 1998, Takeda 1998). Stokes' Law dictates that heavier and larger cells have a greater sinking velocity. Consequently, it has been suggested that diatoms may increase their sinking rate when they are nutrient limited by producing heavier frustules to access nutrient-rich waters deeper in the water column (Raven and Waite 2004). More heavily silicified frustules have also been observed in diatoms exposed to low light conditions (Martin-Jézéquel et al. 2000, Zhang et al. 2017). In contrast to increased silicification as a means for alleviating nutrient limitation, greater silicification of frustules in low light conditions may exacerbate the light stress experienced by diatoms by causing them to sink further down the water column, where light availability is even lower. In terms of CO_2 availability, increased silicification may allow diatoms to sink to more CO_2-rich depths during spring phytoplankton blooms, when surface depletion of CO_2 is often observed (Codispoti et al. 1982, Karl et al. 1991, Murata et al. 2002). Thus, without measuring the CA_{ext} buffering

capacity of more heavily silicified frustules it is not possible to conclude that increased silicification at low CO_2 is solely for the purpose of increasing CA_{ext} activity.

Whilst measurements of the CA_{ext} buffering capacity of poorly silicified frustules have not been made, the effect of exogenous silica availability on CA_{ext} activity in *S. costatum* has been investigated. Specifically, Gong and Hu (2014) reported that decreased silica availability correlated with decreased CA_{ext} activity. These observations provide some, albeit correlative, support for a link between the extent of frustule silicification and CA_{ext} activity in diatoms, since the degree of silicification is mediated by exogenous silica availability. If this were true in *C. muelleri*, it would be expected that when normalised to surface area, CA_{ext} activity would be lower in our silica-limited cells. However, no effect of silica availability on CA_{ext} activity was observed when normalised to surface area (Figure 3.2b). Therefore, whilst it might be expected that if silica-limited cells are not nitrogen or phosphorus limited that they would be able to upregulate CA_{ext} expression to overcome any impact of frustule silica content on CA_{ext} activity in *C. muelleri*, our data suggest that enhanced C_i limitation associated with increased biovolume in silica-limited cells plays a greater role in CCM function in this species.

A $K_{0.5}CO_2$ for photosynthesis less than the K_mCO_2 RUBISCO, coupled with a low RUBISCO content relative to total soluble protein (Young et al. 2016, Heureux et al. 2017), for a given species is indicative of an active CCM. Therefore, since a $K_{0.5}CO_2$ for photosynthesis below the K_mCO_2 RUBISCO of ~23 µM reported for *C. muelleri* (Young et al. 2016) was recorded in silica-limited and silica-replete cells (Table 3.3), it can be concluded that cells from both treatments have an active CCM. If silica-mediated CA_{ext} activity were the regulating factor in the CCM of *C. muelleri*, we would expect the trend observed in CA_{ext} activity to be reflected

in CCM function. However, the lower $K_{0.5}CO_2$ observed in silica-replete cells is indicative of a more efficient CCM, despite an up-regulation of CA_{ext} in silica-limited cells. This supports the idea that C_i limitation as a result of increased biovolume, rather than frustule silica content, is the main driver of CCM regulation in *C. muelleri*.

Any decreases in diatom CCM activity will have implications for CO_2 drawdown. Here, we observed that the CO_2 drawdown capacity of silica-limited *C. muelleri* cultures was approximately half that of silica-replete cultures (Figure 3.4). This is in agreement with field observations where diatom net primary productivity (NPP) is often controlled by Si availability (Dugdale and Wilkerson 1998, Brzezinski et al. 2001). Despite high nutrient availability, low phytoplankton biomass is observed in the surface waters of the equatorial Pacific Ocean (Barber and Chavez 1991). There is evidence that phytoplankton growth and primary productivity in this region is limited by Fe availability, given that the IronEx I and IronExII Fe fertilisation of the South equatorial current, where the sole source of Fe is from the atmosphere, resulted in increased phytoplankton biomass and photosynthesis (Martin et al. 1994, Coale et al. 1996). In contrast, Dugdale and Wilkerson (1998) suggest that phytoplankton biomass in the equatorial upwelling zone (EUZ) of the Pacific Ocean is primarily controlled by low concentrations of Si, since sufficient Fe is likely provided to the surface by upwelled waters. In the equatorial upwelling zone (EUZ) of the Pacific Ocean, new production is dominated by diatoms. In line with our observations for silica-limited cultures, the consistently low silica concentrations observed in the region result in low NPP, and ultimately, CO_2 drawdown in the EUZ. Consequently, the EUZ is a net source of CO_2 to the atmosphere (Dugdale and Wilkerson 1998). It is possible that the reduced CO_2 drawdown in the EUZ is, at least in some part, due to the influence of silica availability on diatom CCM function reported in this study. If so, future climate scenarios are likely to impact the efficiency of diatom CCMs. In particular,

future warming of the surface layer will likely exacerbate thermal stratification of the upper ocean in the tropics and mid-latitudes (Behrenfeld et al. 2006, Doney 2006). This will inhibit mixing and thus the supply of nutrients, including silica, to the photic zone. Any impact of changes in the availability of silica on diatom CCM function ultimately have the potential to influence global CO_2 concentrations.

In this study, we showed that CCM function in *C. muelleri* is mediated by nutrient availability. In particular, we found that silica limitation resulted in slower growing cells that were larger and poorly silicified. We propose that, since larger cells are more prone to CO_2 diffusion limitation, CA_{ext} activity on a 'per cell' basis is upregulated in silica-limited cells. In contrast, we observed no difference in CA_{ext} activity when the variation in cell size between treatments was accounted for. In addition, we found that the CCM of silica-limited cells is less efficient than silica-replete cells. Consequently, we argue that enhanced C_i limitation associated with increased biovolume, rather than frustule silica content, is the main factor regulating CCM function under silica limitation. Ultimately, since any impacts of silica limitation on C_i acquisition and CCM function in diatoms will result in changes to CO_2 drawdown, the availability of silica has the potential to influence global oceanic C cycling.

3.6 ACKNOWLEDGEMENTS

Chapter 4: The Impacts of Silica Limitation on Photosynthesis, Photoprotective Mechanisms and Reactive Oxygen Production

4.1 ABSTRACT

Silicification of diatom frustules is mediated by silica availability, with limitation usually resulting in poorly silicified frustules. The frustule may act as a buffer for external carbonic anhydrase (CA_{ext}), a component of some microalgal carbon dioxide concentrating mechanisms (CCMs). There is also evidence in the literature that CA_{ext} activity is modulated by the silica content of the frustule. The operation of a CCM may act as a sink for excess light energy. Therefore, silica limitation may expose diatoms to excess light energy, which can result in the production of harmful reactive oxygen species (ROS). We investigated the impacts of silica limitation on photosynthesis, photoprotective mechanisms and ROS production in the cosmopolitan marine diatom, *Chaetoceros muelleri*. Whilst silica-limited cells had a greater maximum quantum yield of photosystem II (F_v/F_m) and relative light harvesting efficiency (α) than silica-replete cells, the maximum relative electron transport rate ($rETR_{max}$) was reduced under limitation. Similarly, silica limitation resulted in a reduced capacity to utilise light at high light intensities, indicated by the lower light saturation parameter (I_k) and relative electron transport rates (rETR) at photon flux densities (PFDs) above $240 \, \mu mol \cdot photons \cdot m^{-2} \cdot s^{-1}$ in silica-limited cells. We observed that carotenoid content and non-photochemical quenching (NPQ) capacity were 2 times and 1.6 times greater, respectively, in silica-limited cells. It is likely that these photoprotective mechanisms reduced the formation of ROS, since no difference in ROS concentration was observed between treatments. This physiological plasticity likely allows bloom-forming diatoms to acclimate to constantly changing environmental conditions.

4.2 INTRODUCTION

Despite the plentiful supply of inorganic carbon (C_i) in the marine environment, carbon dioxide (CO_2), the sole substrate for photosynthetic carbon (C) fixation by ribulose-1,5-bisphosphate carboxylase/oxygenase (RUBISCO), is scarce (Zeebe and Wolf-Gladrow 2001, Reinfelder 2011). At the alkaline pH (8-8.3) of seawater, C_i is comprised of 90% bicarbonate (HCO_3^-), >9% carbonate (CO_3^{2-}) and <1% (CO_2) (Raven 1994, Riebesell 2000). The poor supply of CO_2 to the cell is exacerbated by its slow diffusion in water, which is 10^4 times slower than in air (Raven 1994, Granum et al. 2005). The low affinity of RUBISCO for CO_2 (Giordano et al. 2005), coupled with the relatively low supply of CO_2 to the cell, means that all microalgal RUBISCOs are sub-saturated at present day air-equilibrium CO_2 levels (Giordano et al. 2005). To overcome the problems associated with acquiring CO_2 for photosynthesis many microalgae have evolved CO_2 concentrating mechanisms (CCMs) (Giordano et al. 2005, Reinfelder 2011). One such mechanism involves the dehydration of HCO_3^- to CO_2 at the cell surface by external carbonic anhydrase (CA_{ext}), followed by active transport at some other membrane (Giordano et al. 2005). However, the proton (H^+) exchange step involved in the HCO_3^- dehydration reaction is slow in water (Lindskog and Coleman 1973, Silverman and Lindskog 1988). As such, a pH buffer is required to maintain high catalytic rates (Lindskog and Coleman 1973, Silverman and Lindskog 1988, Milligan and Morel 2002).

There is evidence that the polymerised silica in the diatom cell wall, known as the frustule, may act as a buffer for CA_{ext} (Milligan and Morel 2002). Specifically, Milligan and Morel (2002) showed that live cells and cleaned frustules of *Thalassiosira weissflogii* effectively buffered the CA reaction. Further work has suggested that CA_{ext} activity in diatoms is modulated by the extent of frustule silicification. In particular, it has been proposed that

diatoms become more heavily silicified when experiencing CO_2 limitation in order to enhance CA_{ext} activity and, consequently, improve C_i supply (Milligan et al. 2004, Mejía et al. 2013). Silicification of the frustule is mediated by exogenous silica supply, with limitation producing poorly silicified frustules (Guillard et al. 1973, Paasche 1973a, Paasche 1973b, Harrison et al. 1977). Therefore, the observation that CA_{ext} activity is positively correlated with medium silica concentration in *Skeletonema costatum* lends support to the idea that CA_{ext} activity is influenced by the extent of frustule silicification (Gong and Hu 2014). Whilst it seems likely that the impact of silica limitation on cell size, rather than on the degree of frustule silicification, influences CA_{ext} activity in *C. muelleri*, we did observe a downregulation of overall CCM function under silica limitation (Smith-Harding et al. In prep.).

There is evidence that the operation of a CCM may protect cells from photoinhibition by acting as a sink for excess light energy (Tchernov et al. 1997, Tchernov et al. 2003, Qiu and Liu 2004). Therefore, the downregulation of the diatom CCM under silica limitation may enhance the likelihood that excess light energy would lead to photoinhibition. Exposure to excess light energy can lead to the production of harmful reactive oxygen species (ROS) (de Bianchi et al. 2010). Increased production of ROS such as superoxide, hydrogen peroxide, hydroxyl radical and singlet oxygen, results in oxidative stress (Bucciarelli and Sunda 2003) and, in some cases, programmed cell death (Vardi et al. 1999). Photoautotrophs adopt a number of photoprotective strategies to protect themselves from ROS damage induced by excess light. In particular, the formation of ROS can be prevented through the dissipation of excess light energy as heat in a mechanism known as non-photochemical quenching (NPQ) (de Bianchi et al. 2010, Wu et al. 2010). Alternatively, ROS can be detoxified by antioxidant molecules such as carotenoids (de Bianchi et al. 2010). In diatoms, a xanthophyll cycle involving the de-epoxidation of diadinoxanthin (DD) to form diatoxathin (DT) is involved in dissipating excess light energy

arriving at PSII via NPQ (Olaizola and Yamamoto 1994, Dimier et al. 2007). In addition, β-carotene has the potential to detoxify ROS by quenching excited triplet chlorophyll, which can lead to the production singlet oxygen, and dissipating the excess energy as heat ('physical quenching') or by oxidation of β-carotene by singlet oxygen ('chemical quenching') (Ramel et al. 2012). Therefore, if silica limitation induces a downregulation of the CCM in diatoms, then an increased capacity for NPQ and/or carotenoid activity might be expected in silica-limited diatoms.

In this study, we investigated the impacts of silica limitation on photosynthesis, photoprotective mechanisms and ROS production in the cosmopolitan marine diatom *Chaetoceros muelleri* (Lemmerman). Members of the *Chaetoceros* genus are the often the most numerous species in marine phytoplankton communities (Rines and Theriot 2003). Investigating the physiological responses of *C. muelleri* to Si limitation will improve our understanding of the mechanisms that enable diatoms to acclimate to fluctuating environmental conditions.

4.3 MATERIALS AND METHODS

4.3.1 Growth Conditions

Chaetoceros muelleri Lemmerman (CS-176; Australian National Culture Collection, Hobart Australia) was grown in silica-limited (10.6 µM Na_2SiO_3) or silica-replete (106 µM Na_2SiO_3), filter-sterilised (0.2 µm Type GTTP Polycarbonate filters, Millipore, Bayswater VIC, Australia) enriched seawater artificial water (ESAW) medium (Berges et al. 2001). Medium was buffered to pH 8.2 with 10 mM Tris-base (Sigma, St. Louis, Missouri, USA). Cultures were maintained at $18 \pm 1°C$ and stirred continuously at 300 rpm on a magnetic stirrer (RT 15

magnetic stirrer, IKA Werke Staufen, Germany). Light was supplied continuously at 90 µmol photons · m^{-2} · s^{-1} (cool white light, BL75-S LED panel, Enttec, Rowville VIC, Australia). Cells were acclimated to growth conditions for at least 3 generations before experiments commenced. For experiments, triplicate 300 mL semi-continuous batch cultures were prepared in 500 mL square Nalgene Polycarbonate narrow-mouthed bottles (Thermo Scientific Nalgene, Rochester NY, USA). All cultures were inoculated at a density of 10^4 cells · mL^{-1}. Cultures were maintained in mid-exponential phase, at specific growth rates of 0.27 day^{-1} and 0.63 day^{-1} for silica-limited and silica-replete cultures (Smith-Harding et al. In prep.), respectively, by performing daily dilutions with fresh ESAW medium.

4.3.2 Chlorophyll Fluorescence: Photosynthesis and Non-photochemical Quenching (NPQ) Capacity

A number of photosynthetic parameters and the non-photochemical quenching (NPQ) capacity of silica-limited and silica-replete cells were determined using a PhytoPAM Analyser (Heinz Walz GmbH, Effeltrich, Germany). Four mL samples were dark adapted for 15 minutes before analyses. The maximum quantum yield (F_v/F_m), maximum relative electron transport rate ($rETR_{max}$), the relative light harvesting efficiency (α) and the relative electron transport rate (rETR) at photon flux densities (PFD) from 16 – 610 µmol photons · m^{-2} · s^{-1} (Rapid Light Curve analysis) were measured according to Smith-Harding et al. (2017). In addition, the light saturation parameter (I_k) was calculated by the in-built PhytoWIN software (PhytoWIN v2.13), as:

$$I_k = rETR_{max}/\alpha \ (4.1)$$

The NPQ capacity of cells was determined according to Pierangelini et al. (2014b). Briefly, samples were exposed to actinic light of 480 µmol photons · m^{-2} · s^{-1} for 10 minutes with a 60

s cycle of saturating red pulses until the maximum fluorescence yield in the light (F_m') remained stable. The NPQ capacity was then calculated according to the Stern-Volmer equation, as follows:

$$NPQ = (F_m/F_{m'}) - 1 \quad (4.2)$$

4.3.3 Pigments: Chlorophylls and Carotenoids

Samples were harvested for pigment analysis according to Smith-Harding et al. (2017), with minor modifications. Specifically, pigments were extracted in 90% methanol (Merck, French Forest, NSW, Australia) rather than acetone prior to analysis. The extinction coefficients of extracts at 632 and 665 nm were determined in a Cary-50 UV-visible spectrophotometer (Varian, Inc., California USA) and used to calculate chlorophyll a and c concentrations ($\mu g \cdot mL^{-1}$) using Ritchie (2006)'s formulae for diatom chlorophylls extracted in methanol:

$$\text{Chlorophyll } a = 13.2654 * E_{665} - 2.6839 * E_{632} \quad (4.3)$$

$$\text{Chlorophyll } c_1 + c_2 = 28.8191 * E_{632} - 6.0138 * E_{665} \quad (4.4)$$

where E_x denotes the extinction coefficient at wavelength x.

The same extracts were used to determine the carotenoid content of cells. The absorbance of extracts at 480 nm was determined and used to calculate the concentration of carotenoids ($\mu g \cdot mL^{-1}$) according to the diatom-specific formula of Strickland and Parsons (1972):

$$\text{Carotenoids} = (10 * E_{480})/1000 \quad (4.5)$$

where E_{480} is the extinction coefficient at 480 nm.

4.3.4 Hydrogen peroxide

The H_2O_2 (hereafter, ROS) content of cells was determined according to Keston and Brandt (1965), as modified by Mikulic (2015). The method measures the extent of the oxidation of the non-fluorescent probe 2',7'-dichlorodihydrofluorecein (DCFH$_2$) to the fluorescent 2',7'-dichlorofluorecein (DCF) by ROS within the cell in the following manner:

$$H_2DCF - DA \xrightarrow[\text{Deacetylation}]{\text{Esterases in cell}} H_2DCF + DA \xrightarrow[\text{Oxidation}]{\text{ROS}} DCF \text{ (fluorescent)} \quad (4.6)$$

For analysis, cells were harvested by centrifuging culture suspensions at 4,000 g for 15 minutes (Heraeus Multifuge 3ST+, Thermo Scientific, Brookfield, WI, USA) and washed twice in 40 mM in Tris-HCl buffer (Sigma, St. Louis, Missouri, USA; pH 7). Cells were then resuspended at a final density of 1 x 10^7 cells in 4 mL of 40 mM in Tris-HCl with 1 mL of a 0.25 mM solution of the non-fluorescent probe, DCFH$_2$ (Sigma, St. Louis, Missouri, USA; final concentration of non-fluorescent probe was 50 µM). Cells were incubated at 37ºC for 90 minutes, harvested by centrifugation at 4,000 g for 15 minutes and washed twice in 40 mM Tris-HCl buffer before resuspension in 3 mL of the same buffer. Cells were then lysed using a Branson Sonifier 450 probe sonicator (Branson Ultrasonics Corporation, Danbury, Connecticut, USA), cellular debris removed by centrifugation at 4,000 g for 15 minutes and the supernatant retained for analysis. The fluorescence of the supernatant at excitation and emission wavelengths of 485 nm and 525 nm, respectively, were measured in a Hitachi 7500 spectrofluorometer (Hitachi Ltd, Tokyo, Japan). A standard curve of the fluorescence of solutions of known DCF concentrations was used to determine the ROS content of samples.

4.3.5 Statistical Analyses

The statistical significance of any differences observed between silica treatments was tested by performing an unpaired two-tailed t-test in GraphPad Prism 6.07 (GraphPad Software, La Jolla California USA). The statistical significance of any difference in rETR observed between silica treatments over a range of PFDs during Rapid Light Curve analysis was tested using a two-way ANOVA followed by a post hoc Tukey's HSD multiple comparison test in GraphPad Prism 6.07 (GraphPad Software, La Jolla California USA). All differences between silica treatments were considered statistically significant if $p < 0.05$.

4.4 RESULTS AND DISCUSSION

The maximum quantum yield of photosystem II (F_v/F_m) was used to assess the physiological status (Maxwell and Johnson 2000) of our cultures. We observed that F_v/F_m was 11% greater in silica-limited cells than in silica-replete cells (Figure 4.1a; unpaired t test, $t_4 = 8.82$, $p = 0.0009$). Similarly, the relative light harvesting efficiency, α, of silica-limited cells was 13% greater than that of silica-replete cells (Figure 4.1b; unpaired t test, $t_4 = 12.07$, $p = 0.0003$). These results suggest that in *C. muelleri* photosystem II function and the ability to harvest light at low intensities are enhanced under silica limitation. However, cell numbers in silica-replete cultures were 3.5 times higher than in silica-limited cultures at the time of harvest during mid-exponential phase (Table 3.1). Since the potential for self-shading increases with cell number it is more likely that the variation in F_v/F_m and α between treatments reflect differences in light, than silica, availability. Our observation for α contradicts that of Lippemeier et al. (1999), who reported no variation in α with silica concentration in batch cultures of *T. weissflogii*. Our F_v/F_m result is also inconsistent with that observed in *T. weissflogii*, where larger decreases in F_v/F_m

of up to 33% were observed in silica-limited cultures (Lippemeier et al. 1999). Parkhill et al. (2001) reported that whilst F_v/F_m was depressed in nitrogen starved batch cultures of *Thalassiosira pseudonana*, no impact was observed if cultures had been acclimated to nitrogen limited conditions. Therefore, the lesser impact of silica limitation on F_v/F_m observed in *C. muelleri* compared to *T. weissflogii* could be due to the fact that our cultures were acclimated to the silica treatments before measurements, and those of Lippemeier et al. (1999, 2001) were not. In support of this idea, no effect of silica limitation on F_v/F_m was observed in *Pseudo-nitzschia pungens* and *Asterionellopsis glacialis* cultures, which had been in steady state growth for at least five days (Napoléon et al. 2013).

In contrast to our observations for F_v/F_m and α, we observed a negative impact of silica limitation on the maximum relative electron transport rate ($rETR_{max}$). Electron transport rate correlates well with photosynthesis under controlled conditions (Maxwell and Johnson 2000, Ralph and Gademann 2005) and, as such, can be used to assess the photosynthetic performance of phytoplankton cells in the laboratory (Maxwell and Johnson 2000, Napoléon et al. 2013). We observed that $rETR_{max}$ was 22% greater in silica-replete cells (Figure 4.1c; unpaired t-test; $t_4 = 6.73$, $p = 0.0025$). Since silica is not directly involved in photosynthesis (Napoléon et al. 2013), few studies have investigated the impacts of silica limitation on photosynthesis in diatoms. However, our finding agrees with field studies that observed a decrease in photosynthesis within hours of silica depletion in a mixed diatom bloom in the Hudson River (Malone et al. 1980). Similarly, a sharp decline in $rETR_{max}$ was recorded at the onset of silica limitation in *T. weissflogii* (Lippemeier et al. 1999). A 70% recovery in $rETR_{max}$ was observed in silica-starved cells after the re-addition of silica, suggesting that photosynthesis in *T. weissflogii* is, in part, determined by silica availability (Lippemeier et al. 1999). In contrast, whilst electron transport rate was 182% greater in silica-limited *A. glacialis* cells, no significant

impact of silica limitation on electron transport rate was observed in *P. pungens*, (Napoléon et al. 2013), suggesting that the physiological response to silica limitaiton in diatoms may be species specific.

As with rETR$_{max}$, silica availability had a marked impact on the light saturation parameter (I$_k$) in *C. muelleri*. Specifically, I$_k$ was 234 ± 2.7 µmol photons m^{-2} s^{-1} in silica-replete cells, compared to 159 ± 5.5 µmol photons m^{-2} s^{-1} in silica-limited cells (Figure 4.1d; unpaired t-test, t$_4$ = 12.15, p = 0.0003). A similar decline in I$_k$ was observed at the onset of silica limitation in *T. weissflogii* cells (Lippemeier et al. 1999). These results suggest that, in diatoms, silica limitation results in a reduced capacity to utilise light at high photon flux densities (PFDs) (Henley 1993).
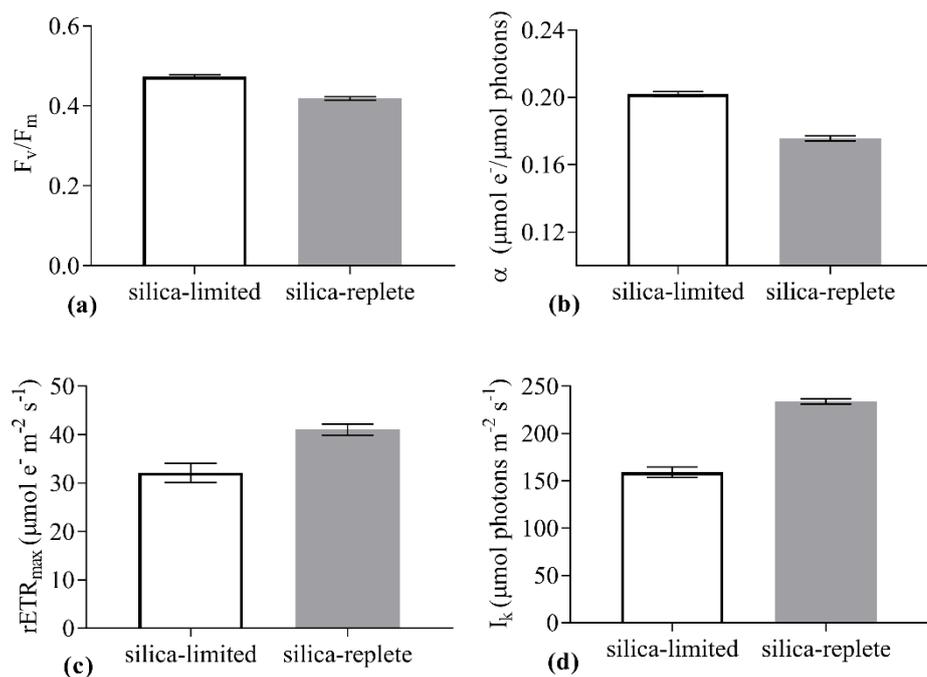
Figure 4.1. The (a) maximum quantum yield of photosystem II (F_v/F_m), (b) relative light harvesting efficiency (α; μmol e$^-$/μmol photons), (c) relative maximum electron transport rate (rETR$_{max}$; μmol e$^-$ m^{-2} s^{-1}) and (d) light saturation parameter (I_k; μmol photons m^{-2} s^{-1}) of silica-limited and silica-replete *Chaetoceros muelleri* cells. Values are means ($\pm$ standard error of the mean) of triplicate independent cultures.

The downturn in rETR observed at high PFDs in cells from both treatments (Figure 4.2) suggests that *C. muelleri* may become photoinhibited at supra-optimal light intensities regardless of silica availability (Ralph and Gademann 2005). However, rETR was significantly higher in silica-replete cells at PFDs greater than 240 μmol photons m^{-2} s^{-1} (Figure 4.2; Tukey's HSD, $p > 0.05$ for all comparisons). Together, these results suggest that silica-limited *C. muelleri* cells are more prone to photoinhibition than their silica-replete counterparts, although

it is possible that silica-limited cells have a greater C demand due to their larger biovolume (Smith-Harding et al. 2018, in prep).
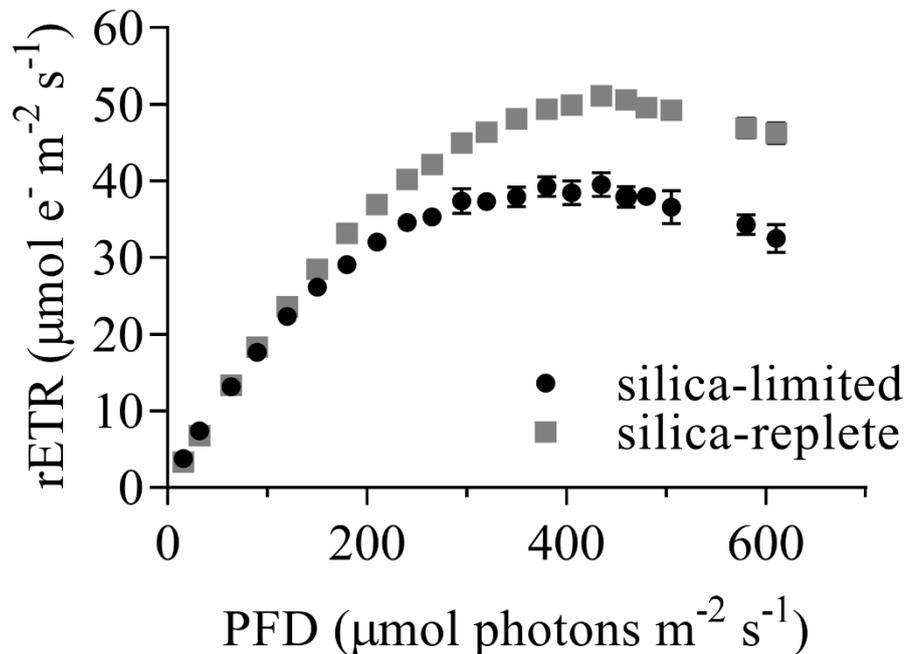
Figure 4.2. Rapid Light Curves showing the relative electron transport rate ($rETR_{max}$; µmol e$^-$ m^{-2} s^{-1}) as a function of photon flux density (PFD; µmol e$^-$ m^{-2} s^{-1}) of silica-limited and silica-replete *Chaetoceros muelleri* cells. Values are means ($\pm$ standard error of the mean) of triplicate independent cultures.

The operation of a CCM, including CA_{ext}, to acquire C_i for photosynthesis consumes energy (Raven et al. 2014). Consequently, it has been suggested that the operation of a CCM may play a role in protecting cells from photoinhibition by acting as a sink for excess light energy (Tchernov et al. 1997, Tchernov et al. 2003, Qiu and Liu 2004). Therefore, if CA_{ext} activity is mediated by silica supply (Gong and Hu 2014) and/or the degree of frustule silicification (Milligan et al. 2004, Mejía et al. 2013), then it might be expected that under silica limitation

cells are more likely to experience photoinhibition at high PFDs, as shown in our Rapid Light Curves (Figure 4.2). Similar differences in rETR were observed between low CO_2 (12.6 µM) grown *Thalassiosira pseudonana* cells in the presence and absence of ethoxyzolamide, a membrane permeable inhibitor of carbonic anhydrase (Wu et al. 2015). In particular, Wu et al. (2015) found that, at higher PFDs, rETR was greater in cells in which CA had not been inhibited compared to those where it had, suggesting that the downregulation of CA may play a role in a decreased ability to utilise light at high PFDs.

A number of physiological strategies allow microalgae to adjust to changes in their light environment, including changing their pigment concentration and composition (Richardson et al. 1983, Napoléon et al. 2013). We observed that silica-limited cells had 2.2 times the chlorophyll content of silica-replete cells (Table 2.1; unpaired t-test, $t_4 = 12.47$, $p = 0.0002$). Varying results on the impacts of silica limitation on chlorophyll content in diatoms have been reported. In some instances silica availability has been reported to have no influence on chlorophyll content (Napoléon et al. 2013), whilst other studies have observed increases (Harrison et al. 1977, Bucciarelli and Sunda 2003) and decreases (Harrison et al. 1977, Lynn et al. 2000) in chlorophyll content per cell under silica limitation. This variation may reflect species specific responses to silica limitation (Harrison et al. 1977), differences in the extent of silica limitation (Bucciarelli and Sunda 2003) or differences in other experimental conditions (such as the availability of nutrients other than silica or light conditions). The higher chlorophyll content of silica-limited cells may be a consequence of normal rates of chloroplast replication, despite slower cell division (Harrison et al. 1977). Alternatively, Bucciarelli and Sunda (2003) suggested that chlorophyll synthesis is upregulated to meet the increased energy demands of CO_2 acquisition resulting from the depression of CA_{ext} activity under silica limitation. Their observation that the chlorophyll content of *T. pseudonana* responded similarly

to CO_2 limitation, but not nitrate or phosphate limitation, supports this hypothesis (Bucciarelli and Sunda 2003). However, some previous studies have found that chlorophyll content per cell scales linearly with cell biovolume (Lynn et al. 2000, Durbin 1977). We observed no impact of silica availability on chlorophyll content when data were normalised to biovolume (data not shown; unpaired t-test, $t_4 = 1.44$, $p = 0.22$). Since silica-limited cells were approximately twice the size of silica-replete cells (Smith-Harding et al. In prep.), it is likely that the higher chlorophyll content observed in limited cells was due to the increase in cell biovolume observed under silica limitation.

Table 4.1. The total chlorophyll concentration ($a + c1,c2$), total carotenoids concentration and carotenoids: total chlorophyll of silica-limited and silica-replete *Chaetoceros muelleri* cells. Values are means (± standard error of the mean) of triplicate measurements.

	silica-limited	silica-replete
Total chlorophyll ($\mu g\ 10^{-6}$ cells)	0.71 ± 0.02	0.33 ± 0.02
Total carotenoids ($\mu g\ 10^{-6}$ cells)	$8.4 \times 10^{-4} \pm 2.7 \times 10^{-5}$	$4.0 \times 10^{-4} \pm 2.3 \times 10^{-5}$
Carotenoids: total chlorophyll	1.18 ± 0	$1.20 \pm 1 \times 10^{-5}$

In addition to an increase in chlorophyll content per cell, we observed that silica-limited cells had twice the carotenoid content of silica-replete cells (Table 4.1; unpaired t-test, $t_4 = 12.65$, $p = 0.0002$). Similar to the increase in chlorophyll content under silica limitation, this increase may be as a consequence of the increased cell biovolume of silica-limited cells, since no

difference in carotenoid content was observed between silica treatments when normalised to biovolume (data not shown; unpaired t-test, $t_4 = 1.26$, $p = 0.28$). In diatoms, the carotenoid fucoxanthin forms part of the light-harvesting complex (Coesel et al. 2008), transferring light energy to chlorophyll a (Goericke and Welschmeyer 1992). Therefore, the observed increase in carotenoids under silica limitation may too have been a response to the increased energy demand for CO_2 acquisition brought on by silica limitation. However, carotenoids in diatoms may also be involved in photoprotection under high light conditions (Goericke and Welschmeyer 1992). More specifically, the thermal dissipation of excess light energy by photosystem II through NPQ involves the increase of a xanthophyll cycle at high PFDs in many photoautotrophs (Olaizola et al. 1994, Dimier et al. 2007). Increases in diadinoxanthin cycle (DD-cycle) activity, which involves the conversion of DD to diatoxanthin (DT) (Olaizola et al. 1994, Dimier et al. 2007), have been associated with high irradiance in many diatom species, including *C. muelleri* (Olaizola and Yamamoto 1994). More specifically, increases in the xanthophyll pool (DD + DT) have been observed to be associated with increasing irradiance (Goericke and Welschmeyer 1992, Dimier et al. 2007), as well as with prolonged exposure to high irradiances (Olaizola et al. 1994). In addition, DT accumulation, either by conversion from DD or *de novo* synthesis, is correlated with enhanced capacity for NPQ under high irradiance (Olaizola et al. 1994, Olaizola and Yamamoto 1994, Dimier et al. 2007). Previous research has shown that the response of the DD-cycle to fluctuating light environments varies between species and may be influenced by ecological niche (Dimier et al. 2007). Coastal bloom-forming species tend to display the greatest physiological plasticity under changing conditions, allowing them to acclimate to the constantly fluctuating abiotic conditions present in coastal environments (Dimier et al. 2007). Whilst the method used here could not distinguish between the different types of carotenoids, we observed that the capacity for NPQ of silica-limited cells was 1.6 times greater than that of silica-replete cells (Table 4.2; unpaired t-test, t_3

= 5.09, p = 0.015). This suggests that the observed increase in carotenoids under silicalimitation may, at least in part, be due to an increase in DT concentration. Similar increases in NPQ were observed in *T. weissflogii* under silica limitation (Lippemeier et al. 1999). The thermal dissipation of excess light energy by NPQ relieves pressure on the electron transport chain (Wu et al. 2010) and prevents the formation of ROS (de Bianchi et al. 2010).

Table 4.2. The non-photochemical quenching (NPQ) capacity and reactive oxygen species (ROS) content of silica-limited and silica-replete *Chaetoceros muelleri* cells. Values are means (± standard error of the mean) of triplicate independent cultures (except for the NPQ measurement for silica-limited cells, where the value is the mean of two independent cultures).

	silica-limited	silica-replete
NPQ	0.46 ± 0.02	0.28 ± 0.03
ROS content (nmol DCF $\cdot$ 10^{-6} cells)	0.019 ± 0.001	0.018 ± 0.003

Changes in temperature, light availability or nutrient supply can disrupt photosynthesis, resulting in the production of harmful ROS (Bucciarelli and Sunda 2003, de Bianchi et al. 2010). A previous study on *Skeletonema marinoi* found that under silica limitation the expression of aldehyde dehydrogenase, glutathione synthase and glycolate oxidase genes, which are known to protect cells from oxidative stress, increased (Wang et al. 2017). In addition, cells exposed to silica limitation were more prone to programmed cell death, likely induced by the greater caspase activity observed in the low silica treatment (Wang et al. 2017). In contrast, we observed no difference in ROS concentration between treatments (Table 4.2;

unpaired t-test, $t_4 = 0.25$, $p = 0.81$). This suggests that, in *C. muelleri*, NPQ is effective at protecting cells from the formation of silica limitation-induced ROS. Similarly, silica-limited *T. pseudonana* cells were found to contain more dimethylsulfoniopropionate, which may be involved in an antioxidant system (Sunda et al. 2002, Bucciarelli and Sunda 2003). The upregulation of mechanisms that protect cells from oxidative stress in our study and that of Bucciarelli and Sunda (2003) provides support for our hypothesis that silica limitation results in excess light energy as a consequence of the downregulation of the CCM.

Our findings suggest that silica limitation may make *C. muelleri* more prone to photoinhibition. We suggest that the downregulation of the CCM, which acts as a sink for excess light energy, may be responsible for the reduced capacity to utilise light at high intensities, the decline in rETR at a lower light intensity and lower $rETR_{max}$ of silica-limited cells compared to silica-replete cells. Consequently, silica-limited *C. muelleri* cells employed a number of physiological strategies to alleviate the stresses associated with downregulation of the CCM. In particular, an increase in carotenoid content, along with an enhanced capacity for NPQ were observed in silica-limited cells. It is likely that these mechanisms reduced the potential for oxidative stress by preventing the production of additional ROS in silica-limited cells. Such physiological plasticity likely enables bloom-formers, such as *Chaetoceros* spp., to acclimate to the constantly changing conditions found in coastal environments. This will likely allow diatoms be competitive under future climate scenarios, where enhanced thermal stratification in the tropics and mid-latitudes will likely inhibit the supply of nutrients to the upper mixed layer of the oceans (Behrenfeld et al. 2006, Doney 2006).

4.5 ACKNOWLEDGEMENTS

Chapter 5: Discussion and Conclusions

5.1 SYNTHESIS

The overall objective of this research was to investigate the role of the silica frustule in diatom CA_{ext} activity, CCM function and photosynthesis using the cosmopolitan marine diatom *Chaetoceros muelleri*. Members of the genus *Chaetoceros* often dominate marine phytoplankton communities, with blooms persisting for weeks (Rines and Theriot 2003). Elucidating the physiological strategies used by *C. muelleri* to respond to fluctuating abiotic conditions will provide insight into the mechanisms that enable diatoms to thrive in marine environments. Initially, this thesis set out to determine if CA_{ext} is a part of the CCM of *C. muelleri* and, if so, whether the role it plays in photosynthesis varies over the course of population growth progression (Chapter 2). The thesis then investigated the impacts of silica limitation on CA_{ext} activity, overall CCM function and photosynthesis in *C. muelleri* (Chapter 3). Lastly, the impacts of silica limitation on photoprotective mechanisms and the production of harmful ROS in *C. muelleri* were investigated (Chapter 4).

It is generally accepted that CA_{ext} activity is induced by low C_i, particularly CO_2, availability. However, a majority of the work investigating the relationship between CA_{ext} activity and CO_2 availability has been conducted on cells that have been pre-acclimated to air-equilibrium concentrations of CO_2. In contrast, few studies have investigated the response of CA_{ext} activity to the depletion of CO_2 that occurs with progression of population growth in phytoplankton blooms or microalgal cultures. Therefore, the role of CA_{ext} in C_i acquisition and photosynthesis at three stages of growth was explored in *C. muelleri* (Chapter 2). A decrease in C_i availability, along with a concomitant increase in pH, was observed with increases in cell number over time. In agreement with the available literature (Berman-Frank et al. 1994, Nimer et al. 1994, Iglesias-Rodriguez and Merrett 1997, Elzenga et al. 2000), CA_{ext} activity in *C. muelleri* was

up-regulated in response to the observed changes in the carbonate system that occurred with the progression of population growth. In addition, we found that the role of CA_{ext} in C_i acquisition for photosynthesis varied over time in response to the depletion of C_i over time, as well as changes in the relative proportion of C_i that occurs with increasing pH. Lowest CA_{ext} activity was measured at our first sampling point. At this point in population growth the theoretical supply of CO_2 by the uncatalysed dehydration of HCO_3^- in the medium exceeded the CO_2 drawdown capacity of the cultures. This suggests that the supply of C_i, specifically CO_2, was sufficient to support photosynthesis without a large contribution by CA_{ext}. In contrast, the CO_2 drawdown capacity of cultures exceeded the theoretical supply of CO_2 by uncatalysed dehydration of HCO_3^- at sampling point 2, suggesting the operation of a CCM (Burns and Beardall 1987). In support of this, marked increases in CA_{ext} activity and the contribution of CA_{ext} to the supply of C_i for photosynthesis were found between the first two sampling points. This up-regulation of CA_{ext} occurred in response to the depletion of CO_2 by exponentially growing *C. muelleri* cultures. Since the operation of a CCM consumes energy and requires investment in capital costs of enzymes needed for C_i transport, the up-regulation of CA_{ext} only when CO_2 supply from the medium is inadequate to maintain the C_i requirements of photosynthesis may act as a resource-saving strategy in *C. muelleri* cells. Whilst the availability of CO_2 decreased further between sampling points 2 and 3, only a small increase in CA_{ext} activity was observed. In addition, the role of CA_{ext} in the supply of C_i for photosynthesis was negligible at the last sampling point. At the high pH, and consequently very low relative CO_2 concentration, present at the last sampling point very high CA_{ext} activity would be necessary to supply sufficient CO_2 for photosynthesis. As such, direct uptake of HCO_3^- at the cell surface by anion exchange transporters, followed by internal conversion to CO_2 by intracellular CA, is likely to be a more efficient means for C_i acquisition at this stage of growth. Overall CCM function in *C. muelleri* increased considerably between sampling points 2 and 3, despite the

small increase in CA_{ext} activity observed over the same time period. Together, these results suggest that *C. muelleri* might rely on direct uptake of HCO_3^- by anion exchange transporters at the cell surface for C_i acquisition later in the growth cycle, rather than CA_{ext}, though this was not tested directly. In contrast to the literature (Rost et al. 2003), we observed a decrease in photosynthesis with the progression of population growth, despite enhanced CCM function. Previous research has suggested that this enhanced CCM function acts to maintain efficient photosynthetic C fixation by RUBISCO under nitrogen-limited conditions. Whilst a large proportion of cellular nitrogen is invested in RUBISCO synthesis under nitrogen-replete conditions, this proportion decreases with decreasing nitrogen availability (Falkowski et al. 1989). Therefore, an enhanced affinity for C_i under nitrogen-limited conditions such as those often found in the stationary phase of growth may act to maintain efficient C fixation despite the lower investment of N in RUBISCO. This would enable cells to preferentially allocate nitrogen to daughter cells and therefore, prolong growth of the population for some time after the onset of nitrogen stress. Overall, the flexibility of the *C. muelleri* CCM in response to fluctuating C_i and nitrogen availabilities may contribute, at least in part, to the dominance and persistence of members of the *Chaetoceros* genus in phytoplankton blooms.

Although C_i availability is thought to be the major factor modulating CCM activity in microalgae, previous research has suggested a role for exogenous silica supply in the modulation of CA_{ext} activity in diatoms. In particular, there is evidence that the silica frustule of diatoms may act as a buffer for the CA_{ext} reaction (Milligan and Morel 2002), increasing the otherwise slow rate of HCO_3^- dehydration at the cell surface. Further studies have suggested that CA_{ext} activity is modulated by the extent of frustule silicification, which is, in turn regulated by the availability of silica in the medium. More specifically, it has been observed that when CO_2 supply is limiting, diatoms produce more heavily silicified frustules (Milligan

et al. 2004, Mejía et al. 2013). In addition, a positive correlation between exogenous silica supply and CA_{ext} activity has been reported in diatoms (Gong and Hu 2014). Together these findings support the hypothesis that CA_{ext} activity is modulated, at least in part, by silica availability. However, the resulting impacts on overall CCM function and photosynthesis have not been explored. Therefore, the impacts of silica limitation on CA_{ext} activity, overall CCM function and photosynthesis were investigated in *C. muelleri* (Chapter 3). As is typically reported for diatoms (Guillard et al. 1973, Paasche 1973a, Paasche 1973b, Paasche 1975, Laing 1985), growth rate and the extent of frustule silicification were lower in silica-limited cells. In addition, silica-limited cells had twice the biovolume of their silica-replete counterparts. Larger cells have a greater demand for CO_2 and are more likely to experience CO_2 diffusion limitation, even if CO_2 availability in the growth medium is the same (Pasciak and Gavis 1974). We observed that when the difference in biovolume between treatments was accounted for, the calculated theoretical maximum diffusive flux of CO_2 to the cell surface was lower in silica-limited cells. This would likely exacerbate CO_2 limitation and induce further up-regulation of the CCM in silica-limited cells. CA_{ext} activity in silica-limited cells was approximately twice that of silica-replete cells on a per cell basis. However, when normalised to cell biovolume, no difference in CA_{ext} activity was observed between treatments. In contrast, silica-limited cells were found to have a more efficient CCM overall. If silica-mediated CA_{ext} activity was the key component of the CCM of *C. muelleri*, the trend in CA_{ext} activity would be expected to be reflected in overall CCM function. Given that this was not the case, we suggested that the CCM of silica-limited cells is up-regulated primarily due to the increased CO_2 limitation experienced as a consequence of their larger cell size, rather than frustule silica content. Due to the greater efficiency of their CCMs, the CO_2 drawdown capacity of silica-replete *C. muelleri* was approximately twice that of silica-limited cells. Similar observations have been made in field studies, particularly in the equatorial upwelling zone of the Pacific Ocean where diatoms

dominate new production (Dugdale and Wilkerson 1998). Low silica concentrations are often observed in the region. The resulting low net primary productivity ultimately makes the equatorial upwelling zone a net source of CO_2 to the atmosphere (Dugdale and Wilkerson 1998). It is predicted that under future climate scenarios enhanced thermal stratification of the surface layer in the tropics and mid-latitudes will inhibit the supply of nutrients to the photic zone (Behrenfeld et al. 2006, Doney 2006). Our results suggest that such a decrease in silica availability may result in less efficient CCMs in silica-limited diatoms. As such, diatoms in these regions would have a reduced capacity for CO_2 drawdown, which may then have consequences for global C cycling.

The operation of a CCM consumes energy (Raven et al. 2014) and, as such, may act as a sink for excess light energy (Tchernov et al. 1997, Tchernov et al. 2003, Qiu and Liu 2004). Exposure to excess light energy can induce the production of harmful reactive oxygen species (de Bianchi et al. 2010), resulting in oxidative stress and even programmed cell death (Vardi et al. 1999). Photoautotrophs can utilise a number of photoprotective strategies to mitigate the impacts of excess light exposure, including dissipation of excess light energy as heat via non-photochemical quenching or detoxification of ROS by antioxidant molecules such as carotenoids (de Bianchi et al. 2010). A down-regulation of the CCM, such as that observed in silica-limited *C. muelleri* cells in Chapter 3, may expose cells to excess light energy, resulting in an increase in oxidative stress. Consequently, an increased capacity for non-photochemical quenching and/or carotenoid concentration might be expected in silica-limited *C. muelleri* cells. Therefore, the impacts of silica limitation on photosynthesis, photoprotective mechanisms and ROS production were investigated in *C. muelleri*. We observed that overall photosystem II health and the ability to harvest light at low light intensities were greater in silica-limited *C. muelleri* cells. The potential for self-shading within cultures increases with

cell number. Since silica-replete cultures were denser than silica-limited cultures, the differences in photosystem II health and the ability to harvest light at lower intensities may reflect differences in light, rather than silica, availability. Given that silica does not play a direct role in photosynthesis, few studies have explored the impacts of silica availability on photosynthesis in diatoms. However, our observation that photosynthetic capacity is reduced under silica limitation agrees with the available literature. In addition to a decrease in photosynthesis, a reduction in the ability to utilise light at higher photon flux densities was observed under silica limitation. Similarly, photosynthesis in silica-replete cells was greater at photon flux densities exceeding 240 µmol photons m^{-2} s^{-1}, with the difference between treatments increasing with light intensity. Whilst a decrease in photosynthesis occurred at supra-optimal light intensities regardless of silica availability, our results suggest that silica limitation makes *C. muelleri* more susceptible to photoinhibition. As anticipated, an up-regulation of photoprotective mechanisms was observed in silica-limited *C. muelleri* cells. In particular, the chlorophyll and carotenoid contents of silica-limited cells were approximately double those of silica-replete cells. This variation in pigment content between treatments may be due to the increase in cell biovolume observed under silica limitation (Chapter 3). Alternatively, diatoms may increase the concentration of light-harvesting pigments, such as chlorophyll and the carotenoid fucoxanthin, to meet additional energy demands for CO_2 acquisition caused by a down-regulation of the CA_{ext} under silica limitation (Bucciarelli and Sunda 2003). In addition, the increase in carotenoids observed under silica limitation may be attributed to an increase in diadinoxanthin cycle activity. In diatoms, up-regulation of the diadinoxanthin cycle, and more specifically increases in the concentration of diatoxanthin, have been associated with an enhanced capacity for non-photochemical quenching (Olaizola et al. 1994, Olaizola and Yamamoto 1994, Dimier et al. 2007). Since silica-limited cells had a greater capacity for non-photochemical quenching, the increase in carotenoids observed under silica

limitation may, at least in part, be due to an increase in diadinoxanthin cycle activity. Non-photochemical quenching acts to dissipate excess light energy as heat and, as such, prevent the formation of reactive oxygen species. Given that the concentration of reactive oxygen species did not differ between silica treatments, increased non-photochemical quenching is likely an effective mechanism for lessening the severity of photoinhibition in silica-limited *C. muelleri* cells. Together, the results presented in Chapter 4 provide support for our hypothesis that the down-regulation of the CCM under silica limitation exposes cells to excess light energy. The physiological plasticity displayed by *C. muelleri* under silica limitation may help bloom formers, such as *Chaetoceros spp.*, to dominate in constantly changing coastal environments.

5.2 LIMITATIONS AND FUTURE DIRECTIONS

In Chapter 2, we suggested that although CA_{ext} plays a considerable role in acquiring C_i for photosynthesis in mid-exponential phase, C_i acquisition in the later stages of growth is likely dominated by direct uptake of HCO_3-by anion exchange transporters. The increase in overall CCM function without corresponding increases in CA_{ext} activity or the contribution of CA_{ext} to photosynthesis between the last two sampling points support this hypothesis. However, stronger support for this hypothesis could be gathered by measuring the contribution of anion exchange transporters to photosynthesis over time. This could be achieved by replacing the CA_{ext} inhibitor acetazolamide with 4,4-diisothiocyanostilbene-2,2-disulphonic acid, a putative inhibitor of anion exchange, in the experiments described under the subheading 'The role of CA_{ext} in photosynthetic O_2 evolution – Inhibition of CA_{ext}' in Chapter 2. In addition, we hypothesised in Chapter 2 that the *C. muelleri* CCM is up-regulated in the later stages of growth to maintain efficient C fixation despite reduced RUBISCO synthesis caused by decreasing nitrogen availability. The decreases in photosystem II health, chlorophyll concentration and

photosynthesis observed in *C. muelleri* over time are good indicators of nitrogen limitation. However, measurements of the proportion of cellular nitrogen allocated to RUBISCO and the RUBISCO content of cells over time would be necessary to confirm our hypothesis. In Chapter 3 we suggested that enhanced C_i limitation associated with the increased biovolume of cells exposed to silica limitation, rather than frustule silica content, is the regulating factor in the CCM of *C. muelleri*. However, a comparison of the CA_{ext} buffering capacity of frustules differing in their silica content would be necessary to definitively conclude that the degree of frustule silicification plays no role in regulating CA_{ext} activity in *C. muelleri*. In Chapter 4, we hypothesised that the greater carotenoid content of silica-limited cells was due, at least in part, to increased diadinoxanthin cycle activity. Our observation of enhanced non-photochemical capacity, which is associated with increased diadinoxanthin cycle activity, in silica-limited *C. muelleri* cells lends support to this idea. However, it is possible that the observed increase in carotenoid content in silica-limited cells is due to an increase in fucoxanthin, a carotenoid that forms part of the light-harvesting complex in diatom. Therefore, it would be necessary to specifically measure diadinoxanthin cycle activity and fucoxanthin concentration to test this hypothesis.

5.3 CONCLUSIONS

This thesis explored the concept that the silica frustule in diatoms plays a role in inorganic carbon acquisition. In particular, it reports on investigations of the physiological mechanisms used by *C. muelleri*, a cosmopolitan marine diatom, to respond to changes in C_i and silicaavailability. Overall, *C. muelleri* showed a high degree of physiological plasticity in response to changes in exogenous C_i and silica availability. This physiological flexibility likely contributes to the observed dominance of bloom-forming diatoms such as *Chaetoceros* species

in coastal environments, where abiotic conditions are constantly fluctuating. In the future, this capacity to acclimate to changes in abiotic conditions may give diatoms a competitive advantage in the tropics and mid-latitudes, where it is predicted that the supply of nutrients to the upper mixed layer will be inhibited due to enhanced thermal stratification under global warming scenarios. However, a study investigating the synergistic response of diatoms to other changes predicted under future climate scenarios, such as increased temperature, CO_2 supply and the availability of nutrients other than silica, would be necessary to more accurately predict the competitive ability of diatoms in the future oceans.

References

Alldredge, A. L., Passow, U. & Logan, B. E. 1993. The abundance and significance of a class of large, transparent organic particles in the ocean. *Deep Sea Res. Part I.* 40:1131-40

Armbrust, E. V. 2009. The life of diatoms in the world's oceans. *Nature* 459:185-92

Armbrust, E. V., Berges, J. A., Bowler, C., Green, B. R., Martinez, D., Putnam, N. H., Zhou, S., Allen, A. E., Apt, K. E. & Bechner, M. 2004. The genome of the diatom *Thalassiosira pseudonana*: ecology, evolution, and metabolism. *Science* 306:79-86

Axelsson, L., Ryberg, H. & Beer, S. 1995. Two modes of bicarbonate utilization in the marine green macroalga *Ulva lactuca*. *Plant, Cell & Environment* 18:439-45

Azam, F. 1998. Microbial control of oceanic carbon flux: the plot thickens. *Science* 280:694-96

Azam, F., Fenchel, T., Field, J. G., Gray, J., Meyer-Reil, L. & Thingstad, F. 1983. The ecological role of water-column microbes in the sea. *Mar. Ecol. Prog. Ser.* 10:257-63

Badger, M. R. & Price, G. D. 1994. The role of carbonic anhydrase in photosynthesis. *Annu. Rev. Plant Biol.* 45:369-92

Badger, M. R. & Price, G. D. 2003. CO_2 concentrating mechanisms in cyanobacteria: molecular components, their diversity and evolution. *J. Exp. Bot.* 54:609-22

Barber, R. & Chavez, F. 1991. Regulation of primary productivity rate in the equatorial Pacific. *Limnol. Oceanogr* 36:1803-15

Beardall, J. 1989. Photosynthesis and photorespiration in marine phytoplankton. *Aquat. Bot.* 34:105-30

Beardall, J. & Giordano, M. 2002. Ecological implication of microalgal and cyanobacterial CO_2 concentrating mechanisms, and their regulation. *Funct. Plant Biol.* 29:335-47

Beardall, J., Johnston, A. & Raven, J. 1998. Environmental regulation of CO_2-concentrating mechanisms in microalgae. *Can. J. Bot* 76:1010-17

Beer, S., Björk, M. & Beardall, J. 2014. *Photosynthesis in the marine environment.* Wiley-Blackwell, United States, 208.

Behrenfeld, M. J., Bale, A. J., Kolber, Z. S., Aiken, J. & Falkowski, P. G. 1996. Confirmation of iron limitation of phytoplankton photosynthesis in the equatorial Pacific Ocean. *Nature* 383:508-11

Behrenfeld, M. J., T O'Malley, R., Siegel, D. A., McClain, C. R., Sarmiento, J. L., Feldman, G. C., Milligan, A. J., Falkowski, P. G., Letelier, R. M. & Boss, E. S. 2006. Climate-driven trends in contemporary ocean productivity. *Nature* 444:752

Berges, J. A., Franklin, D. J. & Harrison, P. J. 2001. Evolution of an artificial seawater medium: Improvements in enriched seawater, artificial water over the last two decades. *J. Phycol.* 37:1138-45

Berman-Frank, I., Zohary, T., Erez, J. & Dubinsky, Z. 1994. CO_2 availability, carbonic anhydrase, and the annual dinoflagellate bloom in Lake Kinneret. *Limnol. Oceanogr.* 39:1822-34

Berman-Frank, I., Kaplan, A., Zohary, T. & Dubinsky, Z. 1995. Carbonic anhydrase activity in the bloom-forming dinoflagellate *Peridinium gatunense*. *J. Phycol.* 31:906-13

Booth, B. & Harrison, P. 1979. Effect of silicate limitation on valve morphology in *Thalassiosira* and *Coscinodiscus* (Bacillariophyceae). *J. Phycol.* 15:326-29

Borowitzka, M. A. & Volcani, B. E. 1978. The Polymorphic Diatom *Phaeodactylum tricornutum*: Ultrastructure of its Morphotypes. *J. Phycol.* 14:10-21

Bowler, C., Vardi, A. & Allen, A. E. 2010. Oceanographic and biogeochemical insights from diatom genomes. *Annu. Rev. Marine. Sci.* 2:333-65

Bozzo, G. & Colman, B. 2000. The induction of inorganic carbon transport and external carbonic anhydrase in *Chlamydomonas reinhardtii* is regulated by external CO_2 concentration. *Plant, Cell & Environment* 23:1137-44

Brzezinski, M., Nelson, D., Franck, V. & Sigmon, D. 2001. Silicon dynamics within an intense open-ocean diatom bloom in the Pacific sector of the Southern Ocean. *Deep Sea Res. Part II.* 48:3997–4018

Brzezinski, M., Olson, R. & Chisholm, S. 1990. Silicon availability and cell-cycle progression in marine diatoms. *Mar. Ecol. Prog. Ser.* 67:83-96

Bucciarelli, E. & Sunda, W. G. 2003. Influence of CO_2, nitrate, phosphate, and silicate limitation on intracellular dimethylsulfoniopropionate in batch cultures of the coastal diatom *Thalassiosira pseudonana*. *Limnol. Oceanogr.* 48:2256-65

Burkhardt, S., Amoroso, G., Riebesell, U. & Sültemeyer, D. 2001. CO_2 and HCO_3^- uptake in marine diatoms acclimated to different CO_2 concentrations. *Limnol. Oceanogr.* 46:1378-91

Burns, B. D. & Beardall, J. 1987. Utilization of inorganic carbon by marine microalgae. *J. Exp. Mar. Biol. Ecol.* 107:75-86

Clement, R., Dimnet, L., Maberly, S. C. & Gontero, B. 2016. The nature of the CO_2-concentrating mechanisms in a marine diatom, *Thalassiosira pseudonana*. *New Phytol.* 209:1417-27

Cleveland, J. & Perry, M. 1987. Quantum yield, relative specific absorption and fluorescence in nitrogen-limited *Chaetoceros gracilis*. *Mar. Biol.* 94:489-97

Coale, K. H., Johnson, K. S., Fitzwater, S. E., Gordon, R. M., Tanner, S., Chavez, F. P., Ferioli, L., Sakamoto, C., Rogers, P. & Millero, F. 1996. A massive phytoplankton bloom induced by an ecosystem-scale iron fertilization experiment in the equatorial Pacific Ocean. *Nature* 383:495

Codispoti, L., Friederich, G., Iverson, R. & Hood, D. 1982. Temporal changes in the inorganic carbon system of the southeastern Bering Sea during spring 1980. *Nature* 296:242-45

Coesel, S., Obornık, M., Varela, J., Falciatore, A. & Bowler, C. 2008. Evolutionary Origins and Functions of the Carotenoid Biosynthetic Pathway in Marine Diatoms. *PLoS ONE* 3:e2896

Colman, B. & Rotatore, C. 1995. Photosynthetic inorganic carbon uptake and accumulation in two marine diatoms. *Plant, Cell & Environment* 18:919-24

de Bianchi, S., Ballottari, M., Dall'Osto, L. & Bassi, R. 2010. Regulation of plant light harvesting by thermal dissipation of excess energy. *Biochem. Soc. Trans.* 38:651-60

De La Rocha, C. L. & Passow, U. 2007. Factors influencing the sinking of POC and the efficiency of the biological carbon pump. *Deep Sea Res. Part II.* 54:639-58

Dickson, A. & Riley, J. 1979. The estimation of acid dissociation constants in seawater media from potentionmetric titrations with strong base. I. The ionic product of water—Kw. *Mar. Chem.* 7:89-99

Dimier, C., Corato, F., Tramontano, F. & Brunet, C. 2007. Photoprotection and xanthophyll-cycle activity in three marine diatoms. *J. Phycol.* 43:937-47

Dixon, G. & Merrett, M. 1988. Bicarbonate utilization by the marine diatom *Phaeodactylum tricornutum* Bohlin. *New Phytol.* 109:47-51

Doney, S. 2006. Plankton in a warmer world. *Nature* 444:695-96

Dugdale, R. & Wilkerson, F. 1998. Silicate regulation of newproduction in the equatorial Pacific upwelling. *Nature* 391:270-73

Durbin, E. G. 1977. Studies on the autoecology of the marine diatom *Thalassiosira nordenskioeldii.* II. The influence of cell size on growth rate, and carbon, nitrogen, chlorophyll a and silica content. *J. Phycol* 13:150-55

Elzenga, J. T. M., Prins, H. & Stefels, J. 2000. The role of extracellular carbonic anhydrase activity in inorganic carbon utilization of *Phaeocystis globosa* (Prymnesiophyceae): A

comparison with other marine algae using the isotopic disequilibrium technique. *Limnol. Oceanogr.* 45:372-80

Falkowski, P., Scholes, R., Boyle, E., Canadell, J., Canfield, D., Elser, J., Gruber, N., Hibbard, K., Högberg, P. & Linder, S. 2000. The global carbon cycle: a test of our knowledge of earth as a system. *Science* 290:291-96

Falkowski, P. G. 1994. The role of phytoplankton photosynthesis in global biogeochemical cycles. *Photosynth. Res.* 39:235-58

Falkowski, P. G., Barber, R. T. & Smetacek, V. 1998. Biogeochemical controls and feedbacks on ocean primary production. *Science* 281:200-06

Falkowski, P. G., Sukenik, A. & Herzig, R. 1989. Nitrogen limitation in *Isochrysis galban*a (Haptophyceae). II. Relative abundance of chlorophyll proteins. *J. Phycol.* 25:471-78

Field, C. B., Behrenfeld, M. J., Randerson, J. T. & Falkowski, P. 1998. Primary production of the biosphere: integrating terrestrial and oceanic components. *Science* 281:237-40

Finkel, Z. V., Beardall, J., Flynn, K. J., Quigg, A., Rees, T. A. V. & Raven, J. A. 2010. Phytoplankton in a changing world: cell size and elemental stoichiometry. *J. Plankton Res.* 32:119-37

Flynn, K. J. & Martin-Jézéquel, V. 2000. Modelling Si–N-limited growth of diatoms. *J. Plankton Res.* 22:447-72

Fuhrman, J. A. 1999. Marine viruses and their biogeochemical and ecological effects. *Nature* 399:541

Fung, I. Y., Doney, S. C., Lindsay, K. & John, J. 2005. Evolution of carbon sinks in a changing climate. *Proc. Natl. Acad. Sci. U S A* 102:11201-06

Ghannoum, O., Evans, J. R., Chow, W. S., Andrews, T. J., Conroy, J. P. & von Caemmerer, S. 2005. Faster Rubisco is the key to superior nitrogen-use efficiency in NADP-malic enzyme relative to NAD-malic enzyme C_4 grasses. *Plant Physiol.* 137:638-50

Giordano, M., Beardall, J. & Raven, J. A. 2005. CO_2 concentrating mechanisms in algae: mechanisms, environmental modulation, and evolution. *Annu. Rev. Plant Biol.* 56:99-131

Giordano, M., Davis, J. S. & Bowes, G. 1994. Organic carbon release by Dunaliella salina (Chlorophyta) under different growth conditions of CO_2, nitrogen, and salinity. *J. Phycol* 30:249-57

Giordano, M., Kansiz, M., Heraud, P., Beardall, J., Wood, B. & McNaughton, D. 2001. Fourier transform infrared spectroscopy as a novel tool to investigate changes in intracellular macromolecular pools in the marine microalga *Chaetoceros muelleri* (Bacillariophyceae). *J. Phycol.* 37:271-79

Goericke, R. & Welschmeyer, N. A. 1992. Pigment turnover in the marine diatom *Thalassiosira weissflogii.* II. The $^{14}CO_2$-labelling kinetics of carotenoids. *J. Phycol.* 28:507-17

Gong, Y. & Hu, H. 2014. Effect of silicate and inorganic carbon availability on the growth and competition of a diatom and two red tide dinoflagellates. *Phycologia* 53:433-42

Granum, E., Raven, J. A. & Leegood, R. C. 2005. How do marine diatoms fix 10 billion tonnes of inorganic carbon per year? *Can. J. Bot* 83:898-908

Guillard, R. R., Kilham, P. & Jackson, T. A. 1973. Kinetics of silicon-limited growth in the marine diatom *Thalassiosira pseudonana* Hasle and Heimdal (= *Cyclotella nana* Hustedt). *J. Phycol.* 9:233-37

Guillard, R. R. & Ryther, J. 1962. Studies of marine planktonic diatoms. I. *Cyclotella nana* Hustedt, and *Detonula confervacea* (Cleve) Gran. *Can. J. Microbiol.* 8:229-39

Hale, M. S. & Mitchell, J. G. 2001. Functional morphology of diatom frustule microstructures: hydrodynamic control of Brownian particle diffusion and advection. *Aquat. Microb. Ecol.* 24:287-95

Hamm, C. E., Merkel, R., Springer, O., Jurkojc, P., Maier, C., Prechtel, K. & Smetacek, V. 2003. Architecture and material properties of diatom shells provide effective mechanical protection. *Nature* 421:841-43

Harrison, P., Conway, H. & Dugdale, R. 1976. Marine diatoms grown in chemostats under silicate or ammonium limitation. I. Cellular chemical composition and steady-state growth kinetics of *Skeletonema costatum*. *Mar. Biol.* 35:177-86

Harrison, P., Conway, H., Holmes, R. & Davis, C. O. 1977. Marine diatoms grown in chemostats under silicate or ammonium limitation. III. Cellular chemical composition and morphology of *Chaetoceros debilis*, *Skeletonema costatum*, and *Thalassiosira gravida*. *Mar. Biol.* 43:19-31

Hein, M. & Sand-Jensen, K. 1997. CO_2 increases oceanic primary production. *Nature* 388:526-27

Henley, W. J. 1993. Measurement and interpretation of photosynthetic light-response curves in algae in the context of photoinhibition and diel changes. *J. Phycol.* 29:729-39

Hetherington, A. M. & Raven, J. A. 2005. The biology of carbon dioxide. *Curr. Biol.* 15:R406-R10

Heureux, A. M., Young, J. N., Whitney, S. M., Eason-Hubbard, M. R., Lee, R. B., Sharwood, R. E. & Rickaby, R. E. 2017. The role of Rubisco kinetics and pyrenoid morphology in shaping the CCM of haptophyte microalgae. *J. Exp. Bot.* 68:3959-69

Hildebrand, M. 2008. Diatoms, Biomineralization Processes, and Genomics. *Chem. Rev.* 108:4855-74

Hopkinson, B. M., Meile, C. & Shen, C. 2013. Quantification of extracellular carbonic anhydrase activity in two marine diatoms and investigation of its role. *Plant Physiol.* 162:1142-52

Hu, H. & Gao, K. 2008. Impacts of CO_2 enrichment on growth and photosynthesis in freshwater and marine diatoms. *Chinese J. Oceanol. Limnol.* 26:407-14

Hutchins, D. A. & Bruland, K. W. 1998. Iron-limited diatom growth and Si: N uptake ratios in a coastal upwelling regime. *Nature* 393:561-64

Iglesias-Rodriguez, M. & Merrett, M. 1997. Dissolved inorganic carbon utilization and the development of extracellular carbonic anhydrase by the marine diatom *Phaeodactylum tricornutum. New Phytol.* 135:163-68

Ihnken, S., Roberts, S. & Beardall, J. 2011. Differential responses of growth and photosynthesis in the marine diatom *Chaetoceros muelleri* to CO_2 and light availability. *Phycologia* 50:182-93

Ingalls, A. E., Whitehead, K. & Bridoux, M. C. 2010. Tinted windows: the presence of the UV absorbing compounds called mycosporine-like amino acids embedded in the frustules of marine diatoms. *Geochim. Cosmochim. Acta* 74:104-15

Jeffrey, S. t. & Humphrey, G. 1975. New spectrophotometric equations for determining chlorophylls a, b, c1 and c2 in higher plants, algae and natural phytoplankton. *Biochem. Physiol. PFL* 167:191-94

John-McKay, M. E. & Colman, B. 1997. Variation in the occurrence of external carbonic anhydrase among strains of the marine diatom *Phaeodactylum tricornutum* (Bacillariophyceae). *J. Phycol.* 33:988-90

Karl, D. M., Tilbrook, B. D. & Tien, G. 1991. Seasonal coupling of organic matter production and particle flux in the western Bransfield Strait, Antartica. *Deep Sea Res. Part I.* 38:1097-126

Keston, A. S. & Brandt, R. 1965. The fluorometric analysis of ultramicro quantities of hydrogen peroxide. *Anal. Biochem.* 11:1-5

Kolber, Z. S., Barber, R. T., Coale, K. H., Fitzwateri, S. E., Greene, R. M., Johnson, K. S.,
Lindley, S. & Falkowski, P. G. 1994. Iron limitation of phytoplankton photosynthesis
in the equatorial Pacific Ocean. *Nature* 371:145-49

Kooistra, W. H. C. F., De Stefano, M., Mann, D. G. & Medlin, K. 2003. The Phylogeny of
the Diatoms. *In*: Müller, W. E. G. [Ed.] *Silicon Biomineralization: Biology —
Biochemistry — Molecular Biology — Biotechnology.* Springer Berlin Heidelberg,
Berlin, Heidelberg, pp. 59-97.

Kroth, P., Chiovitti, A., Gruber, A., Martin-Jezequel, V. & Mock, T. 2008. A Model for
Carbohydrate Metabolism in the Diatom *Phaeodactylum tricornutum* Deduced from
Comparitive Whole Genome Analysis. *PLoS One* 3:e1426

Laing, I. 1985. Growth response of *Chaetoceros calcitrans* (Bacillariophyceae) in batch
culture to a range of initial silica concentrations. *Mar. Biol.* 85:37-41

Lane, T. W. & Morel, F. M. 2000. Regulation of carbonic anhydrase expression by zinc,
cobalt, and carbon dioxide in the marine diatom *Thalassiosira weissflogii*. *Plant
Physiol.* 123:345-52

Lavoie, M., Raven, J. A. & Levasseur, M. 2016. Energy cost and putative benefits of cellular
mechanisms modulating buoyancy in aflagellate marine phytoplankton. *J. Phycol*
52:239-51

Leterme, S. C., Ellis, A. V., Mitchell, J. G., Buscot, M. J., Pollet, T., Schapira, M. & Seuront,
L. 2010. Morphological flexibility of Cocconeis placentula(Bacillariophyceae)
nanostructure to changing salinity levels. *J. Phycol.* 46:715-19

Leterme, S. C., Prime, E., Mitchell, J., Brown, M. H. & Ellis, A. V. 2013. Diatom
adaptability to environmental change: a case study of two *Cocconeis* species from
high-salinity areas. *Diatom Research* 28:29-35

Lewin, J. 1962. Silicification. *In*: Lewin, R. [Ed.] *Physiology and Biochemistry of Algae.* Academic Press, New York, pp. 445-53.

Lewin, J. C. 1955. Silicon metabolism in iatoms. II. Sources of silicon for growth of *Navicula pelliculosa. Plant Physiol.* 30:129

Liang, Y., Beardall, J. & Heraud, P. 2006. Changes in growth, chlorophyll fluorescence and fatty acid composition with culture age in batch cultures of *Phaeodactylum tricornutum* and *Chaetoceros muelleri* (Bacillariophyceae). *Bot. Mar.* 49:165-73

Ligowski, R., Jordan, R. W. & Assmy, P. 2012. Morphological adaptation of a planktonic diatom to growth in Antarctic sea ice. *Mar. Biol.* 159:817-27

Lindskog, S. & Coleman, J. E. 1973. The catalytic mechanism of carbonic anhydrase. *Proc. Natl. Acad. Sci. U S A* 70:2505-08

Lippemeier, S., Hartig, P. & Colijn, F. 1999. Direct impact of silicate on the photosynthetic performance of the diatom *Thalassiosira weissflogii* assessed by on- and off-line PAM fluorescence measurements. *J. Plankton Res.* 21:269-83

Lorimer, G. H. 1981. The carboxylation and oxygenation of ribulose 1, 5-bisphosphate: the primary events in photosynthesis and photorespiration. *Annu. Rev. Plant Physiol.* 32:349-82

Losh, J. L., Young, J. N. & Morel, F. M. 2013. Rubisco is a small fraction of total protein in marine phytoplankton. *New Phytologist* 198:52-58

Lynn, S. G., Kilham, S. S., Kreeger, D. A. & Interlandi, S. J. 2000. Effect of nutrient availability on the biochemical and elemental stoichiometry in the freshwater diatom *Stephanodiscus minutulus* (Bacillariophyceae). *J. Phycol.* 36:510-22

Malone, T., Garside, C. & Neale, P. 1980. Effects of silicate depletion on photosynthesis by diatoms in the plume of the Hudson River. *Marine Biology* 58:197-204

Mann, D. & Droop, J. 1996. Biodiversity, biogeography and conservation of diatoms. *Hydrobiologia* 336:19-32

Martin-Jézéquel, V., Hildebrand, M. & Brzezinski, M. A. 2000. Silicon metabolism in diatoms: Implications for growth. *J. Phycol.* 36:821-40

Martin, C. L. & Tortell, P. D. 2006. Bicarbonate transport and extracellular carbonic anhydrase activity in Bering Sea phytoplankton assemblages: results from isotope disequilibrium experiments. *Limnol. Oceanogr.* 51:2111-21

Martin, C. L. & Tortell, P. D. 2008. Bicarbonate transport and extracellular carbonic anhydrase in marine diatoms. *Physiol. Plant.* 133:106-16

Martin, J. H., Coale, K., Johnson, K., Fitzwater, S., Gordon, R., Tanner, S., Hunter, C., Elrod, V., Nowicki, J. & Coley, T. 1994. Testing the iron hypothesis in ecosystems of the equatorial Pacific Ocean. *Nature* 371:123

Martin, J. H. & Fitzwater, S. E. 1988. Iron deficiency limits phytoplankton growth in the north-east Pacific subarctic. *Nature* 331:341

Martino, A. D., Meichenin, A., Shi, J., Pan, K. & Bowler, C. 2007. Genetic and phenotypic characterization of *Phaeodactylum tricornutum* (Bacillariophyceae) accessions. *Journal of Phycology* 43:992-1009

Matsuda, Y., Hara, T. & Colman, B. 2001. Regulation of the induction of bicarbonate uptake by dissolved CO_2 in the marine diatom, *Phaeodactylum tricornutum*. *Plant. Cell. Environ.* 24:611-20

Matsuda, Y., Hopkinson, B. M., Nakajima, K., Dupont, C. L. & Tsuji, Y. 2017. Mechanisms of carbon dioxide acquisition and CO_2 sensing in marine diatoms: a gateway to carbon metabolism. *Phil. Trans. R. Soc. B* 372:20160403

Maxwell, K. & Johnson, G. N. 2000. Chlorophyll fluorescence—a practical guide. *J. Exp. Bot.* 51:659-68

Mejía, L. M., Isensee, K., Méndez-Vicente, A., Pisonero, J., Shimizu, N., González, C., Monteleone, B. & Stoll, H. 2013. B content and Si/C ratios from cultured diatoms (*Thalassiosira pseudonana* and *Thalassiosira weissflogii*): Relationship to seawater pH and diatom carbon acquisition. *Geochim. Cosmochim. Acta* 123:322-37

Mikulic, P. 2015. *Contrasting zinc toxicity effects on model extremophilic freshwater algal species.* PhD Thesis, Monash University, 301 pp.

Miller, A. G. & Colman, B. 1980. Evidence for HCO_3^- transport by the blue-green alga (cyanobacterium) *Coccochloris peniocystis*. *Plant. Physiol.* 65:397-402

Millero, F. J. 2010. Carbonate constants for estuarine waters. *Mar. Freshwater Res.* 61:139-42

Milligan, A. J. & Morel, F. M. 2002. A proton buffering role for silica in diatoms. *Science* 297:1848-50

Milligan, A. J., Varela, D. E., Brzezinski, M. A. & Morel, F. M. 2004. Dynamics of silicon metabolism and silicon isotopic discrimination in a marine diatomas a function of $p\text{CO}_2$. *Limnol. Oceanogr.* 49:322-29

Mitchell, C. & Beardall, J. 1996. Inorganic carbon uptake by an Antarctic sea-ice diatom, *Nitzschia frigida*. *Polar Biol.* 16:95-99

Mitchell, J. G., Seuront, L., Doubell, M. J., Losic, D., Voelcker, N. H., Seymour, J. & Lal, R. 2013. The role of diatom nanostructures in biasing diffusion to improve uptake in a patchy nutrient environment. *PLoS One* 8:e59548.doi:10.1371/journal.pone.0059548

Miyachi, S., Tsuzuki, M. & Avramova, S. T. 1983. Utilization modes of inorganic carbon for photosynthesis in various species of *Chlorella*. . *Plant and Cell Physiology* 24:441-51

Morel, F. M., Cox, E. H., Kraepiel, A. M., Lane, T. W., Milligan, A. J., Schaperdoth, I., Reinfelder, J. R. & Tortell, P. D. 2002. Acquisition of inorganic carbon by the marine diatom *Thalassiosira weissflogii*. *Funct. Plant Biol.* 29:301-08

Moroney, J. V., Husic, H. D. & Tolbert, N. 1985. Effect of carbonic anhydrase inhibitors on

inorganic carbon accumulation by *Chlamydomonas reinhardtii*. *Plant. Physiol.*

79:177-83

Moroney, J. V., Ma, Y., Frey, W. D., Fusilier, K. A., Pham, T. T., Simms, T. A., DiMario, R.

J., Yang, J. & Mukherjee, B. 2011. The carbonic anhydrase isoforms of

Chlamydomonas reinhardtii: intracellular location, expression, and physiological

roles. *Photosynthesis Research* 109:133-49

Moroney, J. V. & Somanchi, A. 1999. How do algae concentrate CO_2 to increase the

efficiency of photosynthetic carbon fixation? *Plant Physiol.* 119:9-16

Mukerji, D., Glover, H. & Morris, I. 1978. Diversity in the mechanism of carbon dioxide

fixation in *Dunaliella tertiolecta* (Chlorophyceae). *J. Phycol.* 14:137-42

Murata, A., Kumamoto, Y., Saito, C., Kawakami, H., Asanuma, I., Kusakabe, M. & Inoue, H.

2002. Impact of a spring phytoplankton bloom on the CO 2 system in the mixed layer

of the northwestern North Pacific. *Deep Sea Res. Part II.* 49:5531-55

Nakajima, K., Tanaka, A. & Matsuda, Y. 2013. SLC4 family transporters in a marine diatom

directly pump bicarbonate from seawater. *Proc. Natl. Acad. Sci. U S A* 110:1767-72

Nalewajko, C. & O'Mahony, M. A. 1989. Photosynthesis of algal cultures and phytoplankton

following an acid pH shock. *J. Phycol.* 25:319-25

Napoléon, C., Raimbault, V. & Claquin, P. 2013. Influence of nutrient stress on the

relationships between PAM measurements and carbon incorporation in four

phytoplankton species. *PLoS One* 8:e66423

Nelson, D. M., Tréguer, P., Brzezinski, M. A., Leynaert, A. & Quéguiner, B. 1995.

Production and dissolution of biogenic silica in the ocean: revised global estimates,

comparison with regional data and relationship to biogenic sedimentation. *Glob.*

Biogeochem. Cycles 9:359-72

Nimer, N., Guan, Q. & Merrett, M. 1994. Extra-and intra-cellular carbonic anhydrase in relation to culture age in a high-calcifying strain of *Emiliania huxleyi* Lohmann. *New. Phytol.* 126:601-07

Nimer, N. A., Iglesias-Rodriguez, M. D. & Merrett, M. J. 1997. Bicarbonate utilization by marine phytoplankton species. *Journal of Phycology* 33:625-31

Olaizola, M., La Roche, J., Kolber, Z. & Falkowski, P. G. 1994. Non-photochemical flourescence quenching and the diadinoxanthin cycle in a marine diatom. *Photosynth. Res.* 41:357-70

Olaizola, M. & Yamamoto, H. Y. 1994. Short-term response of the diadinoxanthin cycle and fluorescence yield to high irradiance in *Chaetoceros muelleri* (Bacillariophyceae). *J. Phycol.* 30:606-12

Paasche, E. 1973a. Silicon and the ecology of marine plankton diatoms. I. *Thalassiosira pseudonana* (*Cyclotella nana*) grown in a chemostat with silicate as limiting nutrient. *Mar. Biol.* 19:117-26

Paasche, E. 1973b. Silicon and the ecology of marine plankton diatoms. II. Silicate-uptake kinetics in five diatom species. *Mar. Biol.* 19:262-69

Paasche, E. 1975. Growth of the plankton diatom *Thalassiosira nordenskioeldii* Cleve at low silicate concentrations. *J. Exp. Mar. Biol. Ecol.* 18:173-83

Paasche, E. 1980. Silicon content of five marine plankton diatom species measured with a rapid filter method. *Limnol. Oceanogr.* 25:474-80

Pacheco-Vega, J. M. & Sánchez-Saavedra, M. 2009. The biochemical composition of *Chaetoceros muelleri* (Lemmermann) grown with an agricultural fertilizer. *J. World. Aquacult. Soc.* 40:556-60

Parkhill, J. P., Maillet, G. & Cullen, J. J. 2001. Fluorescence-based maximal quantum yield for PSII as a diagnostic of nutrient stress. *J. Phycol* 37:517-29

Pasciak, W. J. & Gavis, J. 1974. Transport limitation of nutrient uptake in phytoplankton. *Limnol. Oceanogr.* 19:881-88

Pasciak, W. J. & Gavis, J. 1975. Transport limited nutrient uptake rates in *Ditylum brightwelli*. *Limnol. Oceanogr.* 20:604-17

Pickett-Heaps, J. D. 1998. Cell division and morphogenesis of the centric diatom *Chaetoceros decipiens* (Bacillariophyceae) I. Living cells. *J. Phycol* 34:989-94

Pierangelini, M., Stojkovic, S., Orr, P. T. & Beardall, J. 2014a. Elevated CO_2 causes changes in the photosynthetic apparatus of a toxic cyanobacterium, *Cylindrospermopsis raciborskii*. *J. Plant. Physiol.* 171:1091-98

Pierangelini, M., Stojkovic, S., Orr, P. T. & Beardall, J. 2014b. Photosynthetic characteristics of two *Cylindrospermopsis raciborskii* strains differing in their toxicity. *J. Phycol.* 50:292-302

Pocker, Y. 2000. Water in enzyme reactions: biophysical aspects of hydration-dehydration processes. *Cellular and Molecular Life Sciences* 57:1008-17

Qiu, B. & Liu, J. 2004. Utilization of inorganic carbon in the edible cyanobacterium Ge-Xian-Mi (*Nostoc*) and its role in alleviating photo-inhibition. *Plant. Cell. Environ.* 27:1447-58

Ralph, P. J. & Gademann, R. 2005. Rapid light curves: a powerful tool to assess photosynthetic activity. *Aquat. Bot.* 82:222-37

Ramel, F., Birtic, S., Cuiné, S., Triantaphylidès, C., Ravanat, J.-L. & Havaux, M. 2012. Chemical quenching of singlet oxygen by carotenoids in plants. *Plant Physiol.* 158:1267-78

Raven, J. 1983. The transport and function of silicon in plants. *Biol. Rev.* 58:179-207

Raven, J. 1995. Scaling the seas. *Plant, Cell & Environment* 18:1090-100

Raven, J. & Waite, A. 2004. The evolution of silicification in diatoms: inescapable sinking and sinking as escape? *New phytologist* 162:45-61

Raven, J. A. 1994. Carbon fixation and carbon availability in marine phytoplankton. *Photosynth. Res.* 39:259-73

Raven, J. A., Beardall, J. & Giordano, M. 2014. Energy costs of carbon dioxide concentrating mechanisms in aquatic organisms. *Photosynth. Res.* 121:111-24

Raven, J. A., Beardall, J. & Sánchez-Baracaldo, P. 2017. The possible evolution and future of CO_2-concentrating mechanisms. *J. Exp. Bot.* 68:3701-16

Raven, J. A., Cockell, C. S. & De La Rocha, C. L. 2008. The evolution of inorganic carbon concentrating mechanisms in photosynthesis. *Philos. T. R. Soc. B.* 363:2641-50

Reinecke, B. 1997. *The effects of increased carbon dioxide on growth and photosynthesis of microalgae.* Honours Thesis, Monash University, 56 pp.

Reinfelder, J. 2011. Carbon Concentrating Mechanisms in Eukaryotic Marine Phytoplankton. *Annu. Rev. Marine. Sci.* 3:291-315

Richardson, K., Beardall, J. & Raven, J. 1983. Adaptation of unicellular algae to irradiance: An analysis of strategies. *New Phytol.* 93:157-91

Riebesell, U. 2000. Photosynthesis: Carbon fix for a diatom. *Nature* 407:959-60

Riebesell, U., Schulz, K. G., Bellerby, R., Botros, M., Fritsche, P., Meyerhöfer, M., Neill, C., Nondal, G., Oschlies, A. & Wohlers, J. 2007. Enhanced biological carbon consumption in a high CO_2 ocean. *Nature* 450:545-48

Riebesell, U., Wolf-Gladrow, D. & Smetacek, V. 1993. Carbon dioxide limitation of marine phytoplankton growth rates.

Rines, J. E. & Theriot, E. C. 2003. Systematics of Chaetocerotaceae (Bacillariophyceae). I. A phylogenetic analysis of the family. *Phycol. Res.* 51:83-98

Ritchie, R. J. 2006. Consistent sets of spectrophotometric chlorophyll equations for acetone, methanol and ethanol solvents. *Photosynth. Res.* 89:27-41

Rost, B., Riebesell, U., Burkhardt, S. & Sültemeyer, D. 2003. Carbon acquisition of bloom-forming marine phytoplankton. *Limnol Oceanogr* 48:55-67

Samukawa, M., Shen, C., Hopkinson, B. M. & Matsuda, Y. 2014. Localization of putative carbonic anhydrases in the marine diatom, *Thalassiosira pseudonana*. *Photosynth. Res.* 121:235-49

Sánchez-Baracaldo, P. 2015. Origin of marine planktonic cyanobacteria. *Sci. Rep.* 5

Shen, C. & Hopkinson, B. M. 2015. Size scaling of extracellular carbonic anhydrase activity in centric marine diatoms. *J. Phycol.* 51:255-63

Silverman, D. N. & Lindskog, S. 1988. The Catalytic Mechanism of Carbonic Anhydrase: Implications of a Rate-Limiting Protolysis of Water. *Acc. Chem. Res.* 21:30-36

Smith-Harding, T. J., Beardall, J. & Mitchell, J. G. 2017. The role of external carbonic anhydrase in photosynthesis during growth of the marine diatom *Chaetoceros muelleri*. *J. Phycol*.10.1111/jpy.12572

Smith-Harding, T. J., Beardall, J. & Mitchell, J. G. In prep. Silica Limitation Effects on Diatom CO_2 Concentrating Mechanism Function, Photosynthesis and CO_2 Drawdown Capacity

Spijkerman, E., Stojkovic, S. & Beardall, J. 2014. CO_2 acquisition in *Chlamydomonas acidophila* is influenced mainly by CO_2, not phosphorus, availability. *Photosynth. Res.* 121:213-21.doi 10.1007/s11120-014-0016-6

Strickland, J. D. & Parsons, T. R. 1972. *A practical handbook of seawater analysis.* Fisheries Research Board of Canada, Ottawa, Ontario, Canada,

Sunda, W., Kieber, D., Kiene, R. & Huntsman, S. 2002. An antioxidant function for DMSP and DMS in marine algae. *Nature* 418:317-20

Szabo, E. & Colman, B. 2007. Isolation and characterization of carbonic anhydrases from the marine diatom *Phaeodactylum tricornutum*. *Physiol. Plant.* 129:484-92

Tachibana, M., Allen, A. E., Kikutani, S., Endo, Y., Bowler, C. & Matsuda, Y. 2011. Localization of putative carbonic anhydrases in two marine diatoms, *Phaeodactylum tricornutum* and *Thalassiosira pseudonana*. *Photosynth. Res.* 109:205-21

Takeda, S. 1998. Influence of iron availability on nutrient consumption ratio of diatoms in oceanic waters. *Nature* 393:774-77

Tchernov, D., Hassidim, M., Luz, B., Sukenik, A., Reinhold, L. & Kaplan, A. 1997. Sustained net CO_2 evolution during photosynthesis by marine microorganisms. *Curr. Biol.* 7:723-28

Tchernov, D., Silverman, J., Luz, B., Reinhold, L. & Kaplan, A. 2003. Massive light-dependent cycling of inorganic carbon between oxygenic photosynthetic microorganisms and their surroundings. *Photosynth. Res.* 77:95-103

Tortell, P. D. 2000. Evolutionary and ecological perspectives on carbon acquisition in phytoplankton. *Limnol Oceanogr* 45:744-50

Tréguer, P. & Pondaven, P. 2000. Global change: silica control of carbon dioxide. *Nature* 406:358-59

Trimborn, S., Lundholm, N., Thoms, S., Richter, K. U., Krock, B., Hansen, P. J. & Rost, B. 2008. Inorganic carbon acquisition in potentially toxic and non-toxic diatoms: the effect of pH-induced changes in seawater carbonate chemistry. *Physiol. Plant.* 133:92-105

Trimborn, S., Wolf-Gladrow, D., Richter, K.-U. & Rost, B. 2009. The effect of pCO_2 on carbon acquisition and intracellular assimilation in four marine diatoms. *J. Exp. Mar. Biol. Ecol.* 376:26-36

Tsuji, Y., Mahardika, A. & Matsuda, Y. 2017a. Evolutionarily distinct strategies for the acquisition of inorganic carbon from seawater in marine diatoms. *J. Exp. Bot.* erx102.doi: 10.1093/jxb/erx102

Tsuji, Y., Nakajima, K. & Matsuda, Y. 2017b. Molecular aspects of the biophysical CO_2-concentrating mechanism and its regulation in marine diatoms. *J. Exp. Bot.* 68:3763-72

Vadrucci, M., Mazziotti, C. & Fiocca, A. 2013. Cell volume and surface area in phytoplankton of Mediterranean transitional water ecosystems: methodological aspects. *Transit. Waters Bull.* 7:100-23.10.1285/i1825229Xv7n2p100

Vance, P. & Spalding, M. H. 2005. Growth, photosynthesis, and gene expression in *Chlamydomonas* over a range of CO_2 concentrations and CO_2/O_2 ratios: CO_2 regulates multiple acclimation states. *Can. J. Bot.* 83:796-809.10.1139/b05-064

Vardi, A., Berman-Frank, I., Rozenberg, T., Hadas, O., Kaplan, A. & Levine, A. 1999. Programmed cell death of the dinoflagellate *Peridinium gatunense* is mediated by CO_2 limitation and oxidative stress. *Curr. Biol.* 9:1061-64

Vardi, A., Thamatrakoln, K., Bidle, K. D. & Falkowski, P. G. 2009. Diatom genomes come of age. *Genome Biol.* 9:245

Wang, H., Mi, T., Zhen, Y., Jing, X., Liu, Q. & Yu, Z. 2017. Metacaspases and programmed cell death in *Skeletonema marinoi* in response to silicate limitation. *J. Plankton Res.* 39:729-43.10.1093/plankt/fbw090

Watson, A., Bakker, D., Ridgwell, A., Boyd, P. & Law, C. 2000. Effect of iron supply on Southern Ocean CO_2 uptake and implications for glacial atmospheric CO_2. *Nature* 407:730-33

Weiss, R. 1974. Carbon dioxide in water and seawater: the solubility of a non-ideal gas. *Mar. Chem.* 2:203-15

Wilbur, K. M. & Anderson, N. G. 1948. Electrometric and colorimetric determination of carbonic anhydrase. *J. Biol. Chem.* 176:147-54

Willén, E. 1991. Planktonic diatoms - An ecological review. *Arch. Hydrobiol. Suppl. Algol. Stud.* 62:69-106

Williams, T. G. & Colman, B. 1993. Identification of distinct internal and external isozymes of carbonic anhydrase in *Chlorella saccharophila*. *Plant Physiol.* 103:943-48

Wolf-Gladrow, D. & Riebesell, U. 1997. Diffusion and reactions in the vicinity of plankton: A refined model for inorganic carbon transport. *Marine Chemistry* 59:17-34

Wu, Y., Beardall, J. & Gao, K. 2015. Physiological responses of a model marine diatom to fast pH changes: special implications of coastal water acidification. *PloS One* 10:e0141163

Wu, Y., Gao, K. & Riebesell, U. 2010. CO_2-induced seawater acidification affects physiological performance of the marine diatom *Phaeodactylum tricornutum*. *Biogeosciences (BG)* 7:2915-23

Young, E., Beardall, J. & Giordano, M. 2001. Inorganic carbon acquisition by *Dunaliella tertiolecta* (Chlorophyta) involves external carbonic anhydrase and direct HCO3- utilization insensitive to the anion exchange inhibitor DIDS. *European Journal of Phycology* 36:81-88

Young, E. B. & Beardall, J. 2003. Photosynthetic function in *Dunaliella tertiolecta* (Chlorophyta) during a nitrogen starvation and recovery cycle. *J. Phycol.* 39:897-905

Young, E. B. & Beardall, J. 2005. Modulation of photosynthesis and inorganic carbon acquisition in a marine microalga by nitrogen, iron, and light availability. *Can. J. Bot* 83:917-28

Young, J. N., Heureux, A. M., Sharwood, R. E., Rickaby, R. E., Morel, F. M. & Whitney, S. M. 2016. Large variation in the Rubisco kinetics of diatoms reveals diversity among their carbon-concentrating mechanisms. *J. Exp. Bot.* 67:3445-56

Zeebe, R. E. & Wolf-Gladrow, D. 2001. *CO$_2$ in Seawater: Equilibrium, Kinetics, Isotopes.* Elsevier, Amsterdam,

Zhang, S., Liu, H., Ke, Y. & Li, B. 2017. Effect of the silica content of diatoms on protozoan grazing. *Frontiers in Marine Science* 4:202